

NATURAL HELPER CELL DEVELOPMENT AND THEIR ROLE IN MEDIATING THE
INNATE TH2 INFLAMMATORY RESPONSE

by

TIMOTHËUS YOU FU HALIM

B.Sc., The University of British Columbia, 2004

A THESIS SUBMITTED IN PARTIAL FULFILLMENT OF
THE REQUIREMENTS FOR THE DEGREE OF

DOCTOR OF PHILOSOPHY

in

THE FACULTY OF GRADUATE STUDIES

(Genetics)

THE UNIVERSITY OF BRITISH COLUMBIA

(Vancouver)

December 2012

© Timothëus You Fu Halim, 2012

Abstract

Overproduction of cytokines by T helper 2 (Th2) cells in the lung is thought to be a cause of allergic lung inflammation. We found that innate lymphocytes termed lung Natural Helper cells are a T cell-independent source of Th2 cytokines in allergen stimulated lungs. When stimulated by IL-33 plus IL-2, IL-7 or thymic stroma lymphopoietin, lung Natural Helper cells (identified as Lineage⁻Sca-1⁺c-Kit^{low/-}CD25⁺CD127⁺) produced large amounts of IL-5 and IL-13. Intranasal administration of the protease allergen, papain, or house dust mite extract induced eosinophilic infiltration and mucus hyper-production in the lungs of wild-type and *Rag1*^{-/-} mice, but not *Rag2*^{-/-}*Il2rg*^{-/-} mice that lack lung Natural Helper cells. Lung Natural Helper cell depletion inhibited papain-induced airway inflammation in *Rag1*^{-/-} mice, whereas adoptive transfer of lung Natural Helper cells enabled *Rag2*^{-/-}*Il2rg*^{-/-} mice to respond. Treatment of lung explants with papain induced IL-33 and thymic stroma lymphopoietin production by stroma cells and IL-5 and IL-13 production by lung Natural Helper cells. We also examined the lineage relationship between Natural Helper cells in different tissues and IL-22 producing retinoid receptor related orphan receptor (ROR) γ t-positive innate lymphoid cells. We found that Natural Helper cells expressed ROR α but not ROR γ t. ROR α deficient, but not ROR γ t-deficient, mice lacked Natural Helper cells in all tissues while all other lymphocytes including ROR γ t⁺ innate lymphocytes were unaffected. Natural Helper cell deficient mice generated by ROR α -deficient bone marrow transplantation had a normal Th2 cell response but failed to develop acute allergic lung inflammation in response to protease allergen. We also identified ROR α -dependent Natural Helper cell progenitors that were distinct from common lymphoid progenitors in the bone marrow. Thus, these results showed that all Natural Helper cells belong to a distinct cell lineage separate from other lymphoid lineages and they are critical for protease allergen-induced airway inflammation.

Preface

A version of Chapter 2 has been published: Halim, T.Y.F., Krauß, R.H., Sun, A.C., and Takei F. (2012) Lung Natural Helper cells are critical source of Th2 cytokines in protease allergen-induced airway inflammation. *Immunity* 36(3):451-463. I designed and conducted 80% of experiments, and wrote 50% of the manuscript. Ramona Krauß conducted 10% of the experiments. Ann Sun conducted 10% of the experiments. Dr. Fumio Takei designed experiments and wrote 50% of the manuscript.

A version of Chapter 3 has been accepted for publication: Halim, T.Y.F., MacLaren A., Romanish, M.T., Gold, M.J., McNaghy K.M., and Takei F. (2012) Retinoic acid receptor-related orphan nuclear receptor alpha is required for Natural Helper cell development and allergic inflammation. *Immunity* 37(3):463-474. I designed and conducted 80% of the experiments, and wrote 50% of the manuscript. Aric McLaren conducted 10% of the experiments. Mark Romanish conducted the qPCR experiments shown in Figure 14E. Matthew Gold conducted the Pep3b bone marrow-transplant experiments shown in Appendix 31. Dr. Kelly McNaghy edited the manuscript. Dr. Fumio Takei designed experiments and wrote 50% of the manuscript.

All animal experimentation was carried out with adherence to the guidelines presented by the University of British Columbia Animal Care Committee. Canadian Council on Animal Care Approval was granted under the certificate number: # A09-0994.

Table of Contents

Abstract.....	ii
Preface	iii
Table of contents.....	iv
List of tables	viii
List of figures.....	ix
List of abbreviations	xi
Acknowledgements.....	xiii
Dedication.....	xiv
Chapter 1 Introduction.....	1
1.1 The immune system	1
1.1.1 Adaptive immune system	1
1.1.2 Innate immune system.....	4
1.1.2.1 Innate lymphocytes	7
1.1.3 Interaction between the innate and adaptive immune system	9
1.2 Natural Helper cells	12
1.2.1 Characterization of Natural Helper cells	14
1.2.2 Natural Helper cell activation.....	14
1.2.3 Function of Natural Helper cells	16
1.2.4 Allergic inflammation and asthma	17
1.3 Development of Natural Helper cells.....	18
1.3.1 Lymphopoiesis	18
1.3.2 Innate lymphocyte development	21
1.3.3 ROR α and ROR γ t.....	23
1.4 Thesis objective	24
Chapter 2 Lung Natural Helper cells are a critical source of Th2 cell-type cytokines in protease allergen-induced airway inflammation	25
2.1 Introduction.....	25
2.2 Materials and methods	28

2.2.1 Mice.....	28
2.2.2 Antibodies, reagents, FACS sorting and analysis	28
2.2.3 Primary leukocyte preparation	29
2.2.4 Isolation of lung NH cells	29
2.2.5 Cytokine production assay	29
2.2.6 Lung explant culture.....	29
2.2.7 Intracellular staining.....	30
2.2.8 ELISA assay	30
2.2.9 RNA isolation and microarray	30
2.2.10 <i>In vivo</i> papain stimulation, lung NH cell depletion and adoptive transplant	30
2.2.10 Statistics.....	31
2.3 Results.....	32
2.3.1 Identification of lung Natural Helper cells in normal mice.....	32
2.3.2 Characterization of lung NH cells	33
2.3.3 Gene expression profile of lung NH cells	36
2.3.4 Cytokine-mediated stimulation of lung NH cells.....	37
2.3.5 lung NH cells are responsible for papain-induced eosinophilia and mucus secretion in RAG1-deficient mice	41
2.3.6 Papain stimulation enhances Th2 cell-type cytokine production from lung NH cells	45
2.4 Discussion	48
Chapter 3 Retinoic acid receptor-related orphan nuclear receptor alpha is required for Natural Helper cell development and allergic inflammation.....	55
3.1 Introduction.....	55
3.2 Materials and methods	56
3.2.1 Mice.....	56
3.2.2 Genotyping and qPCR.....	57
3.2.3 Bone marrow transplantation	57
3.2.4 Antibodies, reagents, FACS sorting and analysis	58
3.2.5 Primary leukocyte preparation	58
3.2.6 Isolation of NH, iNH, CLP and LMPP cells	59
3.2.7 Cytokine production analysis	59
3.2.8 <i>In vitro</i> CD4 ⁺ T-cell stimulation	60
3.2.9 Intestine explant culture	60
3.2.10 Intracellular staining.....	60
3.2.11 ELISA assay	60
3.2.12 RNA isolation and microarray	60
3.2.13 <i>In vivo</i> papain stimulation	61
3.2.14 Statistics.....	61

3.3 Results.....	60
3.3.1 NH cells express <i>Rora</i> and can be distinguished from ROR γ ⁺ ILC by Sca-1 and c-Kit expression.....	61
3.3.2 ROR α -deficient mice do not have functional NH cells.....	64
3.3.3 <i>Rora</i> ^{sg/sg} bone-marrow transplanted mice are NH cell deficient, but have functional Th2 cells and ROR γ ⁺ ILCs.....	66
3.3.4 Immature NH cells in the bone-marrow develop into mature NH cells in mucosal tissues	69
3.3.5 NH cell-deficient mice have defective inflammatory response to allergens.....	75
3.4 Discussion	78
Chapter 4 General summary and discussion.....	83
4.1 Summary	83
4.2 Significance of the work	86
4.3 Strength and limitations	87
4.4 Future directions	88
References.....	89
Appendices	97
Appendix 1 Backgating analysis of lung NH cells in the lung	97
Appendix 2 The frequency, phenotype and cytokine production capacity of lung NH cells in <i>RagI</i> ^{-/-} mice, and myeloid and lymphoid potential of lung NH cells	98
Appendix 3 Lung NH cells do not have myeloid or lymphoid potential.....	99
Appendix 4 Stimulation by PMA plus ionomycin (P/I) induced IL-5 and IL-13 production from WT and <i>RagI</i> ^{-/-} lung explants, but not from <i>Rag2</i> ^{-/-} <i>Il2rg</i> ^{-/-} lung explants.....	100
Appendix 5 Papain stimulation induces a lung NH cell dependent Th2 response	101
Appendix 6 Lung NH cell depletion in <i>RagI</i> ^{-/-} mice followed by intranasal stimulation with protease allergen or house dust mite	102
Appendix 7 TSLP and/or IL-33 neutralization in explant cultures significantly decreases papain or IL-25 induced Th2 cytokine production	104
Appendix 8 Analysis of naive WT NH cell gene expression and lung NH cell cytokine production	105

Appendix 9 Analysis of <i>staggerer</i> mice for NH cells and NH cell function	106
Appendix 10 <i>Rora</i> ^{sg/sg} BM gives rise to normal numbers of lymphocytes and myeloid cells in the spleen and BM of congenic Pep3b hosts.....	107
Appendix 11 BM derived iNH cells and mature lung NH cells respond differently to in vitro culture conditions.....	108
Appendix 12 BM derived iNH cells have more efficient NH cell repopulation capacity, and are more restricted to NH cell lineage, than LMPP or CLP	109
Appendix 13 Gating strategies for myeloid cell populations.....	111
Appendix 14 Analysis of IL-25 stimulated gut NH cells	112
Appendix 15 Supplementary experimental procedures	113
Appendix 16 Table of primers	116
Appendix 17 Table of antibodies	117
Appendix 18 Table of cytokines	119

List of tables

Table 1 Consolidated review of Natural Helper cells in different tissues and animals.....	13
Table 2 List of primers	116
Table 3 List of antibodies	117
Table 4 List of cytokines	119

List of figures

Figure 1 Classes of innate lymphocytes	9
Figure 2 Th2-skewing of CD4 ⁺ Th0 cells.....	11
Figure 3 Natural Helper cell activation	15
Figure 4 Th2-mediated lung inflammation.....	17
Figure 5 Haematopoiesis	20
Figure 6 Innate lymphocyte development	22
Figure 7 Lung contains Lin ⁻ Sca-1 ⁺ c-Kit ^{+/-low} CD127 ⁺ CD25 ⁺ cytokine secreting cells.....	33
Figure 8 Characterization of lung NH cells.....	35
Figure 9 Gene expression analysis of Lung NH cells.....	37
Figure 10 Lung NH cells rapidly produce Th2 cell-type cytokines in response to IL-33 plus co-stimulation	40
Figure 11 Lung NH cells are required for T cell independent eosinophil infiltration and mucus secretion in papain induced lung inflammation	42
Figure 12 Lung NH cell depletion and adoptive transplant show that lung NH cells are required for papain-induced mucus production and eosinophil infiltration	44
Figure 13 Lung NH cells respond to lung stroma derived cytokines, and are the main producers of IL-5 and IL-13 following papain treatment	47
Figure 14 <i>Rora</i> and <i>Rorct</i> expressing innate lymphocyte subsets in naive WT mice	63
Figure 15 <i>Rora</i> ^{sg/sg} mice are deficient in NH cells but not <i>Rorct</i> -dependent ILC	66
Figure 16 <i>Rora</i> deficiency affects NH cell development	68
Figure 17 Lin ⁻ Sca-1 ^{hi} c-Kit ⁻ (LSK ⁻) cells contain <i>Rora</i> -dependent CD127 ⁺ CD25 ⁺ T1/ST2 ⁺ immature NH cells.....	70
Figure 18 iNH cells are more NH cell lineage restricted and efficient than LMPP or CLP at generating NH cells	74
Figure 19 NH cell deficient <i>Rora</i> ^{sg/sg} BM chimeras have an impaired innate Th2-response	77
Figure 20 Model of NH cell mediated lung inflammation	84
Figure 21 RORα in NH cell development	85
Figure 22 Backgating analysis of lung NH cells in the lung	97
Figure 23 The frequency, phenotype and cytokine production capacity of lung NH cells in <i>Rag1</i> ^{-/-} mice, and myeloid and lymphoid potential of lung NH cells.....	98
Figure 24 Lung NH cells do not have myeloid or lymphoid potential	99
Figure 25 Stimulation by PMA plus ionomycin (P/I) induced IL-5 and IL-13 production from WT and <i>Rag1</i> ^{-/-} lung explants, but not from <i>Rag2</i> ^{-/-} <i>Il2rg</i> ^{-/-} lung explants.....	100
Figure 26 Papain stimulation induces a lung NH cell dependent Th2 response	101
Figure 27 Lung NH cell depletion in <i>Rag1</i> ^{-/-} mice followed by intranasal stimulation with protease allergen or house dust mite	102
Figure 28 TSLP and/or IL-33 neutralization in explant cultures significantly decreases papain or IL-25 induced Th2 cytokine production.....	104
Figure 29 Analysis of naive WT NH cell gene expression and lung NH cell cytokine production	105
Figure 30 Analysis of <i>staggerer</i> mice for NH cells and NH cell function	106

Figure 31 <i>Rora</i> ^{sg/sg} BM gives rise to normal numbers of lymphocytes and myeloid cells in the spleen and BM of congenic Pep3b hosts	107
Figure 32 BM derived iNH cells and mature lung NH cells respond differently to in vitro culture conditions	108
Figure 33 BM derived iNH cells have more efficient NH cell repopulation capacity, and are more restricted to NH cell lineage, than LMPP or CLP.....	109
Figure 34 Gating strategies for myeloid cell populations.....	111
Figure 35 Analysis of IL-25 stimulated gut NH cells.....	112

List of abbreviations

Ab	antibody
APC	allophycocyanin
APCs	antigen presenting cells
B6	C57Bl/6
BAL	bronchioalveolar lavage
BCR	B cell receptor
BM	bone marrow
BMT	bone marrow transplant
Breg	regulatory B cells
DC	dendritic cell
CLP	common lymphoid progenitor
CTL	cytotoxic T cell
eGFP	enhanced green fluorescent protein
ELISA	enzyme linked immunosorbent assay
FACS	fluorescence activated cell sorting
FALC	fat associated lymphoid cells
Fc	constant heavy chain
FcR	receptor for Fc portion of antibodies
Flt3L	Fms-like tyrosine kinase ligand
FMO	fluorescence minus one
GATA3	GATA-binding protein 3
GI	gastrointestinal
HDM	house dust mite
HIS	humanized immune system
HSC	haematopoietic stem cell
i.n.	intranasal injection
i.p.	intraperitoneal injection
i.v.	intravenous injection
IFN	interferon
IFN γ	interferon gamma
Ig	immunoglobulin
Ih2	innate helper type 2
IL	interleukin
IL-17RB	IL-25 receptor
ILC	innate lymphoid cell
ILC17	IL-17 producing innate lymphocyte
ILC22	IL-22 producing innate lymphocyte
iNH	immature Natural Helper
KIR	killer-inhibitory immunoglobulin-like receptor
KO	knock-out
Lin	lineage
L. Int.	large intestine
LMPP	lymphoid primed multipotent progenitor
LN	lymph node
LSK	lineage-negative, Sca-1-positive, c-Kit-negative
LT β R	lymphotoxin-beta receptor
LTi	lymphoid tissue inducing

Ly49	lymphocyte antigen 49 complex
MØ	macrophage
MHC	major histocompatibility complex
MHC I	major histocompatibility complex type I
MHC II	major histocompatibility complex type II
MLN	mesenteric lymph node
MPP type 2	multipotent progenitor type 2
nd	not determined
NH	Natural Helper
NK	natural killer
NKT	natural killer T cell
NOD/SCID	non obese diabetic/severe combined immunodeficient
NSG	NOD/SCID IL-2 receptor gamma chain knockout
OVA	ovalbumin
PAMPs	pathogen associated molecular patterns
PAS	periodic acid-Schiff
PBS	phosphate buffered saline
PCR	polymerase chain reaction
pDC	plasmacytoid dendritic cell
PE	phycoerythrobilin
PI	propidium iodide
P/I	phorbol 12-myristate 13-acetate/ionomycin
PMA	phorbol 12-myristate 13-acetate
PPR	pattern recognition receptor
qPCR	quantitative PCR
RAG	recombinase activating gene
RGS	RAG knockout/IL-2 receptor gamma chain knockout
ROR	retinoic acid receptor orphan receptor
Sca-1	stem cell antigen 1
SCF	stem cell factor
Scid	severe combined immunodeficiency
S. Int.	small intestine
STAT	signal transducers and activator of transcription
TCR	T cell receptor
TF	transcription factor
Tfh	follicular helper T cell
TGFβ	transforming growth factor-beta
Th	T helper
TLR	toll like receptor
TNF-α	tumour necrosis factor-alpha
Treg	regulatory T cells
TSLP	thymic stromal lymphopoietin
VCAM-1	vascular cell adhesion molecule-1
WT	wild-type

Acknowledgements

First and foremost, I would like to acknowledge my supervisor Dr. Fumio Takei without whose exceptional guidance, mentorship and patience none of my work could have been accomplished. I would also like to extend special thanks to Dr. Linnea L. Veinotte who trained me during my first year and with whom I collaborated as a co-first author on experiments published in *Blood* 111(8):4201-4208. I would also like to acknowledge my PhD committee members Dr. Dixie Mager, Dr. Kelly M. McNagny, Dr. Andrew P. Weng and Dr. Fabio M. Rossi who provided constructive advice throughout my education and reviewed this thesis. Furthermore I would like to acknowledge Dr. Kelly McNagny again for his role as a collaborator, as well as his student Matthew J. Gold, and Dr. Mark T. Romanish who both worked on experiments in Chapter 3 of this thesis.

I would also like to acknowledge the co-op, summer and research students who provided invaluable help in the laboratory. They include Laura Matha, Catherine Steer, Aric MacLaren, Ramona Krauß, Ann Sun, Ashley Erdman, Eric Ma, Andrew Wong and Jennifer Mead.

Lastly I would like to acknowledge the present and past lab members for useful advice, help with experiments and great friendship. Takei Laboratory members include Dr. Yuh-Ching Twu, Laura Guillon, Kathrin Warner, Valeria Rytova, Boxiang Jiang, Dr. Claudia Luther, Dr. Evette Haddad, Dr. Emily Mace, Dr. Eva Backstrom, Dr. Nooshin Tabatabaei and Dr. Valeria Alcon. Terry Fox Laboratory members include Dr. Jens Ruschmann, Dr. David Kent, Dr. Florian Kuchenbauer, Dr. Benjamin Lai, Dr. Andrew Muranyi Dr. Julie Brind'Amour, Victoria Garside and Sam Guscott. Core facility staff includes David Ko, Wenbo Xu, Gayle Thornbury, Lindsey Laycock and the ARC facility.

I dedicate this thesis to my parents who instilled in me the love for science.

Chapter 1 Introduction

1.1 The immune system

Our immune system wields great power. Without its constant protection we would be overrun by invading organisms, and yet without control it can quickly overwhelm and destroy us. The human and mouse immune systems are composed of multiple specialized cell types, most of which do not act alone, but in concert with other cells to mount the appropriate response to pathogens. These responses can be roughly grouped into either the innate or adaptive immune system. The innate immune system provides a first line of defence, is evolutionary more primitive than the adaptive immune system, and most importantly, has no long-lasting immune memory. The adaptive immune system confers a highly specific response to pathogens that takes longer to ramp-up. The adaptive immune system is evolutionary more recent, with evidence of classical adaptive immune cells evolving in jawed vertebrates (Flajnik and Du Pasquier, 2004). The hallmark feature of the adaptive immune system is long-lasting immunity to previously encountered pathogens using an unlimited repertoire of randomly rearranged receptors. Another vital, yet often underappreciated function of the immune system is its anti-tumour activity.

1.1.1 Adaptive immune system

The adaptive immune system in mice and humans consists of two types of cells that belong to the lymphoid lineage, namely T and B cells (Murphy et al., 2007). T cells are generated in the thymus and exert their function via their T cell receptor (TCR), which detects peptides presented by other cells using the major histocompatibility complex (MHC) molecule. T cells can detect an almost unlimited variety of peptides bound to MHC by means of genomic rearrangement of the TCR during development. T cells can be further sub-

grouped based on their function and corresponding protein and/or gene expression. CD8⁺ cytotoxic T cells (CTL) detect peptides bound to MHC class I (MHC I) on target cells, and destroy infected or transformed cells (Murphy et al., 2007). CD4⁺ T helper (Th) cells detect peptide presented by MHC class II (MHC II) on antigen presenting cells (APCs). Activated naïve CD4⁺ Th cells develop into mature Th cells, whose primary role is secretion of cytokines that influence other immune functions. Several types of Th cells are known: Th1 cells secrete interferon-gamma (IFN γ) and IL-2, which propagate an immune response against intracellular bacterial or viral pathogens; Th2 cells secrete primarily IL-4, IL-5 and IL-13, which induce an immune response against extracellular pathogens such as parasites; Th17 cells secrete IL-17A and IL-17F, which promotes an immune response against bacterial infection (O'Shea and Paul, 2010). Another subset, follicular helper T (Tfh) cells, play an important role in directing cell interactions and activation in secondary lymphoid structures such as the lymph node (LN) (Crotty, 2011). The factors that direct naïve Th cells towards a specific fate include cytokines and receptor-ligands, which subsequently influence the regulation of transcriptional programs within Th cells. The milieu created by the innate immune system is believed to influence the fate-decisions made by T cells (covered in greater detail in Chapter 1.1.3). A third subset of T cells is the Natural Killer T (NKT) cell, which share properties with innate Natural Killer (NK) cells. NKT cells have a more limited repertoire of TCR that detects lipids and glycolipids presented by the CD1d molecule on target cells (Brigl et al., 2003). A fourth subset is the T regulatory (Treg) cells, whose function is to down-regulate the immune system and induce tolerance to antigens and resolve inflammation after pathogen clearance. Treg cells are dependent on Foxp3 transcription factor (TF) for their development, and express CD4 and CD25 on their cell surface (Sakaguchi et al., 2007).

B cells, unlike T cells, are generated in the bone marrow (BM) and confer antibody (Ab) mediated humoral immunity (Murphy et al., 2007). B cells express rearranged B cell receptors (BCR) on their cell surface, which detect antigens without the need for MHC presentation. Activated B cells secrete Abs, which bind to specific epitopes on antigens and initiate a range of immune responses. When naïve B cells first encounter an antigen recognized by their BCR, they produce immunoglobulin (Ig) M Abs, which form pentamers when secreted. IgM bound to target causes activation of the complement pathway (discussed in section 1.1.2), opsonizes targets for phagocytosis, or neutralizes targets. Depending on various extrinsic signals, activated naïve B cells may undergo further somatic hyper-mutation and class-switching, which result in the production of higher affinity Abs of a different isotype (IgG, IgE or IgA) (Murphy et al., 2007). Different classes of Abs have different functions imparted by their constant heavy chain (Fc), which binds to different Fc-receptors (FcR) on effector cells. Furthermore, the Fc region also determines which anatomical locales are accessible. While IgM is restricted to blood and lymph due to its large size as a pentamer, IgG and IgE monomers freely diffuse into tissues from the blood (Murphy et al., 2007). IgA can form dimers, and is actively transported across the mucosal epithelium where it plays an important role in neutralizing pathogens and toxins.

In addition to their ability to produce different types of Abs, B-cells can also be divided into subsets based on inherited differences in lineage and function, often associated with cell-surface phenotype, anatomical location and genetic program. B2 cells are considered classical B cells as previously described above. B1 cells, like NKT cells, straddle the divide between innate and adaptive immunity (Cerutti et al., 2011). B1 cells are a source of innate-Abs, protective against pathogen derived repetitive epitopes such as carbohydrates. Furthermore, a significant percentage of the Ab-repertoire of B1 cells is directed against self-

antigens. B1 produced self-Abs are thought to play a role in homeostasis, while innate Abs are protective against commonly encountered pathogens (Martin and Kearney, 2000). B-regulatory (Breg) cells are another subset that play an important role in maintenance of tolerance via suppression of pathogenic T cells (Mauri and Ehrenstein, 2008)

1.1.2 Innate immune system

The innate immune system is evolutionarily conserved and found in virtually all multi-cellular organisms. In humans (and mice), the innate immune system forms the first-line of defence against pathogens. Some components of the innate immune system are: the skin and mucosal epithelia, complement proteins, myeloid immune cells and innate lymphocytes. The most primitive, but also most effective part of the immune system is our skin and mucosal epithelia (Duerr and Hornef, 2012). The outer layer of our skin composed of keratinocytes forms a virtually impenetrable barrier to most pathogens. Antimicrobial peptides secreted also keep harm at bay, while commensal flora is allowed to flourish and out-compete pathogenic bacteria. Mucosal tissues in our gastro-intestinal (GI) tract, respiratory system and urogenital system form an epithelial monolayer via tight junctions, secrete mucous, and support the growth of non-pathogenic commensal flora. Complement proteins are found in sera and have the ability to attack pathogens by binding to their cell-wall or cell-membrane causing damage to the pathogen, to opsonise pathogens or induce inflammation. The complement system is activated via several pathways, all involving the formation of complexes at the surface of pathogens which initiate an auto-catalytic cascade. Myeloid immune cells respond to pathogens by releasing toxic compounds, phagocytosis of pathogens, or modulating the immune response via production of chemokines and cytokines. Another important function carried out by many myeloid immune cells is the initiation and regulation of the adaptive immune response. Myeloid immune cells include mast-cells,

monocytes, macrophages (MØ) and granulocytes, which can be grouped into neutrophils, eosinophils and basophils. Certain dendritic cells (DC) also belong to the myeloid lineage. Neutrophils are short lived leukocytes, which infiltrate inflamed tissues from the blood where they release bactericidal compounds and phagocytose pathogens. Eosinophils also infiltrate tissues, are activated by pattern recognition receptors (PRR) or cytokines such as IL-5, and attack immunoglobulin (Ig) A or IgE coated antigens (Kita, 2011). Basophils, like eosinophils, bind to the constant region of IgE via Fc receptors on their cell-surface. Activated basophils secrete histamines, as well as other inflammatory molecules, and play a role in parasitic infection and allergy (Siracusa et al., 2012). Mast-cells serve a similar purpose by releasing histamine granules upon IgE cross-linking, which induces inflammation (Galli and Tsai, 2012). Monocytes migrate from the blood into tissue, where they differentiate into tissue resident macrophages. Macrophages together with DCs in the skin and mucosal epithelia function as sentinels at the barrier between sterility and the outside environment.

To differentiate friend from foe, MØs and DCs (as well as other immune cells) employ germ-line encoded receptors that detect pathogen-associated-molecular-patterns (PAMPs). Toll-like-receptors (TLRs) were the first PRR identified and this class of receptors now includes over 18 other PRRs (Mogensen, 2009). Essentially, TLRs and other PRRs evolved to detect vital components of different groups of pathogens, but alien to humans. Examples include virus derived double-stranded RNA (detected by TLR3); essential bacterial components such as flagellin (detected by TLR5); parasitic lipoprotein (detected by TLR2) or fungal plasma membrane derived β -Glucan (detected by Dectin-1). As such, the detection of these markers by receptors signals the presence of foreign material (danger signals), likely derived from invading organisms. The innate immune system has evolved

together with pathogens to adapt to the type of enemy it must repel. Different PRRs evolved to detect different types of pathogens, while different signalling cascades associated with classes of PRRs has allowed cells to specialize and activate specific molecular or genetic programs tailored to the type of infection detected. Tissue resident MØs or DCs are activated when they encounter PAMPs. Activated MØs absorb and degrade pathogens by phagocytosis, in addition to secreting cytokines, chemokines and other biologically active molecules. DCs, like MØs, phagocytose pathogens. Additionally DCs perform macropinocytosis, a process where they constantly sample their surroundings. Pathogens and other extracellular components absorbed by MØs and DCs are enzymatically degraded and short amino-acid sequences derived from digested proteins are loaded into MHC II and expressed on the cell surface. Similarly, exogenous antigens absorbed by DCs can also be degraded in the cytosol and loaded into MHC I and subsequently presented to CD8⁺ T cells via a process called cross-presentation (Murphy et al., 2007). In addition, activated MØs and (especially) DCs change their phenotype, which facilitates their mobilization into the lymphatic system and migration into the LN. It is in this location where DCs present their antigens in the context of MHC II molecules to CD4⁺ Th cells of the adaptive immune system or cross-present MHC I to CD8⁺ T cells (Murphy et al., 2007). In addition to presenting antigens to T cells via their TCR, innate immune cells produce numerous cytokines which influence the adaptive immune response. Production of IL-12 and IFN γ induces a Th1 immune response against viral pathogens or intracellular bacteria. IL-4 production by innate immune cells promotes a Th2 immune response, while IL-6 and tumour growth factor-beta (TGF β) induce a Th17 response (O'Shea and Paul, 2010).

In addition to the TLR family, C-type lectin receptors, NOD-like receptors and RIG-1-like receptors have been recognized to be important PAMP receptors. Detailed description of these receptors are beyond the scope of this thesis.

1.1.2.1 Innate lymphocytes

Lymphocytes, unlike myeloid immune cells, can be divided based on their association with the innate or adaptive immune system. The hallmark feature of adaptive immunity is the generation of receptors of diverse specificities; lymphocytes which do not possess such receptors are generally classified as innate. Recent work suggests that the divide between innate and adaptive immunity is not clear-cut, as immune memory is observed in cells without rearranged receptors such as Natural Killer (NK) cells (Sun et al., 2009), whereas some innate lymphocytes bear invariant receptors that are dependent on gene-rearrangement, such as invariant NKT cells and B1 cells.

NK cells are lymphocytes that have innate cytotoxic functions. Inhibitory NK cell receptors recognize MHC I on target cells. MHC I is expressed on virtually all healthy nucleated cells. NK cells bind MHC I via the killer- immunoglobulin-like-receptor (KIR) family membrane proteins in humans and the Ly49 family receptors in mice. Binding and activation of KIR or Ly49 receptors to MHC I imparts an inhibitory signal to NK cells, countering the signals from activating receptors. An ever expanding number of activating receptors can be found on NK cells, which aid in the detection of infected or transformed cells (Bryceson et al., 2006). Virally infected or transformed cells often express stress-related molecules to notify the immune system. Furthermore, these same cells might also down-regulate MHC I to evade CD8⁺ cytotoxic T cells (CTL), which decreases the inhibitory signalling by KIR or Ly49 receptors on NK cells and in turn increase overall activation

signal. This method of NK cell activation is derived from the “missing self hypothesis” based on the observation that NK cells were able to reject cells that lack self MHC I (Karre et al., 1986). Activated NK cells directly kill target cells by releasing cytotoxic granules or via FAS receptors; NK cells also release interferon-gamma ($\text{IFN}\gamma$) and other cytokines, which activate the immune function of other cells. NK cells are also activated by cytokines released by other immune cells. IL-12 and IL-18 are potent stimuli for NK cell activation and production of $\text{IFN}\gamma$, while IL-2 and IL-15 might be required for priming of cytotoxic function in NK cells (Bryceson et al., 2006).

Other innate lymphocytes include lymphoid-tissue inducing (LTi) cells and cytokine producing innate lymphocytes (ILC). This newly discovered family includes retinoid acid receptor-related orphan receptor gamma t ($\text{ROR}\gamma\text{t}$)-dependent ILCs, which produce IL-17 (ILC17) and IL-22 (ILC22), and $\text{ROR}\alpha$ -dependent T helper-type 2 (Th2) cytokine producing cells called Natural Helper (NH) cells. Cells of this family are primarily found in, or associated with mucosal tissues such as the airway and GI tract. (Covered in greater detail in Chapter 1.2) Unlike most other immune cells, these ILC do not respond directly to pathogens, but instead respond to cytokines produced by damaged or activated tissues and other immune cells. Their primary known function is the regulation of downstream immune responses.

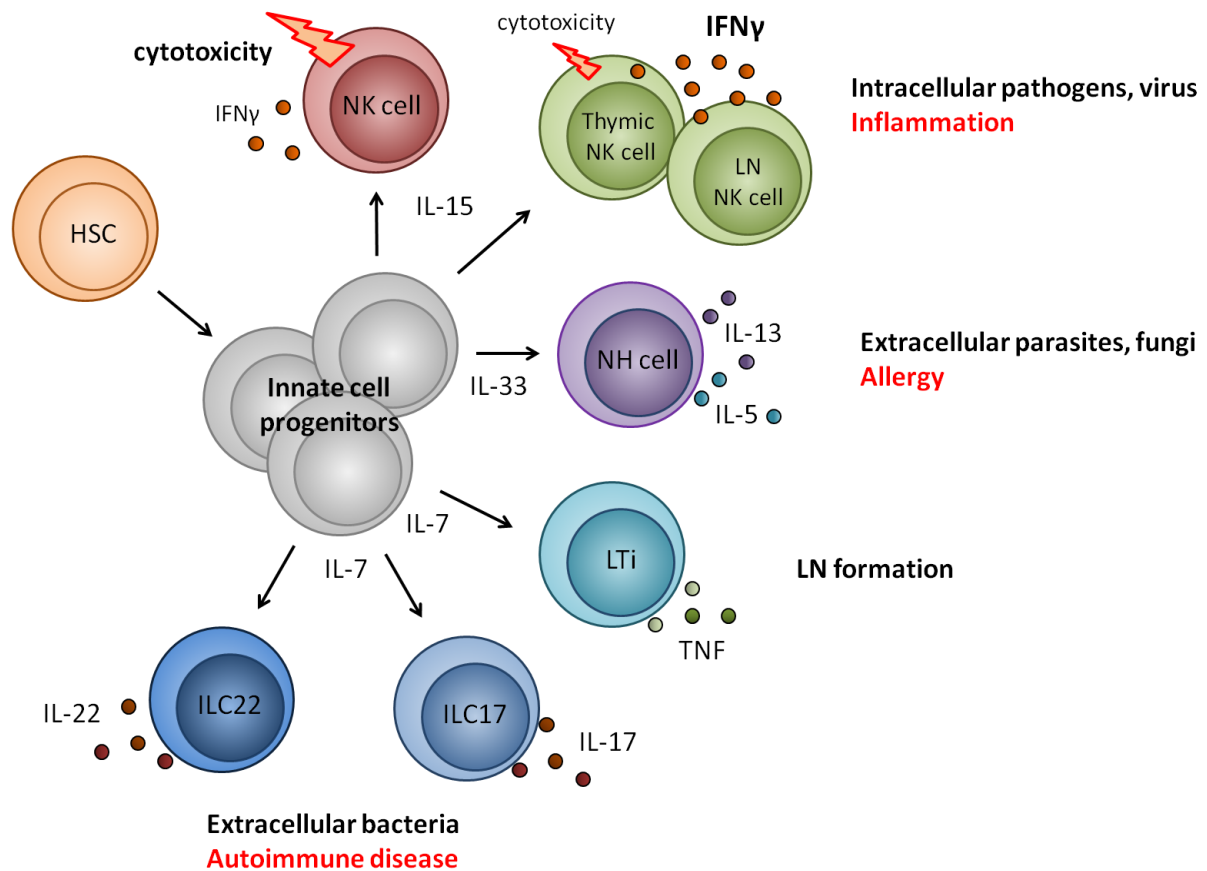


Figure 1: Classes of innate lymphocytes

Recent work has led to the identification of several distinct classes of ILCs, which derive from a haematopoietic stem cell or progenitor in an *Id2*-dependent manner. In mice, their development into mature ILCs is known to depend on several key cytokines, including IL-7, IL-15 and IL-33. ILCs are functionally diverse but, with the exception of NK cells, are primarily cytokine producing cells that influence the downstream immune response. Different classes of ILCs respond to distinct immune challenges (black), and are also implicated in pathology when deregulated (red).

1.1.3 Interaction between the innate and adaptive immune system

It is known that an intricate interplay exists between the innate and adaptive immune system. In addition to antigen presentation by APCs to T cells, there are numerous interactions between different immune and non-immune cells. Such interactions can be mediated by direct cell-cell contact, or through the production of cytokines, chemokines or other biologically active molecules. Recent studies have started to unravel the important role

of ILC in modulating the immune response. IL-22 produced by ILC22 acts directly on epithelial cells in the intestine, and increases the production of anti-microbial peptides (Spits and Cupedo, 2012). ILC22 in turn depend on interactions with DCs, and lymphotoxin-beta receptor (LT β R) and IL-23 receptor signalling. IL-17 produced by ILC17 is thought to play an important role in mediating mucosal inflammation during infection. While IL-22 is believed to play a protective role during infection, IL-17 induces mucosal pathology, and is implicated in Crohn's disease. *Rorct*-dependent ILCs in the intestine interact with the adaptive immune system by promoting IgA class switching (Tsuji et al., 2008). Th2 cytokines produced by NH cells in mucosal tissues initiate acute Th2-type inflammation in response to allergens and helminth infection. Their influence on the adaptive immune response is currently unknown.

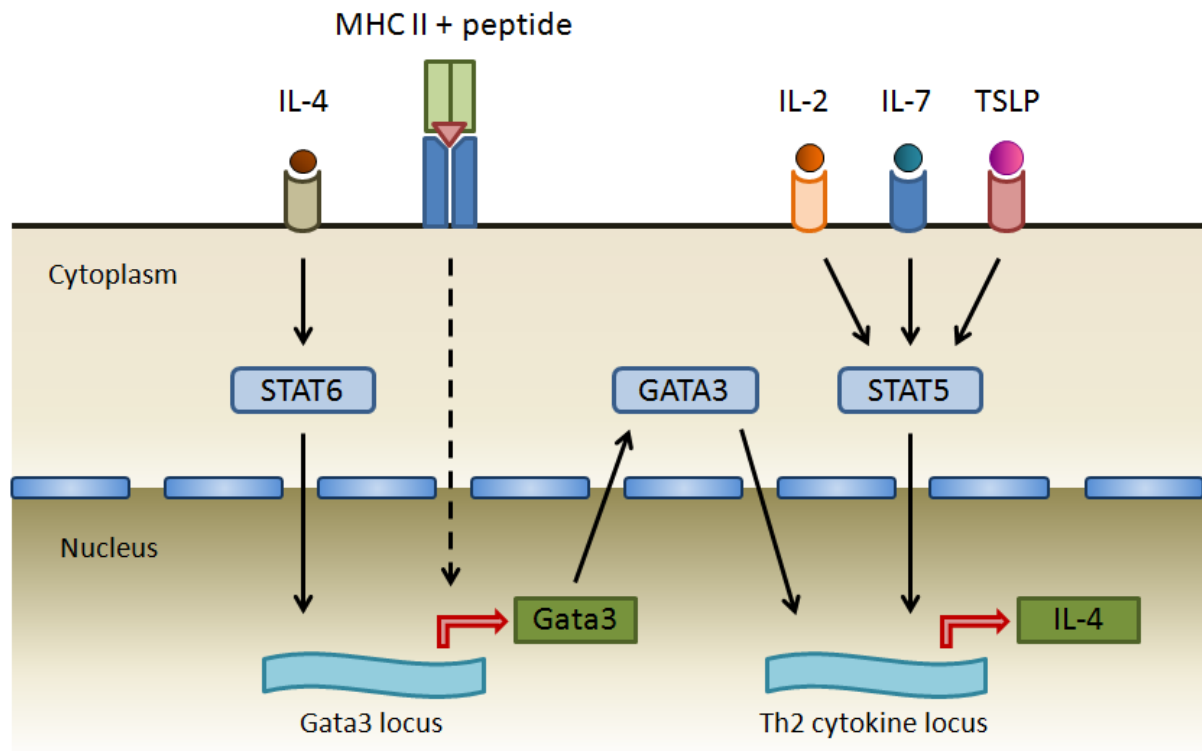


Figure 2: Th2-skewing of CD4⁺ Th0 cells

Th2 skewing of naive CD4⁺ Th0 cells is dependent on TCR signalling and IL-4 dependent STAT6 activation. STAT6 in turn regulates the expression of GATA3, a critical transcription factor for Th2 differentiation in T cells.

CD4⁺ Th2 cells are important in mediating the immune response to extracellular pathogens and allergens. Th2-skewing occurs when naive CD4⁺ Th0 cells are activated by APCs in a Th2-response promoting milieu. Several cytokines act directly on naive Th0 cells to induce Th2 differentiation; IL-4 induces STAT6 signalling, which upregulates GATA-binding protein 3 (GATA3), the main Th2 regulatory transcription factor (Paul and Zhu, 2010). IL-13 has also been reported to induce Th2-skewing in the absence of IL-4 (McKenzie et al., 1998). STAT5 activation via IL-2, IL-7 or thymic stromal lymphopoietin (TSLP) signalling is also required for Th2 cell differentiation (Paul and Zhu, 2010).

1.2 Natural Helper cells

The drive for a Th2-cytokine producing innate cell was initiated by findings of Th2-mediated inflammation in T/B-cell deficient *Rag*^{-/-} mice (Oboki et al., 2010). NH cells were simultaneously discovered by three groups as innate lymphocytes associated with the gut. Although also termed Nuocytes, multipotent progenitor type 2 (MPP type 2), type 2 ILC, or innate helper type 2 (Ih2) cells, it appears that these cells represent more or less the same population, with the exception of MPP type 2, which have progenitor function (Moro et al., 2010; Neill et al., 2010; Price et al., 2010; Saenz et al., 2010b). Nuocytes, MPP-type-2 and Ih2 were discovered in the gut-associated lymphoid tissues using IL-4-eGFP or IL-13-eGFP reporter mice, while gut and lung NH cells were discovered in naïve C57Bl/6 (WT) mice. Although these groups employed different characterization methods, a consolidated review highlights many similarities in cell-surface phenotype and function (Table 1).

tissue	gut						airway		
location	mesenteric	sm int	lar int	MLN	MLN	GALT	various	lung	lung
name	FALC NH [*]	Sm int NH [†]	Lar int NH [†]	MLN NH [†]	Nuocyte [‡]	MPP type 2 [¥]	Ih2 [£]	Lung NH cell [†]	NH cell [@]
background	B6	B6	B6	B6	B6	B6	B6	B6 (BALB/c)	BALB/c
reporter					IL13	IL4	IL4, IL13		
function	IL6, IL5, L13	IL5, IL13	IL5, IL13	IL5, IL13	IL5, IL13	IL5, IL13	?	IL5, IL13	IL5, IL13
stimulation (<i>in vivo</i>)	IL-33	IL-25	IL-25	IL-25	IL-25, IL-33	IL-25	IL-33, IL-25	IL-25	
function	<i>N. Brasiliensis</i>				<i>N. Brasiliensis</i>	<i>N. Brasiliensis</i>	<i>N. Brasiliensis</i>		<i>Influenza</i>
Lineage	CD3, CD4, CD8a, TCRb, TCRd, CD5, CD19, B220, NK1.1, Ter119, Gr-1, CD11b, CD11c FcR1a	CD3, CD19, NK1.1, Gr-1, Ter119, CD11b	CD3, CD19, NK1.1, Gr-1, Ter119, CD11b	CD3, CD19, NK1.1, Gr-1, Ter119, CD11b	CD11b, CD4, CD8, B220, Ter119 (after bead depletion)	CD3, CD8a/b, TCRb, TCRgd, B220, CD19, CD11b, Gr-1, NK1.1, Ter119	CD3, CD4, CD8, SiglecF, CD11b, CD49b, IgE, CD131	CD3, CD19, NK1.1, Gr-1, Ter119, CD11b	CD3, CD19, CD11b, CD11c, CD49b, F4/80, FcR1
eGFP					IL13	IL4	IL4, IL13		
CD127	+	+	+	+	+	+		+	
CD25	+	low/+	+	+				+	+
CD122							low	low	
IL33R (ST2)	+	-	+	+	+			+	+
IL17RB					+				
c-Kit	+	low/-	low/-	low/-	+	+	low	low/-	+
CXCR4								+	
ICOS		+	+	+	+			+	
CCR6		-	-	-				-	
Thy1 (CD90)	+		+			+	+	+	+
Sca-1	+	hi	hi	hi	+	+	-	+	-
CD45	+	+	+	+	+			+	
CD45RA	-	-	-	-	-	-		-	
CD69	+							+	
CD27	+							med	
CD38	+								
CD44	+						+		

Table 1: A consolidated review of NH cells in different tissues and animals.

This table consolidates the phenotypic and functional characteristics of Th2-type cytokine producing innate lymphocytes identified in different mouse tissues. With the exception of MPtype2, all cell types are thought to belong to the same lineage. Minor differences are speculated to be strain or location dependent, or due to applied stimulus such as cytokine administration or infection. White fill indicate not tested. * Moro et al. 2010, [†] Halim et al. 2012, [‡] Neill et al. 2010, [¥] Saenz et al. 2010, [£] Price et al. 2010, [@] Chang et al. 2011.

1.2.1 Characterization of Natural Helper cells

Naïve mouse NH cells are similar in morphology to resting lymphocytes having small round shape (~10-15 µm) and a high nuclear to cytoplasm ratio (Halim et al., 2012a; Moro et al., 2010). Using flow cytometry analysis, mouse NH cells are defined by their lack of cell-surface markers commonly found on known mature leukocyte populations (referred to as lineage-marker negative, or Lin⁻). NH cells in all tissues express the IL-7Rα chain (CD127), IL-2Rα (CD25), inducible T cell stimulatory co-receptor (ICOS), Thy1.2 (CD90.2), Ly-6e and Ly-6a (Sca-1) and CD45. NH cells in most tissues also express low levels of steel factor receptor c-Kit (CD117), activation marker CD69 and the IL1RL1 (T1/ST2) chain of the IL-33 receptor complex. Low levels of the IL-15 receptor, or low affinity IL-2 receptor beta (CD122) were also detected on lung NH cells.

1.2.2 Activation of Natural Helper cells

The activation of NH cells in all locations depends on stroma derived IL-33, but the requirement for co-stimulation differs based on the anatomical location. In the gut, NH cells from MLN are readily activated by IL-33 and IL7, whereas fat-associated lymphoid cluster (FALC) NH cells respond to only IL-33, but require IL-2 or IL-7 co-stimulation for more efficient *in vitro* function (Moro et al., 2010; Neill et al., 2010; Saenz et al., 2010b). Lung NH cells also require IL-33 in addition to co-stimulation from IL-7, IL-2, or TSLP (Halim et al., 2012a). IL-25 also activates NH cells by direct or indirect means. IL-33, TSLP, and IL-25 are stroma-derived cytokines, produced by cells in response to cell damage or detection of PAMPs or other pathogen derived signals. IL-33 is an IL-1-like cytokine, found localized in the nuclei of endothelial, epithelial, and brain tissues during homeostasis (Pichery et al., 2012). IL-33 likely functions as an alarmin, and is released upon cell-damage. TSLP is

produced by epithelial cells, and signals through the IL-7R α and TSLP-receptor. IL-25 is produced by Th2 cells, basophils, and airway epithelial cells after allergen exposure or viral infection (Kool et al., 2012).

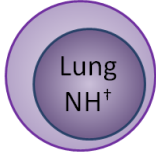
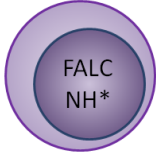
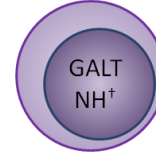
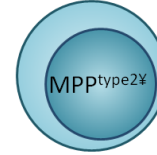
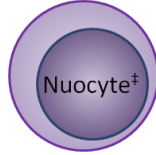
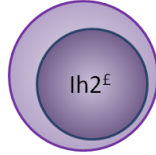
							
		Lung	FALC	GALT		MLN	
In vivo	IL25	+		+	+	+	+
	IL33		+			+	+
In vitro	IL25			+			
	IL33	+	+		+	+	
	TSLP	+			+		
	IL2		+	+			
	IL7			+		+	
Produced	IL4	-	-				
	IL5	+	+	+		+	+
	IL6	-	low			+	
	IL9	-					
	IL10					low	
	IL13	+	+	+		+	
	IL17A	low					

Figure 3: Natural Helper cell activation

Natural Helper cells identified by different groups in the lung, fat associated lymphocytes (FALC) in the mesentery, gut associated lymphoid tissue (GALT) and mesenteric lymph nodes (MLN) were tested for *in vivo* response to IL-25 or IL-33 (green), or *in vitro* response to cytokines (blue). Cytokines produced *in vitro* were tested (red). Empty cells indicate non-tested conditions in all fields; plus-sign indicates tested condition (green), requirement for stimulation (blue), or cytokine produced (red); negative-sign indicates none-produced; low indicates lower levels of cytokines produced (qualitative). *Moro et al. 2010, [†] Halim et al. 2012, [‡] Neill et al. 2010, [¥] Saenz et al. 2010, [£] Price et al. 2010.

1.2.3 Function of Natural Helper cells

The main role of Th2-responses is removal of extracellular pathogens such as fungi and parasites such as helminths. The latter currently infects over 1 billion people worldwide, primarily in under-developed countries (Ziegelbauer et al., 2012). The cardinal Th2-type cytokines IL-4 and IL-13 are instrumental in driving the development of CD4⁺ Th2 cells, which aid in the production of Th2-cytokines and IgE class switching of B cells. IL-5 and IL-9 attract and activate eosinophils and mast-cells respectively. Mast-cells in turn detect Ag-specific IgE coated parasites via their cell surface FcεR1 causing a release of histamine, while eosinophils degranulate and release cytotoxic-cationic peptides and cytokines such as IL-4. IL-13 also induces goblet cell hyperplasia and mucus hyperproduction at mucosal surfaces, resulting in the expulsion of parasites. T cells were originally postulated to be the principal source of Th2-type cytokines until the discovery of NH cells. New data demonstrated that NH cells are a critical innate source of Th2-type cytokines for helminth infection (Moro et al., 2010; Neill et al., 2010; Saenz et al., 2010a), and are sufficient in the expulsion of *Nippostrongylus brasiliensis* in T/B-cell deficient animals (Price et al., 2010). Additionally, FALC NH cells can induce B1 cell activation in the peritoneum and play a role in airway hyper-reactivity and tissue repair in the lungs following influenza virus infection (Chang et al., 2011; Mjosberg et al., 2011; Monticelli et al., 2011; Moro et al., 2010). In the developed world, Th2-type inflammation is more often involved with allergic reactions in the gut and lung, such as inflammatory bowel disease, oesophagitis and asthma. Asthma in particular is commonly caused by aberrant Th2-type inflammation in response to allergens or infection.

1.2.4 Allergic inflammation and asthma

Asthma affects over 300 million people worldwide, with an increasing prevalence in the Western world (Kim et al., 2010). While asthma is a chronic condition typified by tissue remodelling in the lung and airway hyper-reactivity, the primary cause of morbidity and mortality are acute asthma attacks due to inflammation. Triggers for inflammation are diverse and include exercise, viral infection, and exposure to allergens. Th2-type inflammation is most commonly associated with allergic asthma, which also constitutes the major asthma subtype (Kim et al., 2010). Th2-type inflammation is mediated largely by IL-4, IL-5, IL-9 and IL-13 cytokines and IgE production (Figure 4). Although Th2-type cytokines were historically thought to derive from Th2 cells, we now know that multiple myeloid and innate lymphoid cells, as well as new CD4⁺ T cell classes, constitute important cellular sources of these cytokines (Lloyd and Hessel, 2010).

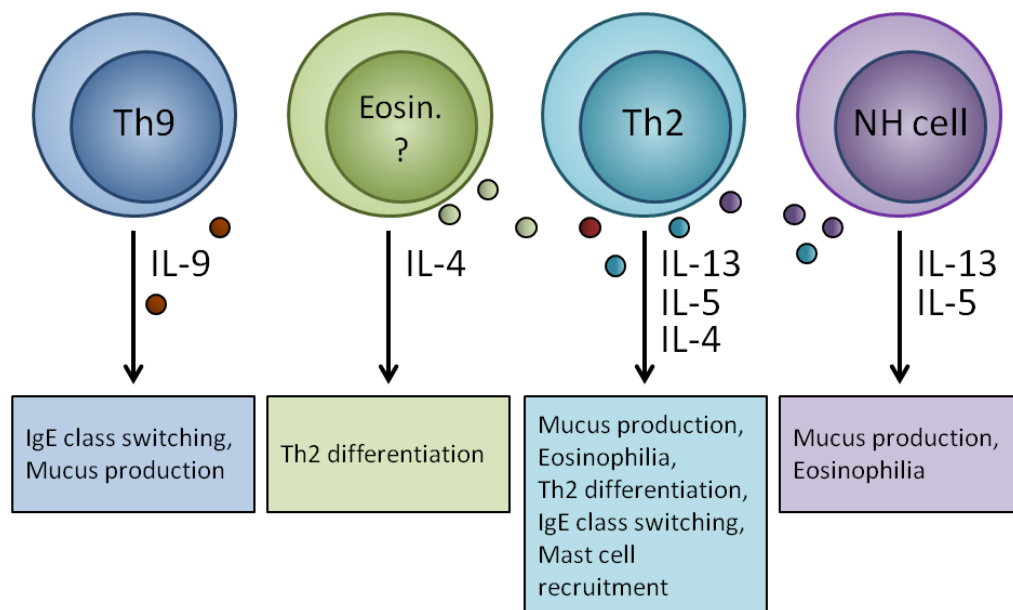


Figure 4: Th2-mediated lung inflammation

Th2 cytokines are produced in the lungs by various types of immune cells, including Th2, Th9 cells, NH cells and eosinophils. IL-4 promotes Th2-differentiation in Th0 cells, IL-5 recruits and causes maturation of eosinophils, IL-9 promotes IgE class switching of activated B cells and IL-13 causes Th2-differentiation and mucus production.

1.3 Development of Natural Helper cells

Since the discovery of NH cells, efforts have been made to delineate the pathway of their development from hematopoietic stem cells or precursors. Initial analysis of mutant mice provided hints that led to the generation of several conclusions. Firstly, NH cells are present in T/B/NKT-cell deficient *Rag*-knockout or Nod/Scid mice but absent in lymphodeficient *Rag*^{-/-}*Il2ry*^{-/-} or Nod/Scid/*Il2ry*^{-/-} mice, thus suggesting that NH cells are common cytokine receptor γ chain (γ -chain) dependent (Halim et al., 2012a; Moro et al., 2010). Secondly, NH cells are reduced in *Il7*^{-/-} mice, suggesting that NH cells are likely lymphocytes dependent on IL-7 for maturation or survival (Moro et al., 2010). Additionally, normal NH cell numbers found in athymic nude mice tells us that NH cell development occurs independently of the thymus.

1.3.1 Lymphopoiesis

All blood cells derive from haematopoietic stem cells (HSC) located in the BM of adult mice and humans. HSC have the ability to self-renew and differentiate into all types of mature blood cells via a process of lineage commitment. During this process, HSC lose self-renewal capacity and become increasingly lineage-committed by differentiating into multipotent progenitors, which in turn give rise to lineage-restricted immature cells. Early during this process, cells become primed and then restricted to either the myeloid or lymphoid lineage (Figure 5). By FACS, populations of cells can be purified based on cell-surface marker expression, which may then be analyzed for HSC or progenitor function using *in vitro* culture methods or *in vivo* adoptive transplantation. HSC were identified in WT mice by their cell-surface expression of Lin⁻Sca-1⁺c-Kit^{hi}Flt3⁻ (A more recent definition of HSC is based on the expression of SLAM family cell surface markers: CD150⁺CD48⁻

CD244⁻) (Kiel et al., 2005; Zhao et al., 2000). HSC differentiate into common myeloid progenitors (Lin⁻Sca-1⁻c-Kit⁺CD34⁺CD16/32⁺), which are primed to become myeloid cells, whereas Lin⁻Sca-1⁺c-Kit^{hi}Flt3⁺ lymphoid primed multipotent progenitors (LMPP) represent a population of cells that is primed for lymphocyte development but still retain some myeloid potential. Common lymphoid progenitors (CLP), classically defined as Lin⁻Sca-1^{lo}c-Kit^{low}CD127⁺ are downstream of LMPPs, and have efficient B and NK cell potential. T cells, unlike B and most NK cells are generated in the thymus from a BM derived thymus-seeding progenitor (Kondo et al., 1997). The identity of this progenitor is currently not clear, although expression of CCR9 and CCR7, critical for thymic homing, are present on subsets of both LMPP and CLPs in the bone-marrow (Chi et al., 2009). The BM microenvironment and cytokine signalling are critical in directing haematopoiesis by influencing genetic and epigenetic changes in HSC and progenitor cells. Master regulators such as Pax-5, Notch1 and Id2 are expressed early during lymphoid development and drive precursors towards a B, T or ILC fate respectively. Knockout or reporter mice for these, and other genes, highlight their importance in specific stages of development. *Pax5*^{-/-} mice cannot develop B-cells past the pro-B cell stage, while other lymphoid lineages are unaffected (Urbanek et al., 1994). Likewise, *Id2*^{-/-} mice have severely reduced numbers of ILCs due to an inability to sequester E proteins that skew progenitors towards a T or B cell fate (Rankin and Belz, 2011). As discussed in Section 1.3 we know that knockout mice also highlight the importance of cytokines for development and survival of leukocytes.

One caveat underlying most research in this field is that FACS purified progenitors often show great plasticity *in vitro*, an artificial feature that is perhaps not representative of its eventual fate *in vivo*. Even *in vivo* adoptive transplant of progenitors creates a situation

where the original microenvironment is disturbed, and the eventual fate of progenitors after entry into the host bloodstream might be artificially skewed.

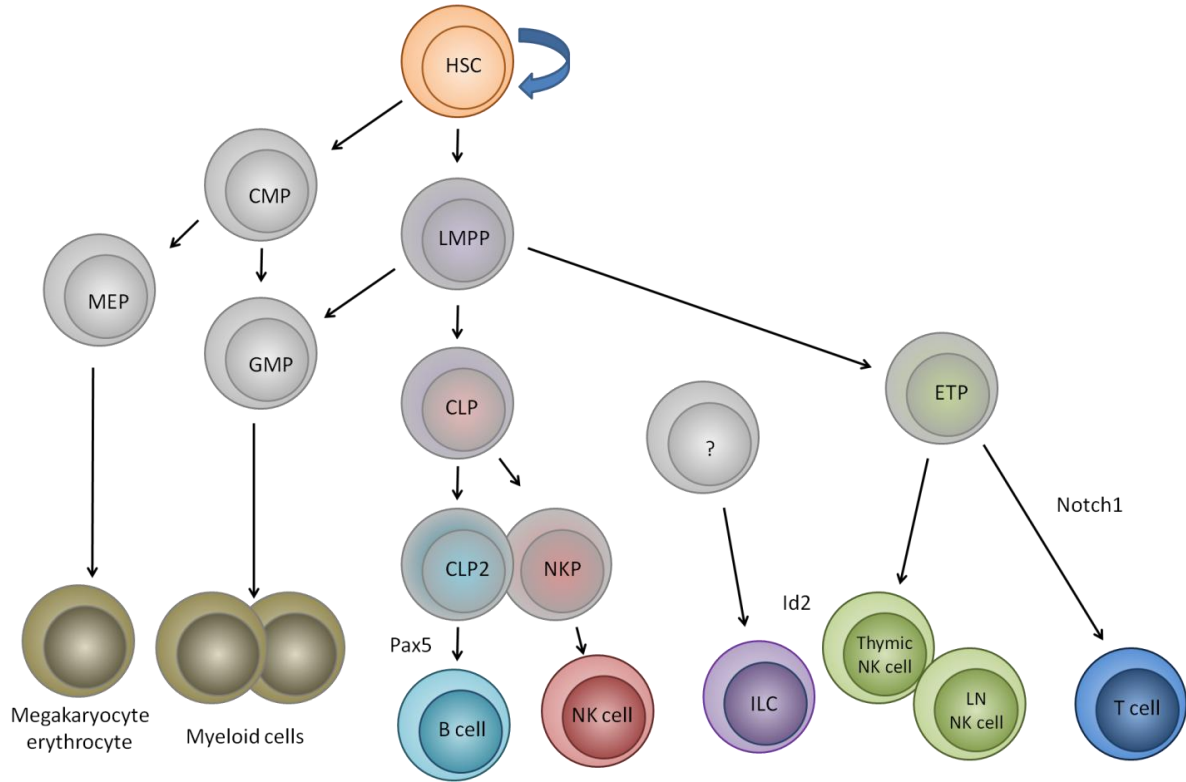


Figure 5: Haematopoiesis

Haematopoiesis occurs in mice from a self-renewing haematopoietic stem cell (HSC) which gives rise to the myeloid lineage through differentiation into a common myeloid progenitor (CMP) followed by myeloid-erythroid progenitors (MEP) or granulocyte-monocyte progenitors (GMP) which in turn give rise to their respective lineages. Lymphocytes develop from a multipotent lymphoid-primed multipotent progenitor (LMPP), which retains some myeloid potential. T cells and some NK cells subsets are believed to arise from an early thymus seeding progenitor (ETP), directly derived from LMPPs. B cells and BM derived NK cells are thought to develop from the common lymphoid progenitor (CLP), which gives rise to NK cell progenitors (NKP) or B cell progenitors (CLP2). The development of other ILCs (LTi, ILC17, ILC22 and NH cells) is not well defined.

1.3.2 Innate lymphocyte development

Unlike T and B cells, the development of innate lymphocytes is currently not well characterized, with the exception of NK cells. This is likely due to their discovery well before ILC17, ILC22, LT_i and NH cells. CLPs, by definition, are assumed by many to be the precursor for all lymphoid lineages, both adaptive and innate. Indeed, CLPs retain *in vitro* potential for most lymphocyte lineages. However, recent work shows that CLPs, although plastic in their lineage potential, may not give rise to all lymphocyte lineages under physiological conditions *in vivo* (Halim et al., 2012b). Furthermore, the phenotype of CLPs has evolved since its discovery, and remains a topic of debate. Indeed, recent findings of committed NK cell progenitors within the most current definition of CLPs shows that this population is heterogeneous (Fathman et al., 2011).

Additionally, many innate lymphocytes depend on the expression of *Id2* for their development. NH cells show high levels of *Id2* expression, and NH cells are absent in *Id2*-knockout mice (Moro et al., 2010). Some *Id2*-dependent innate lymphocytes, including LT_i, ILC17 and ILC22 are known to require *Rorct* for their development. *Rorct*-knockout mice do not have lymph nodes or functional ILC17 and ILC22, but do have normal numbers of functional NH cells. Furthermore, *Rorct* expression in NH cells is low or negative. However, another ROR-family member, *Rora*, is highly expressed in NH cells, and *Rora*-knockout mice have greatly reduced numbers of NH cells (Figure 6) (Wong et al., 2012).

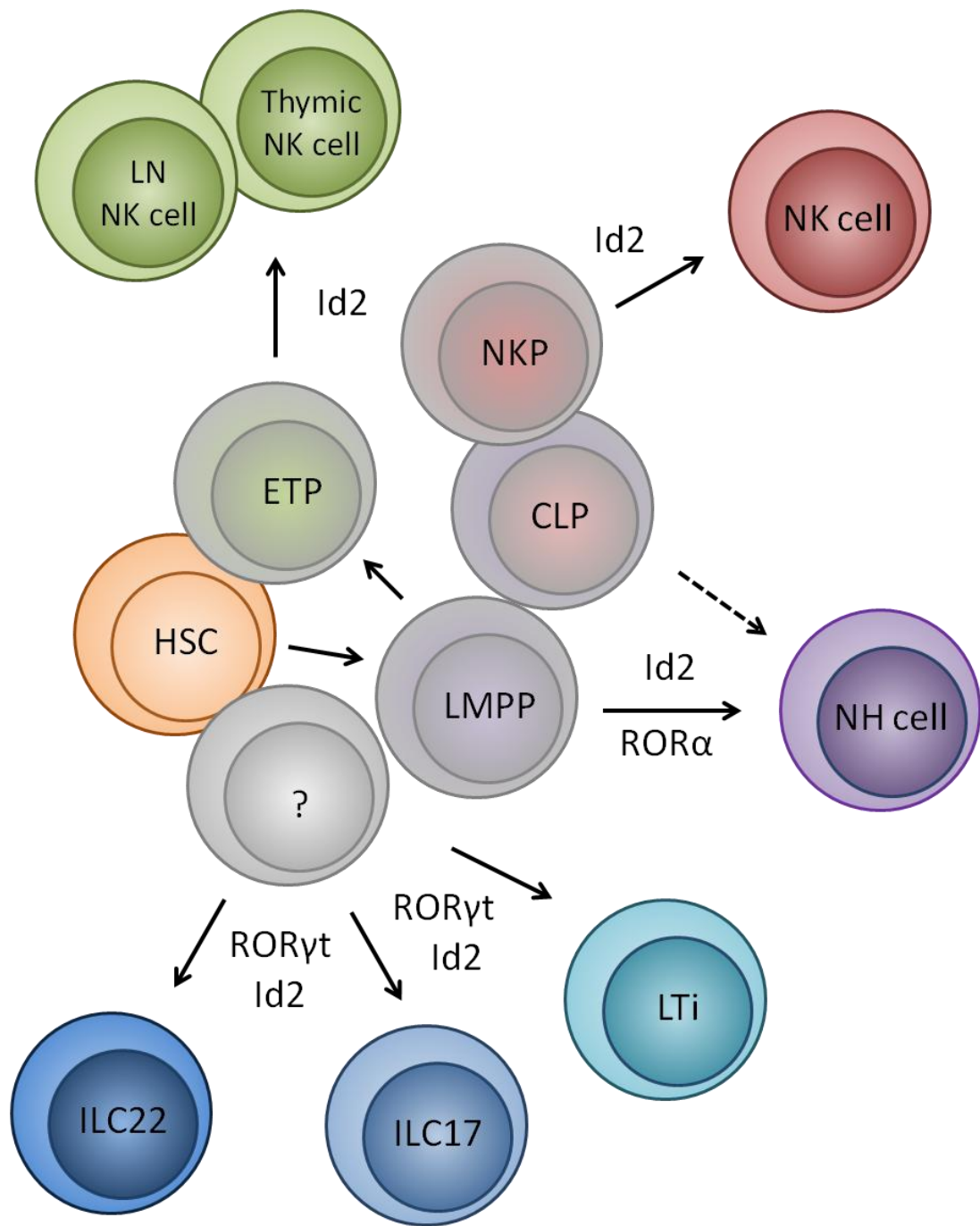


Figure 6: Innate lymphocyte development

All ILCs are *Id2*-dependent, and can be further divided into other lineages. NK cells develop either in the LN or thymus from ETP-like cells, or in the BM from a CLP derived NKP. *Rorct*-dependent ILC, including LTi, ILC17 and ILC22 develop from an unknown progenitor. *Rora* is critical for NH cell development from LMPP or CLP.

1.3.3 ROR α and ROR γ t

The ROR family of proteins constitutes a group of steroid-hormone nuclear receptors that are involved in regulating transcription which in mice and humans includes: ROR α , ROR β and ROR γ (Jetten, 2009). ROR family proteins are involved in the regulation of various physiological functions, and are expressed in a tissue-specific manner. To date ROR α and ROR γ have been implicated in the regulation or development of the immune system. In mice *Rorc* generates two isoforms via alternative promoter usage, namely ROR γ 1 and ROR γ 2 (also known as ROR γ t) . While ROR γ 1 is expressed in various tissues, ROR γ t is expressed only in a small number of cells of the immune system, where it plays an important role in the development of ILC22, ILC17 and LTi (Cupedo et al., 2009; Eberl et al., 2004). Both ROR γ and ROR γ t-deficient mice lack LN's and Peyer's patches due to the absence of LTi. Furthermore, ROR γ t also plays an important role in thymopoiesis and the development of Th17 cells (Guo et al., 2002; Ivanov et al., 2006).

ROR α , like ROR γ t, is a ligand-dependent nuclear hormone receptor (Giguere et al., 1994). Its expression is upregulated in several organs, including the brain, liver, testes, lung and skin (Becker-Andre et al., 1993). In the brain, ROR α plays a critical role in Purkinje cell development and astrocyte regulation (Journiac et al., 2009; Matsui et al., 1995). *Staggerer* *Rora*^{sg/sg} mice have severe neurological and immunological defects due to a deletion mutation (Matsui et al., 1995; Trenkner and Hoffmann, 1986). The *Rora* gene in mice is located on chromosome 9, and encodes for a protein that consists of several domains which compose a DNA-binding region containing two zinc-finger motifs, hinge domain and C-terminal ligand-binding-domain. Alternative splicing gives rise to four isoforms (ROR α 1-4) which are differentially expressed based on the tissue, and due to variations in N-terminal

domain, have specific DNA-binding site preferences (Giguere et al., 1994). The ligand for ROR α is currently undefined, but suspected to be cholesterol or a cholesterol derivative.

1.4 Thesis objectives

The overall objective of this thesis was to characterize lung NH cells, their role in acute Th2-type lung inflammation and establish the role of *Rora* in NH cell development. In continuation of my previous work on the development of NK cells in the LN of mice from a novel progenitor (Veinotte et al., 2008), I started looking at NK cell development in the lung. I found lung NK cell progenitors in the lungs of naïve WT mice, characterized by a Lin⁻ NK1.1⁻CD122⁺B220^{+/-} phenotype with *in vitro* and *in vivo* NK cell potential (unpublished). Further analysis of Lin⁻ lung leukocyte populations for putative NK cell progenitors led to the discovery of a Lin⁻Sca-1⁺c-Kit^{low/-} fraction, which closely resembled FALC NH cells. Exploratory experiments uncovered their potential to produce Th2-cytokines when stimulated with PMA and ionomycin (P/I). This and reports of T/B-cell independent inflammation in the lungs of *Rag1*^{-/-} mice led me to hypothesize that lung Lin⁻Sca-1⁺c-Kit^{low/-} cells are innate Th2-cytokine producing lung NH cells. Furthermore, I hypothesized that these putative lung NH cells are involved in acute Th2-type lung inflammation. Subsequent characterization of lung NH cells led to the discovery of *Rora* as a highly enriched gene transcript. As *Rora*-deficient mice have a reported defect in Th2-cytokine production and attenuated Th2-type lung inflammation in response to OVA challenge, I made the hypothesis that *Rora* is required in NH cell function or development.

Chapter 2 Lung Natural Helper cells are a critical source of Th2 cell-type cytokines in protease allergen-induced airway inflammation

2.1 Introduction

Asthma is a chronic inflammatory disease of the lower airways characterized by recurrent airway obstruction and wheezing. It is induced by allergen such as pollen, moulds and dust mites as well as air-borne irritants and infections. Asthma is a heterogeneous disease, and includes allergic, non-allergic and intrinsic forms, of which allergic asthma is the most common form (Kim et al., 2010). Allergic asthma is thought to be driven by T helper 2 (Th2) cytokines including IL-4, IL-5 and IL-13. IL-4 promotes the production of IgE by B cells and the expression of vascular cell adhesion molecule-1 (VCAM-1) on endothelial cells (Steinke and Borish, 2001). IL-5 induces eosinophil development, recruitment to the lung and activation (Hamelmann and Gelfand, 2001). Activated eosinophils produce a broad range of cytokines and chemokines and are a potent source of the lipid mediator leukotriene C4 and platelet activating factor, which induce mucus secretion and smooth muscle contraction. IL-13 is thought to mediate the effector phase of asthma by inducing airway remodelling and hyper-responsiveness as well as mucus hyper-production (Wills-Karp, 2004). Whereas basophils, mast cells and eosinophils, which can produce some Th2 cytokines are found in the lungs of asthma patients (Voehringer et al., 2006), Th2 cells are generally thought to be the critical source of those cytokines (Cohn et al., 2004).

A version of Chapter 2 has been published: Halim, T.Y.F., Krauß, R.H., Sun, A.C., and Takei F. (2012) Lung Natural Helper cells are a critical source of Th2 cytokines in protease allergen-induced airway inflammation. *Immunity* 36(3):451-463, with permission from Elsevier.

In most mouse models of induced asthma, T cells are first sensitized by allergens such as ovalbumin (OVA) to induce a Th2-polarized response; sensitized mice are then challenged by intranasal administration of the same allergen, resulting in cytokine production by Th2 cells recruited to the lung and eosinophilic inflammation (Kim et al., 2010). While these mouse models have clearly indicated the importance of Th2 cells in lung inflammation, recent studies have revealed that innate cells also play a significant role in asthma. Lung epithelial cells can produce multiple cytokines in response to stress, including IL-25, IL-33 and thymic stromal lymphopoietin (TSLP), which induce Th2 cytokine production and eosinophilic lung inflammation. Intranasal administration of IL-25 reproduces many asthma symptoms (Hurst et al., 2002), and OVA-induced allergic airway inflammation is inhibited by anti-IL-25 antibody (Ballantyne et al., 2007). It is thought that IL-25 stimulates natural killer (NK) T cells, which express the IL-25 receptor (IL-17RB) (Terashima et al., 2008). IL-33 acts on mast cells and basophils (Schmitz et al., 2005; Schneider et al., 2009). Activated basophils produce IL-4 and TSLP, which promote Th2 responses. Anti-IL-33 antibody inhibits eosinophilic lung inflammation, indicating the importance of IL-33. TSLP activates dendritic cells (DC) and enhances the Th2 response (Ziegler and Artis, 2010). These epithelial cell-derived cytokines are thought to promote Th2 cell responses and induce lung inflammation. However, intranasal administration of IL-25 or IL-33 induces lung eosinophilia in recombinaase activating gene (RAG)-deficient mice, which lack all T and B cells, indicating that an innate cell population is capable of inducing lung inflammation (Hurst et al., 2002; Kondo et al., 2008).

Recently, novel innate lymphocytes termed multipotent progenitor type 2 (MMP^{type2}), Natural Helper cells and Nuocytes have been discovered in the gut-associated mucosa tissues (Moro et al., 2010; Neill et al., 2010; Saenz et al., 2010b). Phenotypically, these cells do not

express mature hematopoietic lineage markers (Lin⁻), and produce Th2 cytokines when stimulated by IL-25 or IL-33. They have been implicated in immune responses in the gut against helminth infections and allergens. Similar Lin⁻ cells that produce IL-4 and IL-13 have also been found in other tissues, including the liver, spleen and lung using IL-4 reporter and IL-13 reporter mice (Price et al., 2010). The detection of these cells in the lung is dependent on the expression of fluorescent reporter proteins, which are induced by IL-25 stimulation. The discovery of Th2 cytokine-producing innate lymphocytes has led to speculation that they may play a role in lung eosinophilic inflammation and asthma (Kaiko and Foster, 2011; Kim et al., 2010; Lloyd and Hessel, 2010). However, IL-4/eGFP⁺ cells are at the threshold of detectable in naive mouse lung, and even after stimulation with IL-25 or *N. brasiliensis* infection, very few have been detected. Recently, Chang et al. reported the presence of Lin⁻ ST2⁺Sca-1⁺c-kit⁺ cells in virus infected BALB/c mouse lung, and indicated their importance in viral induced airway inflammation and macrophage infiltration (Chang et al., 2011). Unlike mesenteric Natural Helper cells, Lin⁻ST2⁺Sca-1⁺c-kit⁺ cells do not induce eosinophil infiltration. Furthermore, their cytokine production capacity is strikingly lower than those of Nuocytes/mesenteric Natural Helper cells. Thus, Th2 cytokine-producing innate lymphocytes in the lung have not been characterized beyond their initial detection, and their functional significance remains speculative. Here, we have characterized in detail innate lymphocytes in normal mouse lungs that rapidly produce multiple Th2 cytokines, and studied their regulation in the lung environment. We show that these innate lymphocytes play a critical role in T cell-independent lung eosinophilia and mucus hyper-secretion induced by protease allergen.

2.2 Materials and methods

2.2.1 Mice

C57BL/6 (WT), NOD/SCID and NOD/SCID/*Il2rg*^{-/-} mice were maintained in the BCCRC pathogen free animal facility. B6.*Rag1*^{-/-} mice were purchased from The Jackson Laboratories. B6.*Rag2*^{-/-}/*Il2rg*^{-/-} mice were purchased from Taconic Farms. Mice were used at 4-8 weeks of age. All animal use was approved by the animal care committee of the University of British Columbia, and animals were maintained and euthanized under humane conditions in accordance with the guidelines of the Canadian Council on Animal Care.

2.2.2 Antibodies, reagents, FACS sorting and analysis

Phycoerythrin (PE)-conjugated anti-CD4, CD11c, CD90, CD122, CD127, FITC-conjugated anti-CD3 ϵ , CD19, NK1.1, Mac-1, Gr-1, Ter119, MHCII, CD45.2, Allophycocyanin (APC)-conjugated anti-CD117, IL5, CD25, Alexa 647-conjugated anti-CCR3, PerCP-cy5.5 conjugated anti-CD25, NK1.1, CD3, B220, and PE.cy7-conjugated Sca-1 were purchased from BD Biosciences, PE-conjugated anti-NKp46, ICOS, IL-5, IL-13 was purchased from eBioscience. FITC-conjugated anti-T1/ST2 was purchased from MD Bioproducts. Propidium Iodide (PI), eFluor® 780 (eBioscience) or DAPI reagents were used to exclude non-viable cells. IL-2, 7, 25, 33, SCF and TSLP were purchased from eBioscience, IL-4 was purchased from STEMCELL Technologies, PMA and Ionomycin were purchased from Sigma Aldrich. Polyclonal goat anti-mouse IL-33 IgG was purchased from R&D Systems. BD Caliber (Cytex 6 color upgrade) and Canto II were used for phenotypic analysis; BD FACS Aria II was used for cell sorting and phenotypic analysis. Flowjo v. 8.6 was used for data analysis.

2.2.3 Primary leukocyte preparation

Cell suspensions were prepared from lung, spleen, LN, blood or BM tissue as described (Veinotte et al., 2008).

2.2.4 Isolation of lung NH cells

Lung cells were incubated with 2.4G2 to block Fc receptors and then stained with FITC-conjugated lineage marker mAbs (CD3, CD19, NK1.1, Mac-1, GR-1, and Ter119), PE-CD127, PE.cy7-Sca-1, PerCP-cy5.5-CD25, and APC-CD117 and purified by FACS.

2.2.5 Cytokine production assay

FACS purified B6 or *Rag1*^{-/-} mouse lung NH cells were cultured in 200 µl RPMI-1640 media containing 10% FBS, penicillin and streptomycin (P/S), 50 mM 2-mercaptoethanol (2ME) at 37°C. Cells were stimulated with IL-25 (10 ng/ml), PMA (30 ng/ml) and ionomycin (500 ng/ml), IL-2 (1000 U/ml), IL-7 (10 ng/ml), TSLP (10 ng/ml), IL-33 (10 ng/ml).

2.2.6 Lung explant culture

Mice were sacrificed by CO₂ asphyxiation. Lungs were instilled via 18G catheter with 1.5 ml 1% low melting point agar in RPMI-1640 + 10% FCS, 2-Me, P/S at 37°C and cooled on ice. Lungs were sliced by razor into ~0.5 mm thick sections placed in 2 ml RPMI-1640, 10% FCS, 2ME, P/S, and stimulated with IL-25 (10 ng/ml), PMA (30 ng/ml) and ionomycin (500 ng/ml), papain (10 µg/ml), IL-2 (1000 U/ml) IL-7 (10 ng/ml), PBS or blocked with anti-IL-33 (2 µg/ml). Lung explants from one animal were divided into 6 separate cultures; total cell number per culture was counted to allow normalization of ELISA data. For intracellular cytokine staining GolgiPlug™ (BD Biosciences) was added to the lung explant cultures 6 h before collection, and lung explants were passed through a 70 µm filter to make single cell suspension.

2.2.7 Intracellular staining

Intracellular staining for IL-17A, IL-5 and IL-13 was performed using the Cytofix/Cytoperm™ Plus kit (BD Biosciences) according to the manufacturer's protocol. Dead cells were stained with eFluor® 780 (eBioscience) fixable viability dye before fixation/permeabilization and were gated out during analysis.

2.2.8 ELISA assay

IFN γ , IL-5, IL-6, IL-12, IL-13, IL-17A, IL-25, IL-33, TSLP (eBioscience) and IL-4 (R&D Systems), IL-3 (BD Biosciences) ELISAs were performed according to the manufacturer's protocol.

2.2.9 RNA isolation and microarray

Total RNA was isolated from FACS purified un-stimulated cells or cells stimulated for 12 h with PMA plus ionomycin by Trizol (Invitrogen). RNA was quantified and checked for quality by Nanodrop. Agilent Bioanalyzer 2100, RNA amplification, and microarray services were performed by McGill University and Génome Québec Innovation Centre using the Affymetrix Mouse Gene 1.0 arrays. All data analysis was performed with FlexArray 1.5 (Genome Quebec). Microarray data sets for other cells were obtained from data assembled by the ImmGen consortium (Heng et al., 2008).

2.2.10 *In vivo* papain stimulation, lung NH cell depletion and adoptive transplant

For lung NH cell depletion, mice were twice injected intra-peritoneally every 24 h with 200 μ g of anti-CD25 produced from PC61 5.3 hybridoma two days before papain stimulation. For lung NH cell adoptive transplant, lung NH cells were purified from WT mice by FACS and expanded in IL-25 and IL-33 (10 ng/ml) for 5 d. Expanded lung NH cells or PBS control were injected by tail vein on d 0. Mice were anaesthetized by isofluorane inhalation, followed by intranasal injection of papain or heat-inactivated papain (10 μ g) in 40

µl of PBS on d 0-2. Blood was collected from the tail vein on d 1 and 2 and cardiac puncture on d 3. Mice were sacrificed on d 3 and lungs and BAL (1 ml PBS) were collected or airways were instilled with 50:50 Tissue-Tek® O.C.T. Compound/PBS (Adwin Scientific) and fixed in formalin. Lung tissue was processed as described previously; lung and BAL cells were then counted and identified by flow cytometry (van Rijt et al., 2004). Fixed lungs were embedded in paraffin and processed for H&E or PAS staining by the Centre for Translational and Applied Genomics (Vancouver, Canada). Eosinophils were quantified in 20× fields of view of H&E stained lung sections (Axioplan 2 Imaging, Carl Zeiss), captured by camera (Retiga EX, QImaging). Using the digital image (Openlab 5.5.1, PerkinElmer) to define field boundaries, eosinophils were then positively identified at 63× using immersion oil. Total eosinophil number in ten 20× fields of view was calculated per mouse lung (5 fields of view per section, 2 sections taken at different depths, separated by 500 µm).

2.2.11 Statistics

Data were analyzed using GraphPad Prism 5 (GraphPad Software). A Student's t test was used to determine statistical significance between groups, with $p \leq 0.05$ being considered significant. The statistical analysis of microarray results was carried out using FlexArray (Genome Quebec).

2.3 Results

2.3.1 Identification of lung Natural Helper cells in normal mice

Flow cytometric analysis of normal B6 mouse lung leukocytes revealed the presence of cells that did not express leukocyte lineage specific cell surface markers (Lin: CD3 ϵ , CD19, CD11b, Gr-1, NK1.1 and Ter119) (Figure 7A). The Lin⁻ leukocyte population contained a sub-population which co-expressed stem cell antigen-1 (Sca-1) and stem cell factor (SCF) receptor CD117 (c-Kit). These Lin⁻Sca-1⁺c-Kit⁺ cells were further divided into two subsets based on co-expression of IL-2R α (CD25) and IL-7R α (CD127) (Figure 7A). The CD25⁺CD127⁺ and CD25⁻CD127⁻ subsets made up ~0.35% and ~0.55% of lung leukocytes (approximately 1.5×10^4 cells and 2.5×10^4 cells) respectively, in each 4-8 week old naive B6 mouse lung (Figure 7B). Back-gating analysis of the lung Lin⁻Sca-1⁺c-Kit⁺CD25⁺CD127⁺ cells indicated that they formed a distinct population, although a small fraction is c-Kit^{low} (Appendix 1A). When the two subsets of Lin⁻Sca-1⁺c-Kit⁺ cells were purified and stimulated by a combination of phorbol 12-myristate 13-acetate (PMA) and ionomycin, the CD25⁺CD127⁺ subset produced large amounts of IL-3, IL-5 and IL-13 and more moderate amounts of IL-17A and low amounts of IL-4 and IFN γ . In contrast, the CD25⁻CD127⁻ subset did not produce any detectable level of the tested cytokines in response to PMA plus ionomycin (Figure 7C). Purified Lin⁻Sca-1⁺c-Kit^{low}CD25⁺CD127⁺ cells were also capable of producing Th2 cytokines when stimulated with PMA plus ionomycin (Appendix 1B). Thus, the phenotype and the function of lung Lin⁻Sca-1⁺c-Kit^{+/low}CD25⁺CD127⁺ cells are similar to those of Nuocytes, innate type 2 helper cells, Natural Helper cells and MPP^{type2} cells in the gut (Saenz et al., 2010a). We termed lung Lin⁻Sca-1⁺c-Kit^{+/low}CD25⁺CD127⁺ cells lung NH cells.

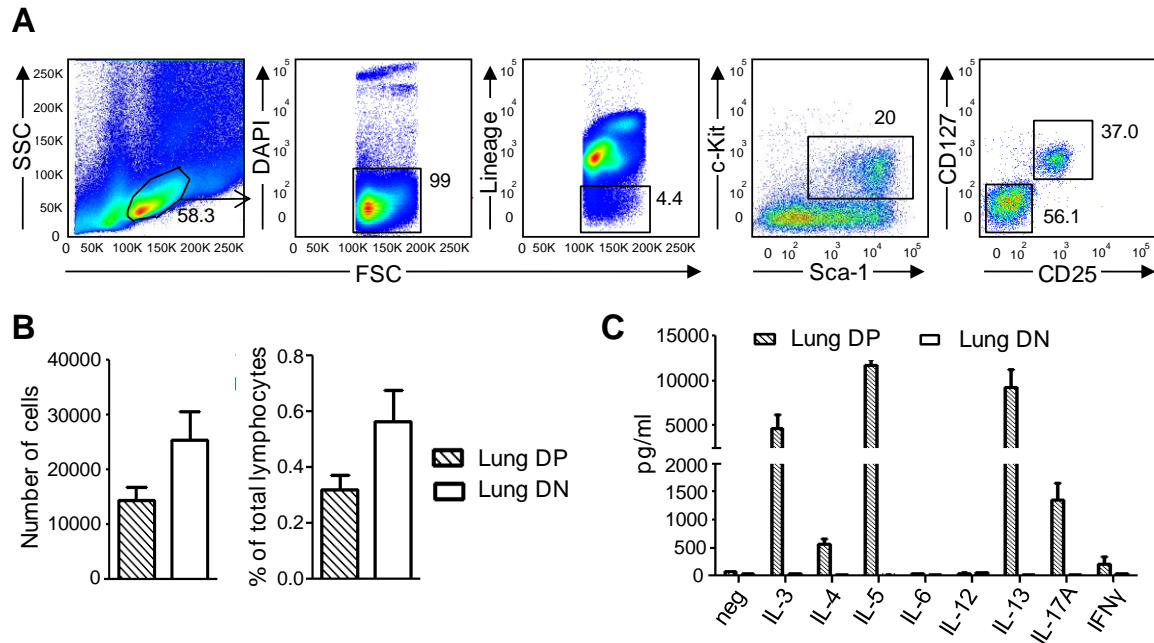


Figure 7 Lung contains Lin⁻Sca-1⁺c-Kit^{+/-low}CD127⁺CD25⁺ cytokine secreting cells.

(A) Gating strategy for identifying lung NH (Lin⁻Sca-1⁺c-Kit^{+/-low}CD127⁺CD25⁺) cells in naïve B6 mouse lungs by flow cytometer is illustrated. The numbers in the plots indicate the percentages of cells in the indicated gates.

(B) Total numbers per whole naïve B6 mouse lung and the percentages of Lin⁻Sca-1⁺c-Kit⁺CD127⁺CD25⁺ (DP) or Lin⁻Sca-1⁺c-Kit⁺CD127⁻CD25⁻ (DN) cells among lung lymphocytes are shown.

(C) FACS purified lung DP and lung DN cells (3.5×10^3 cells in 200 μ l media per well) were stimulated with PMA plus ionomycin (P/I) for 3 days, and cytokines in culture supernatants were measured by ELISA. Un-stimulated negative control (neg) for IL-3 is also shown.

Data are representative of three independent experiments (mean and SEM in B, C) (See also Appendix 1)

2.3.2 Characterization of lung NH cells

Further FACS analysis showed that lung NH (Lin⁻Sca-1⁺c-Kit^{+/-low}CD25⁺CD127⁺) cells were negative for CD4, CD11c, NKp46, CD34 and CD122 (not shown), while they expressed the pan-leukocyte marker CD45, CD90.2 (Thy1.2), the IL-33 receptor chain T1/ST2 and the T cell co-stimulatory molecule ICOS (Figure 8A), thus excluding CD4⁺ lymphoid-tissue inducing (LTi) cells, CD11c⁺ dendritic cells (DC), NKp46⁺ NK cells,

CD34⁺ mast cells and immature hematopoietic progenitors. Lung NH cells were similar in morphology to resting lymphocytes, having a small, round shape with a high nuclear to cytoplasm ratio (Figure 8B). Analysis of other primary and secondary immune organs showed that Lin⁻Sca-1⁺c-Kit^{+/low}CD25⁺CD127⁺ cells were barely detectable in the bone marrow, lymph node, spleen and blood (Figure 8C). Furthermore, no Lin⁻Sca-1⁺c-Kit^{+/low}CD25⁺CD127⁺ cells were detected in mediastinal lymph nodes in naïve B6 mice (data not shown), indicating that lung NH cells are resident lung lymphocytes. Lung NH cells were present in *Rag1*^{-/-} and non-obese diabetic/severe combined immunodeficient (NOD/SCID) mice, which are deficient for T and B cells, but they are absent in *Rag2*^{-/-}*Il2rg*^{-/-} (RGC) and NOD/SCID/*Il2rg*^{-/-} (NSG) mice (Figure 8D). The percentage of lung NH cells in wild-type (WT) and *Rag1*^{-/-} mice were similar (Appendix 2A). Furthermore, CD25⁺ was almost exclusively expressed on lung NH cells in *Rag1*^{-/-} mice (Appendix 2B). Therefore, lung NH cells in *Rag1*^{-/-} mice could be identified by CD25 staining alone. Purified lung NH cells from *Rag1*^{-/-} mice were functionally competent, secreted Th2 cytokines when stimulated *in vitro* (Appendix 2C), and produced similar amounts of cytokines as WT lung NH cells (Appendix 2D). Although the phenotype of lung NH cells was similar to that of early hematopoietic progenitors and gut MPP^{type2} cells, lung NH cells did not form myeloid cell colonies *in vitro* and did not differentiate into T, B or NK cells in the lymphoid differentiation cultures on OP9/OP9-DL1 stroma (Appendix 3). Culture of lung NH cells on OP9 stroma with IL-2 or IL-7 supported survival and maintenance of cell-surface phenotype, but not expansion, and transplanted lung NH cells also failed to engraft or differentiate into T/B/NK-cells in NSG recipient mice (data not shown).

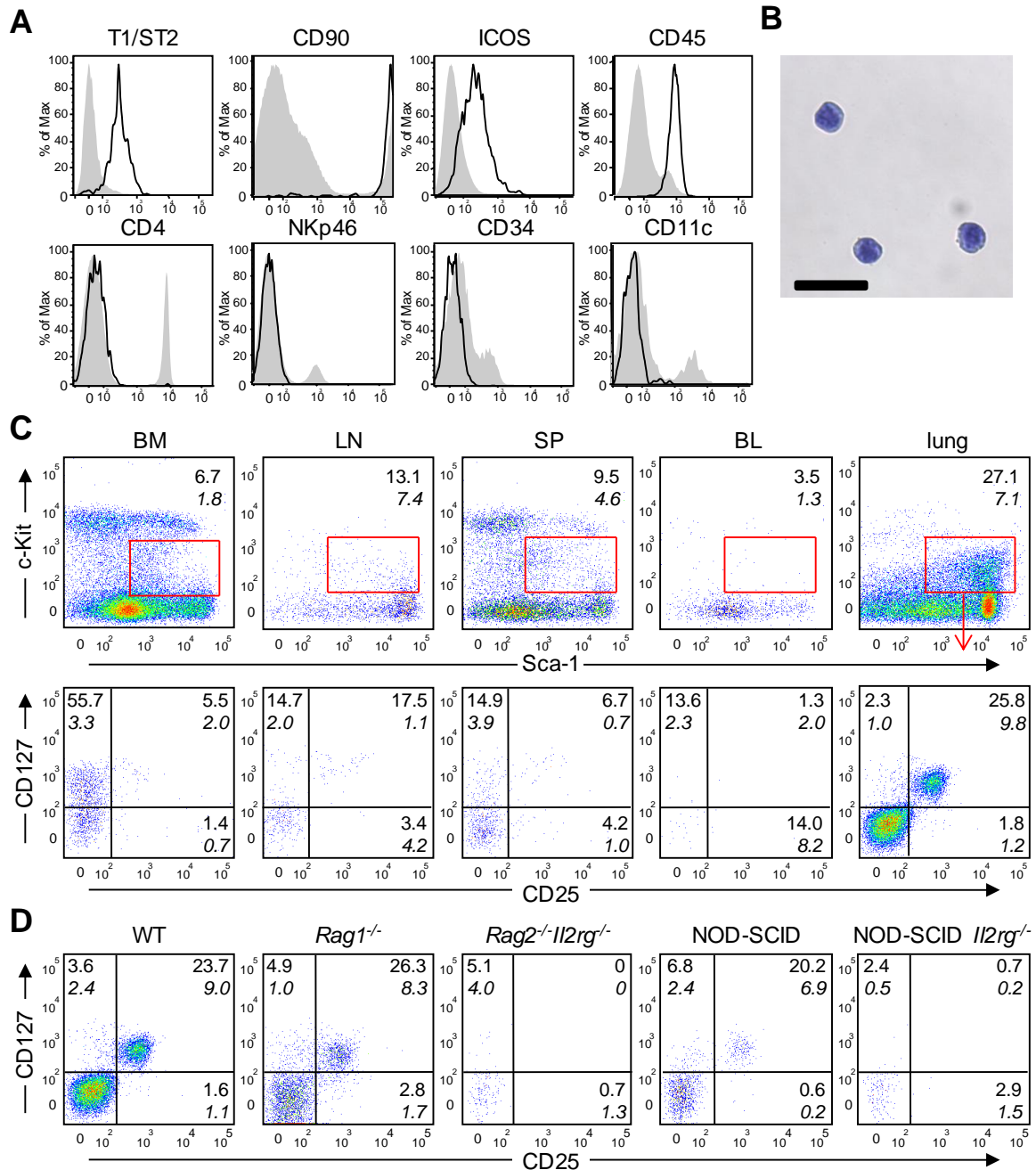


Figure 8 Characterization of lung NH cells.

(A) Surface expression of indicated molecules on lung $\text{Lin}^- \text{Sca-1}^+ \text{c-Kit}^{+/low} \text{CD127}^+ \text{CD25}^+$ cells (black line histograms) and control cells (shaded grey histograms) was analyzed by FACS. For CD45 and CD34 staining, BM cells were used as control. For all others, spleen cells were used as control.

(B) The morphology of FACS purified lung NH cells were examined by Diff-Quick® staining. Scale bar represents 25 μm .

(C) Bone marrow (BM), lymph node (LN), spleen (SP), blood (BL) and lung cells were analyzed by flow cytometry for lung NH cells. Live (DAPI⁻) lymphocytes (FSC/SSC) were first gated, and Lin⁻ cells were then gated for the analysis of c-Kit and Sca-1 expression. Lin⁻ Sca-1⁺c-Kit⁺ cells were gated as indicated by red boxes (top row) and further analyzed for CD25 and CD127 expression (bottom row). The numbers in the plots indicate the mean percentages (upper) and SEM (lower in *italic*) of cells in the gates and quadrants, calculated from 3 independent analyses.

(D) Lin⁻Sca-1⁺c-Kit^{+/low} cells in B6 (WT) and indicated mouse strains (n=4) were analyzed for the expression of CD25 and CD127.

Data are representative of at least 3 independent experiments. Numbers in FACS plot are mean (top) and SEM (below in *italics*). (See also **Appendix 2**)

2.3.3 Gene expression profile of lung NH cells

To further characterize lung NH cells, the global gene expression patterns of purified lung NH cells before and after stimulation with PMA plus ionomycin were analyzed by Affymetrix microarray. The gene expression profile of resting lung NH cells differed from those of lung macrophages, lung DCs, CD4 T cells, NK cells, $\gamma\delta$ T and regulatory T cells (Figure 9A). Lung NH cells expressed high levels of *Gata3*, *Cd69*, *Il2ra* and *Rora*, and low levels of *Notch1* and *Rorc* transcripts. As expected from the flow cytometer analysis, lung NH cells expressed high levels of the c-kit (*kit*), CD127 (*Il7r*), CD25 (*Il2ra*) transcripts. They also expressed the genes encoding the receptors for IL-2 (*Il2ra* and *Il2rg*), IL-4 (*Il4ra*), IL-25 (*Il17rb*) and IL-33 (*Il1rl1*). However, the *Il1rap* gene encoding the other chain of the IL-33 receptor was not highly expressed in lung NH cells. Stimulation of lung NH cells with PMA plus ionomycin induced upregulation of IL-3 (*Il3*), IL-4 (*Il4*), IL17A (*Il17a*) and IL-17F (*Il17f*) transcripts (Figure 9B). Interestingly, unstimulated lung NH cells expressed the IL-5 gene (*Il5*), and it was only slightly upregulated by the stimulation with PMA plus ionomycin, while the IL-33R (*Il1rl1*) and IL-25R (*Il17rb*) transcripts were down-regulated by the stimulation.

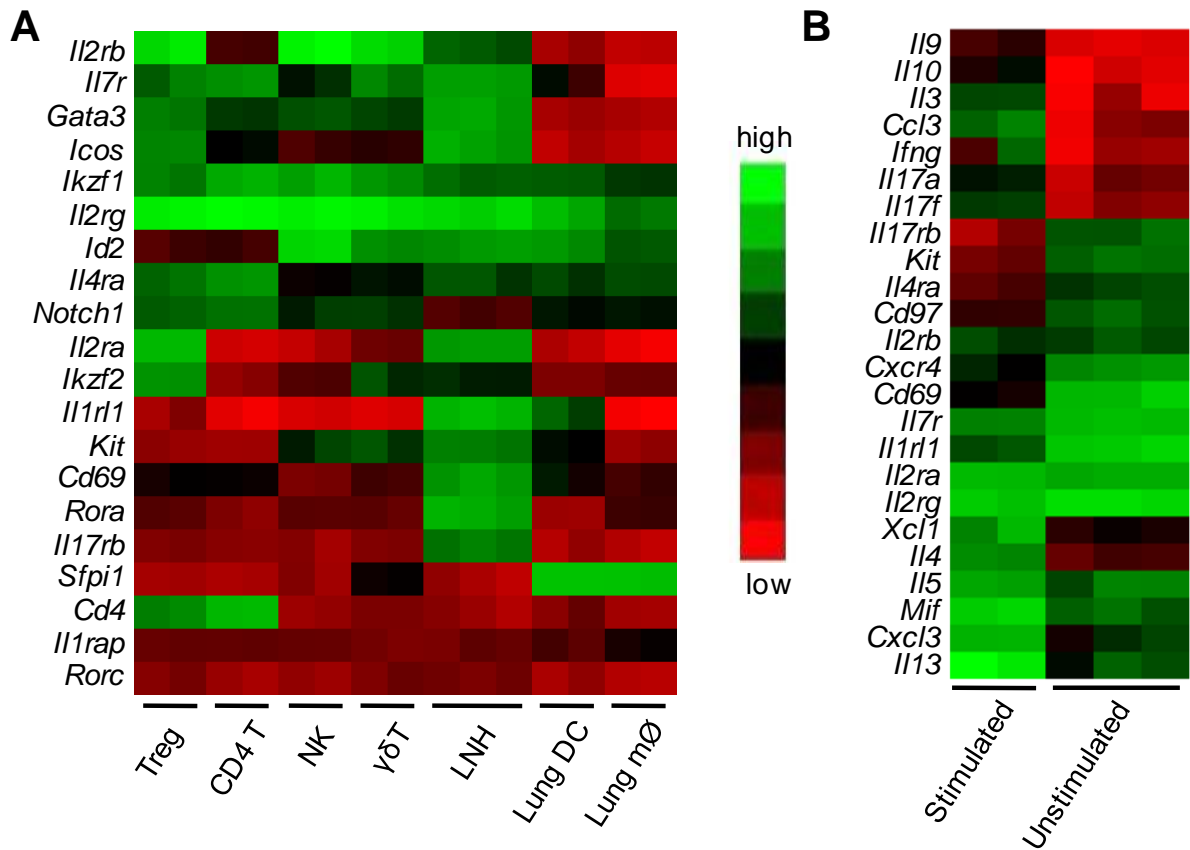


Figure 9 Gene expression analyses of lung NH cells.

(A) FACS purified lung NH cells were analyzed for gene expression by Affymetrix microarray. The expression of the indicated genes in lung NH cells (triplicate experiment) were compared to available microarray results (duplicates) of other known leukocyte lineages.

(B) FACS purified lung NH cells were stimulated with PMA plus ionomycin for 12 h and analyzed for gene expression by microarray. The expression levels of the indicated genes in stimulated lung NH cells (duplicates) were compared to those of non-stimulated samples (triplicates).

2.3.4 Cytokine-mediated stimulation of lung NH cells

Lung NH cells were purified and cultured in the presence of various combinations of cytokines, including IL-2, IL-3, IL-4, IL-7, IL-15, IL-25, IL-33, TSLP, stem cell factor (SCF) and Fms-like tyrosine kinase ligand (Flt3L). The flow cytometer and microarray analyses mentioned above showed that lung NH cells expressed the receptors for IL-2, IL-4,

IL7 and IL-25, while IL-33 has been reported to be important in stimulating other innate helper cells. Unlike gut Natural Helper cells, which readily respond to IL-2, IL-7 and IL-33 alone (Moro et al., 2010), purified lung NH cells only produced low levels of Th2 cytokines in response to IL-33 alone (Figure 10A). While IL-33 is required, co-stimulation with other cytokines was critical in the activation of purified lung NH cells. Combinations of IL-33 and IL-2, IL-7 or TSLP resulted in very large amounts of IL-5 (>0.4 pg/cell) and IL-13 (~1.5 pg/cell) production. IL-25 failed to activate lung NH cells by itself or with IL-33 but enhanced IL-13 production by lung NH cells stimulated with IL-33 plus IL-7. IL-7 had a dampening effect on IL-33 plus TSLP stimulation. None of the cytokine combinations induced IL-3, IL-4 or IL-17A production from purified lung NH cells (data not shown).

As the activation of lung NH cells might require factors derived from the lung microenvironment, we employed lung explant cultures, which mimic the physiological state of the lung *in vivo* (Henjakovic et al., 2008). Freshly isolated lungs were cut into slices of approximately 0.5 mm thickness, cultured *in vitro* with cytokines, and the amounts of IL-17A, IL-5 and IL-13 secreted into the media were measured. IL-25 alone or IL-2 plus IL-7 readily induced IL-5 and IL-13 (Figure 10B) secretion by the lung explants prepared from WT and *Rag1*^{-/-} mice, which have lung NH cells but no B/T/NKT cells. In contrast, *Rag2*^{-/-} *Il2rg*^{-/-} mouse lung explants, which have no lung NH cells or other lymphocytes, did not secrete significant amount of IL-13 or IL-5 upon stimulation with cytokine or PMA plus ionomycin (Appendix 4A and B). The production of IL-5 was rapid, and substantial amounts of IL-5 were secreted even in un-stimulated cultures, although IL-25 and IL-2/7 significantly increased the amount of IL-5 production. This was consistent with the microarray analysis above, which showed high baseline expression of the IL-5 transcript in lung NH cells (Figure 9A). IL-33 did not enhance IL-5 or IL-13 production above the PBS control. None of the

tested conditions except PMA and ionomycin resulted in secreted IL-17A from lung NH cells in explant cultures (data not shown). Intracellular cytokine staining of lung explants confirmed that CD25⁺ cells in *RagI*^{-/-} mice were the main producers of IL-5 (Figure 10C). As lung NH cells were the only CD25⁺ cells in the lungs of *RagI*^{-/-} mice, these results show that IL-25 or IL-2 plus IL-7 stimulate lung NH cells and induce the production of IL-5 and IL-13 in lung explants cultures. Co-staining for intracellular IL-17A and IL-5 in *RagI*^{-/-} mouse explants stimulated with PMA plus ionomycin showed that some lung NH produced both IL-5 and IL-17A while other lung NH cells produced either cytokine, but not both (Figure 10D).

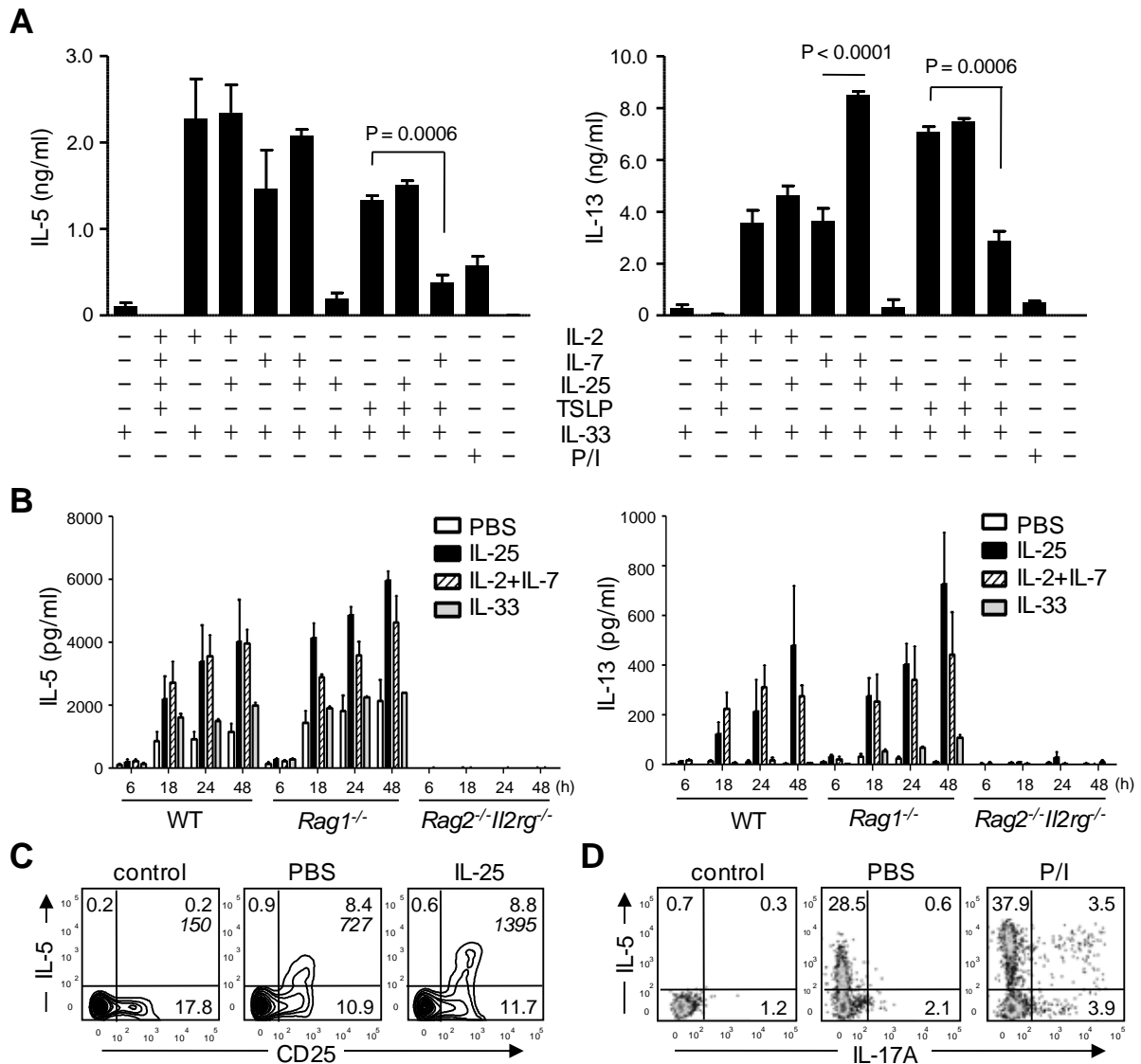


Figure 10 lung NH cells rapidly produce Th2 cytokines in response to IL-33 plus co-stimulation.

(A) Purified lung NH cells (1.0×10^3 cells in 200 μ l media per well) were stimulated with cytokines, or PMA plus ionomycin (P/I) as indicated for 3 days, followed by ELISA analysis for IL-5 and IL-13 in culture supernatants.

(B) Lung explants from indicated mouse strains were stimulated with cytokines or PBS. The amounts of IL-5 (left) and IL-13 (right) in the culture supernatants were assayed by ELISA at the times indicated on the x-axis.

(C) *Rag1*^{-/-} lung explants were stimulated with IL-25 or PBS for 6 h, followed by analysis for intracellular IL-5 production. Cells were first electronically gated to exclude blood cells, debris (FSC/SSC), dead cells and NK cells (NK1.1). Fluorescence minus one (FMO) staining was used as control. The numbers indicate the percentages of cells in the quadrant (top) with mean fluorescence intensity of IL-5 positive cells (italicized below).

(D) *Rag1*^{-/-} mouse lung explants were stimulated with P/I or PBS for 12 h. Explants were processed and surface-stained as in C and CD25⁺ lung NH cells were analyzed for intracellular IL-5 and IL-17A by flow cytometry. Fluorescence minus intracellular stain was used for control. The numbers in the plots show the percentage of cell in each quadrant.

Data are representative of at least 3 independent experiments (mean and SEM in A and B). (See also Appendix 4)

2.3.5 Lung NH cells are responsible for papain-induced eosinophilia and mucus secretion in RAG1-deficient mice

Papain is a protease known to cause occupational asthma (Novey et al., 1979). It also causes asthma-like symptoms in RAG-deficient mice (Oboki et al., 2010). Therefore, we tested whether lung NH cells are involved in papain-induced lung inflammation. Intranasal administration of papain (Appendix 5A) into WT and *Rag1*^{-/-} mice, which have lung NH cells, and *Rag2*^{-/-}*Il2rg*^{-/-} mice, which have no lung NH cells, showed striking differences among those mice. Eosinophil counts in bronchioalveolar lavage (BAL) were significantly elevated in papain stimulated WT and *Rag1*^{-/-} mice, compared to *Rag2*^{-/-}*Il2rg*^{-/-} mice (Figure 11A). Tissue infiltrating eosinophils were also increased in papain stimulated WT and *Rag1*^{-/-} mice, but not *Rag2*^{-/-}*Il2rg*^{-/-} mice (Figure 11B). Histological analysis of lung sections mirrored our flow cytometry findings, showing eosinophilia only in lungs of WT and *Rag1*^{-/-} mice treated with papain (Appendix 5B). Furthermore, BAL levels of IL-5 and IL-13 were significantly increased in papain treated WT and *Rag1*^{-/-} mice, but not *Rag2*^{-/-}*Il2rg*^{-/-} mice (Figure 11C). Periodic acid-Schiff (PAS) staining for mucus in papain treated lungs also showed mucus production from airway goblet cells in WT and *Rag1*^{-/-} mouse lungs, whereas *Rag2*^{-/-}*Il2rg*^{-/-} mouse lungs showed no mucus production (Figure 11D). Similar results were obtained with NOD/SCID and NSG mice, which was mirrored by increased serum concentration of IL-5 in WT and NOD/SCID, but not NSG mice (Appendix 5C).

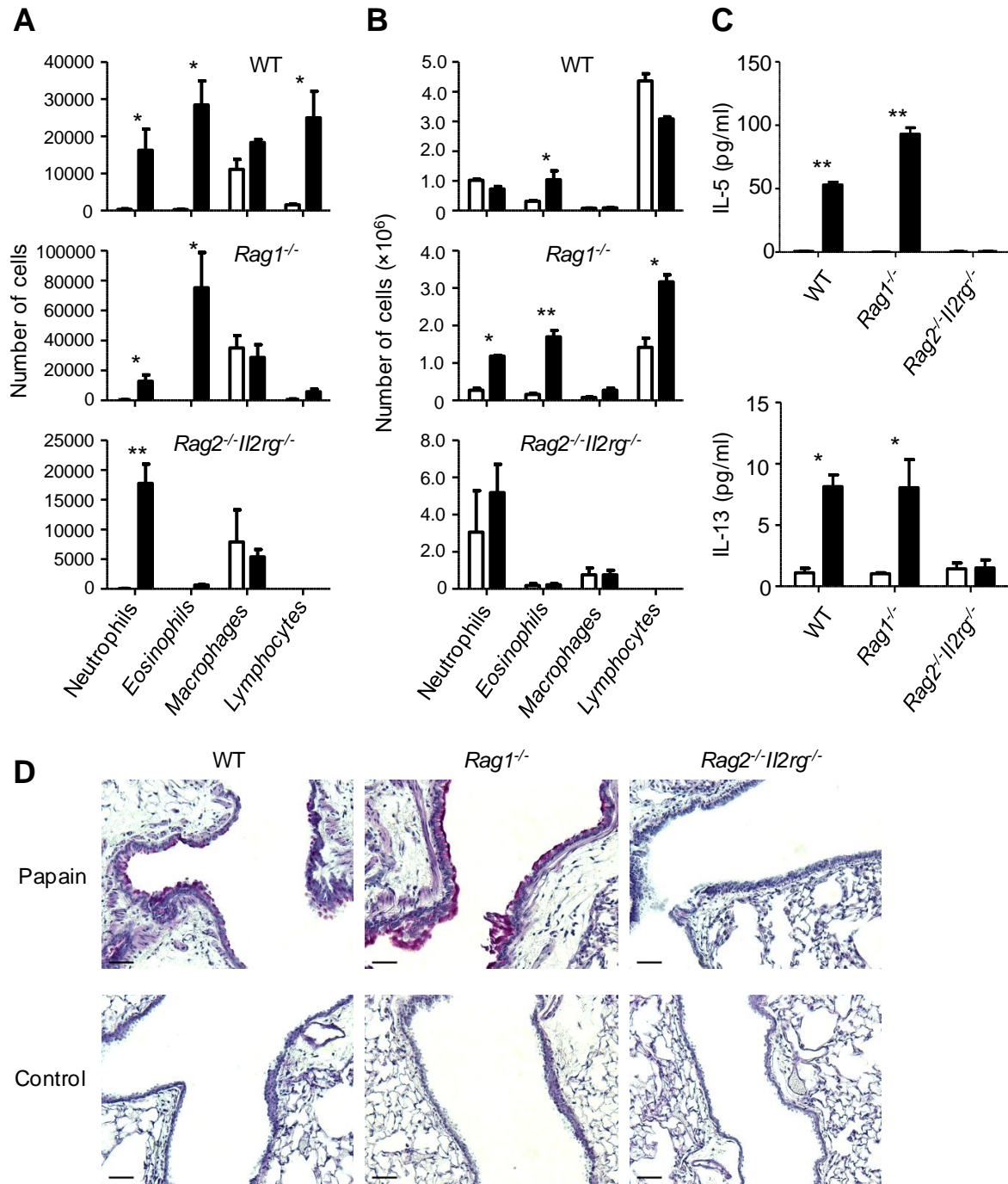


Figure 11 lung NH cells are required for T cell independent eosinophil infiltration and mucus secretion in papain induced lung inflammation.

(A) Bronchioalveolar lavage (BAL) cells from mice treated with heat-inactivated papain (white) or papain (black) were identified by flow cytometry and quantified.

(B) Leukocytes from whole lung tissue from mice treated with heat-inactivated papain (white) or papain (black) were analyzed by flow cytometry and quantified.

(C) BAL fluid from heat-inactivated papain (white) or papain (black) treated mice was analyzed for IL-5 (top panel) and IL-13 (bottom panel) concentration by ELISA.

(D) Mucus secretion from heat-inactivated papain (control) or papain treated mice was analyzed by PAS staining of formalin fixed paraffin embedded lung sections. Scale bar represents 50 μ m.

* $p < 0.05$ ** $p < 0.001$ (two-tailed Student's t-test). Data are representative of 3 independent experiments (mean and SEM in A, B and C). (See also Appendix 5)

To further investigate the role of lung NH cells in T cell independent lung inflammation, we depleted lung NH cells from *Rag1*^{-/-} mice by anti-CD25 antibody injection (Appendix 6A). lung NH cells identified by CD127 and CD25 (stained by different mAb) expression were barely detectable in the treated mice (Figure 12A). lung NH cell depleted mice showed a significant decrease in allergen-induced eosinophilia (Figure 12B). Histological analysis also showed that lung NH cell depletion significantly inhibited lung eosinophilia in papain-treated *Rag1*^{-/-} mice (Figure 12C). PAS staining showed decreased mucus production in lung NH cell depleted *Rag1*^{-/-} mouse lungs (Figure 12D). In addition to depletion, we also transplanted lung NH cells into *Rag2*^{-/-}*Il2rg*^{-/-} mice, followed by papain stimulation (Appendix 6B). Transplanted lung NH cells were detectable in *Rag2*^{-/-}*Il2rg*^{-/-} mouse lungs (Figure 12E), and promoted allergen-induced eosinophilia (Figure 12F). Enhanced mucus production was also observed in papain stimulated *Rag2*^{-/-}*Il2rg*^{-/-} mouse lungs after lung NH cell transplant (Figure 12G). Similar results were observed in mice stimulated with house dust mite (HDM) extract (Appendix 6C and D) or IL-25 (Appendix 6E and F).

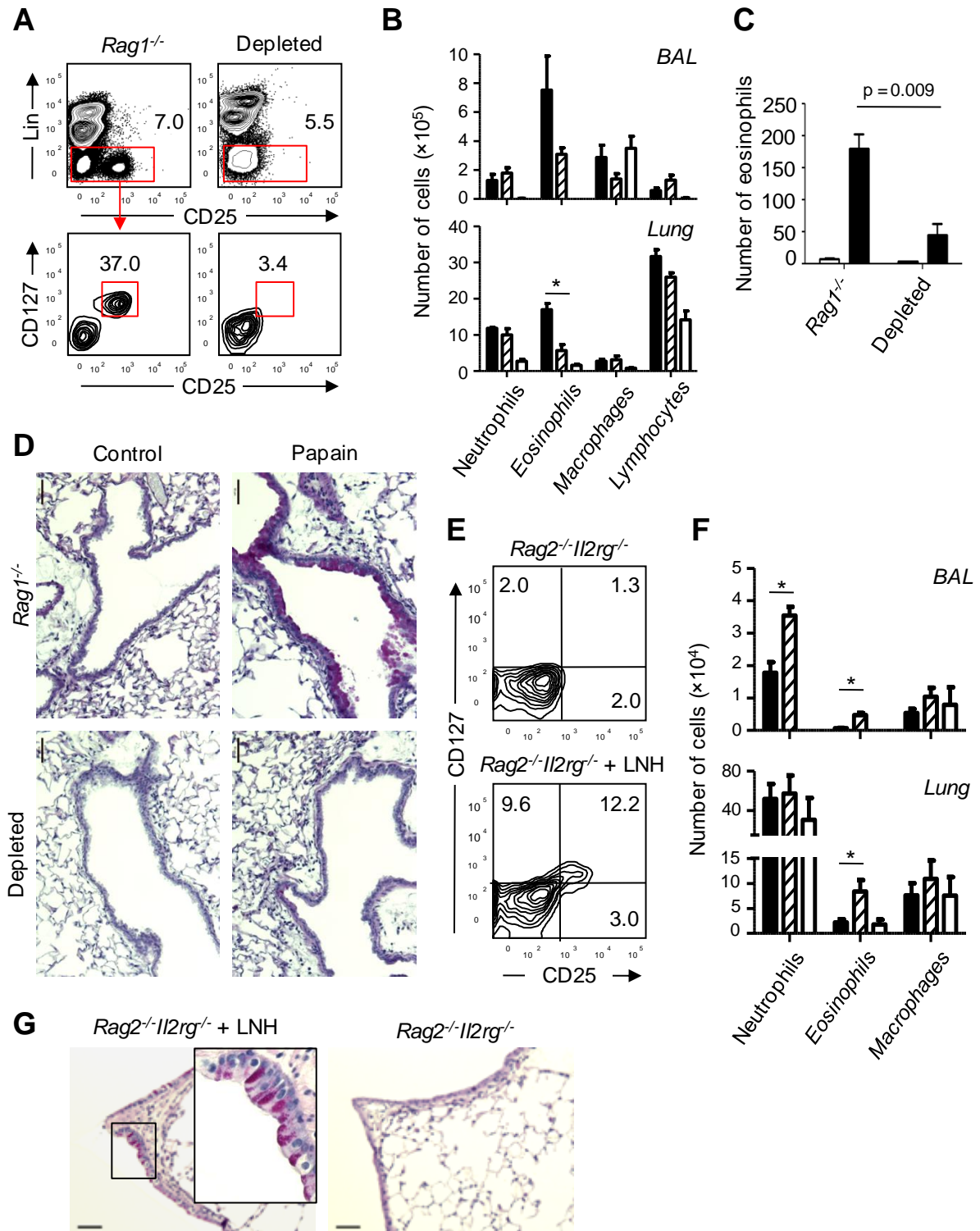


Figure 12 lung NH cell depletion and adoptive transplant show that lung NH cells are required for papain-induced mucus production and eosinophil infiltration.

(A) lung NH cells were depleted by intraperitoneal injection of anti-CD25 mAb (clone PC61 5.3) into *Rag1*^{-/-} mice. Two days later, lung lymphocytes were stained with Lin-cocktail mAb, anti-CD25 (clone 7D4) and anti-CD127 mAb and analyzed by flow cytometer to confirm

lung NH cell depletion. The numbers in the plots show the percentages of cells in the indicated gates.

(B) *Rag1*^{-/-} mice were non-depleted and treated with papain (black), lung NH -depleted and treated with papain (striped) or non-depleted and treated with heat-inactivated papain (white), and Leukocytes in BAL and lung tissue were analyzed by flow cytometry and quantified.

(C) Eosinophils were quantified in H&E stained lung sections of papain (black) or heat-inactivated papain (white) treated depleted and non-depleted *Rag1*^{-/-} mice.

(D) Mucus secretion was analyzed by PAS staining of formalin fixed paraffin embedded lung sections of heat-inactivated papain (control) or papain treated, lung NH depleted and non-depleted *Rag1*^{-/-} mice. Scale bar represents 50 μ m.

(E) In vitro expanded purified lung NH cells were intravenously injected (5×10^4 cells per mouse) into *Rag2*^{-/-}*Il2rg*^{-/-} (*RGC*) mice, and lymphocytes in the recipient mouse lungs were analyzed by flow cytometry 24 h after adoptive transplant. Live, Lin⁻Sca-1⁺c-Kit^{+/low} cells were first gated and analyzed for cells expressing CD127 and CD25. Top plot shows control without lung NH injection, and bottom plot shows lung lymphocytes of mice injected with lung NH cells. The numbers in the plots indicate the percentage of cells in each quadrant.

(F) BAL and lung tissue of *RGC* + papain (black), *RGC* + lung NH cell + papain (striped) or *RGC* + lung NH cell + heat-inactivated papain (white) treated mice were analyzed by flow cytometry and quantified.

(G) Mucus secretion in lungs was analyzed by PAS staining of papain treated *RGC* mice with or without transplanted NH cells. Scale bar represents 50 μ m, magnified image taken with 40 \times objective.

*p < 0.05 (two-tailed Student's t test). Data are representative of at least 3 independent experiments (mean and SEM in B, C, and F). (See also Appendix 6)

2.3.6 Papain stimulation enhances Th2 cytokine production from lung NH cells through the release of stroma-derived IL-33, IL-25 and TSLP.

IL-5 and IL-13 are known to drive eosinophil maturation and infiltration, goblet cell hyperplasia and mucus secretion. To investigate the role and regulation of lung NH cells in response to papain, we stimulated lung explants from WT, *Rag1*^{-/-} and *Rag2*^{-/-}*Il2rg*^{-/-} mice, and assessed IL-25, IL-33, TSLP, IL-5 and IL-13 production by ELISA. Papain induced IL-5 and IL-13 secretion in WT and *Rag1*^{-/-}, but not in *Rag2*^{-/-}*Il2rg*^{-/-} mouse lung explant cultures (Figure 13A, B), consistent with the above *in vivo* results. These results also indicate that papain induces IL-5 and IL-13 production by lung resident lymphocytes rather than

recruiting cytokine-producing cells from circulation to the lung. IL-33, IL-25 and TSLP were produced in lung explant cultures from all mouse strains (Figure 13C-E). Stimulation with papain caused increased IL-25 and TSLP production. IL-33 was constitutively produced in lung explant cultures, and papain stimulation induced a minor but significant increase in concentration. Neutralization of TSLP and/or IL-33 in papain stimulated explants resulted in a significant reduction of IL-5 and IL-13 production (Appendix 7). Heat-inactivated papain did not induce cytokine production above PBS levels (Appendix 4C).

Intracellular IL-13 staining of cells in papain-treated *Rag1*^{-/-} mouse lung explant cultures showed that the main producers of IL-13 in *Rag1*^{-/-} mouse lung explants were CD25⁺ lung NH cells (Figure 13F). Intracellular IL-5 staining of WT and *Rag1*^{-/-} mouse explants indicated that papain stimulation causes rapid IL-5 production almost exclusively from CD25⁺ lung NH cells and not from NK, NKT or T cells (Figure 13G). The majority of papain stimulated lung NH cells from WT and *Rag1*^{-/-} mice produced IL-5 but not IL-13 while small fractions produced IL-13 alone or both IL-5 and IL-13 (Figure 13H).

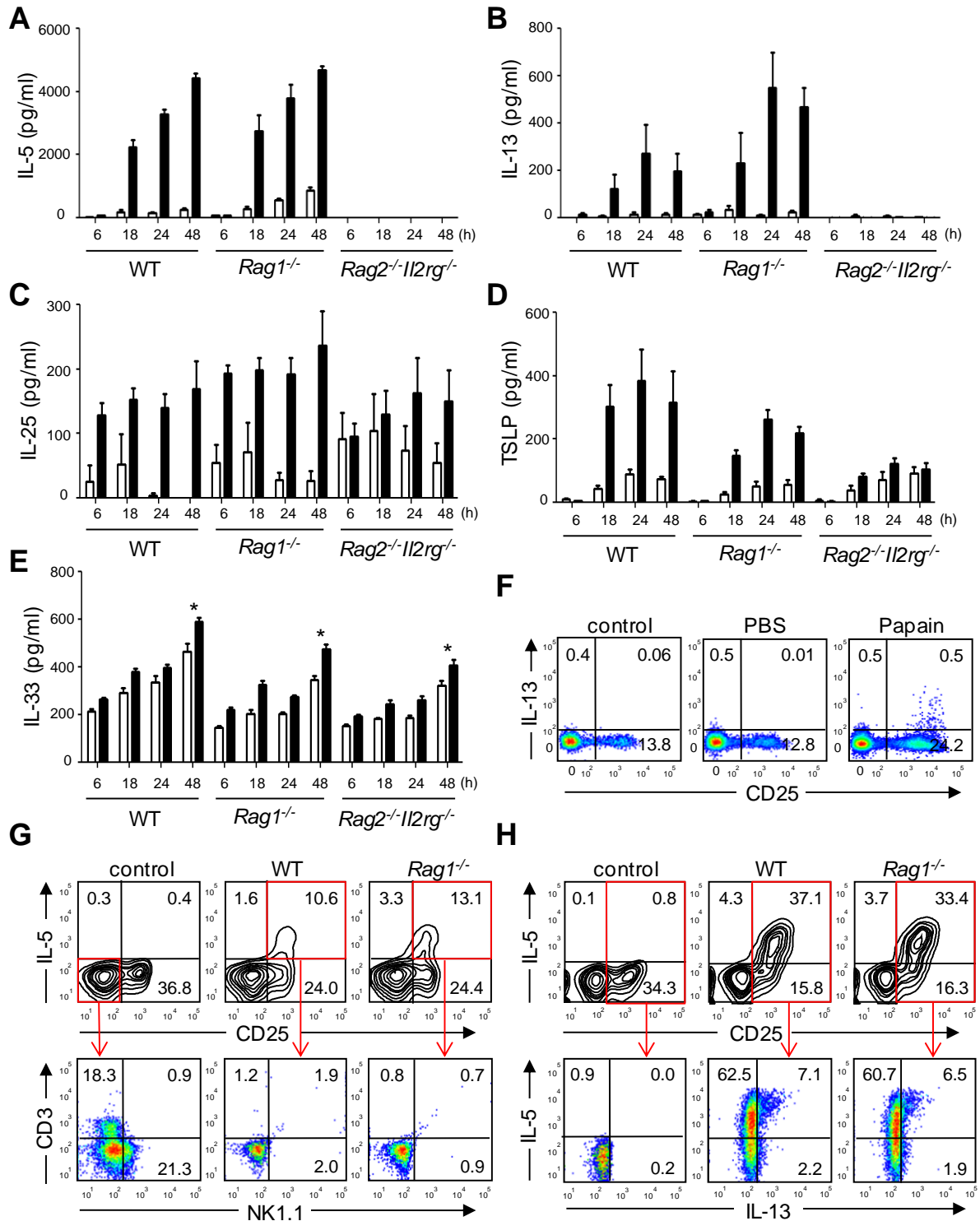


Figure 13 lung NH cells respond to lung stroma derived cytokines, and are the main producers of IL-5 and IL-13 following papain treatment.

(A-E) Lung explants of indicated mouse strains were stimulated with papain (black) or PBS (white). The amount of indicated cytokine in the culture supernatants were assayed by ELISA at the times indicated on the x-axis.

(F) *Rag1*^{-/-} lung explants were cultured for 18 h with PBS or papain and analyzed for intracellular IL-13 and surface expression of CD25. Cells were first electronically gated to exclude blood cells and debris (FSC/SSC), dead cells and NK cells (NK1.1). FMO (minus anti-IL-13 staining) of papain-treated explants is also shown (control).

(G) *Rag1*^{-/-} and WT mouse lung explants were stimulated with papain for 12 h and analyzed for intracellular IL-5 by flow cytometry. IL-5 producing cells were gated and analyzed for surface expression of CD3 and NK1.1 (below). Cells were first electronically gated to exclude blood cells and debris (FSC/SSC) and dead cells. FMO was used as a negative control.

(H) Co-staining for intracellular IL-5 and IL-13 in *Rag1*^{-/-} and WT mouse lung. Lung explants were stimulated with papain for 18 h and analyzed by flow cytometry. CD25⁺ cells were gated (top row) and analyzed for intracellular IL-5 and IL-13 (bottom). Cells were first electronically gated to exclude blood cells and debris (FSC/SSC), dead cells and NK (NK1.1) and T (CD3) cells. Fluorescence minus intracellular stain was used as a negative control.

*p < 0.05 (two-tailed Student's t test). Data are representative of at least 3 independent experiments (mean and SEM in A-E). (See also Appendix 7)

2. 4 Discussion

We have identified Lin⁻Sca-1⁺c-Kit^{+/low}CD25⁺CD127⁺ cells in normal C57BL/6 mouse lung and termed them lung NH cells. They have the capacity to rapidly produce large amounts of Th2 cytokines, and they are critical for induction of eosinophilic lung inflammation by protease allergens, which are known to cause asthma in humans. Whereas T cells are thought to be important for asthma in general, papain has been shown to induce asthma-like symptoms in RAG-deficient mice, indicating the presence of a T cell-independent mechanism. We have demonstrated that intranasal administration of papain into *Rag1*^{-/-} mice, but not *Rag2*^{-/-}*Il2rg*^{-/-} mice, rapidly causes lung eosinophilia, mucus hypersecretion and elevation in BAL IL-5 and IL-13 levels. lung NH cells are present in the former mice but absent in the latter. Furthermore, depletion of lung NH cells in *Rag1*^{-/-} mice by anti-CD25 mAb injection significantly reduces lung eosinophilia and mucus secretion upon papain administration. Conversely, adoptive transplant of lung NH cells into *Rag2*^{-/-}

Il2rg^{-/-} mice reconstitutes these symptoms, thus providing convincing proof that lung NH cells are critical in T cell independent allergic lung inflammation. Indeed, lung NH cells are the main source of IL-5 and IL-13 in both *Rag1*^{-/-} and WT lung explant cultures treated with papain. Taken together, those results suggest that lung NH cells are a critical early source of IL-5 and IL-13 in protease allergen-induced lung inflammation. HDM is another allergen known to depend largely on protease activity (Gregory and Lloyd, 2011). Our results show that lung NH cells play an important role in mediating a rapid Th2 response to HDM exposure.

Proteases are important components of many allergens (Reed and Kita, 2004), and thought to not only disrupt mucosa integrity but also thought to act on protease-activated receptors and activate airway epithelial cells (Thompson et al., 2001). Activated epithelial cells produce a range of cytokines including TSLP, IL-25 and IL-33 (Strickland et al., 2010). Our current study has shown that papain-treated lung explants produce IL-25 and TSLP, while IL-33 production is enhanced upon papain stimulation. IL-33 is known to be constitutively expressed in endothelial and epithelial cells and is released as an alarmin upon cell damage (Moussion et al., 2008). The process of explant preparation likely damages lung epithelial cells causing some release of IL-33, because even unstimulated explants have residual levels. Neutralization of IL-33 in explant cultures significantly decreases Th2 cytokine production, and simultaneous neutralization of TSLP and IL-33 effectively blocks IL-13 production. Purified lung NH cells are stimulated by a combination of IL-33 and TSLP and secrete very large amounts of IL-5 and IL-13. Therefore, lung stroma-derived IL-33 and TSLP likely stimulate lung NH cells and induce IL-5 and IL-13 production in papain-treated lungs, resulting in lung eosinophilia, goblet cell hyperplasia and mucus production. Interestingly, unstimulated lung NH cells express IL-5 transcript and have intracellular IL-5,

although purified lung NH cells do not secrete IL-5 without stimulation. Thus, lung NH cells seem to be poised to respond to cytokines produced by activated lung stromal cells and rapidly release pre-existing IL-5.

Intranasal administration of IL-25 or IL-33 is known to induce lung eosinophilia in RAG-deficient mice (Hurst et al., 2002; Kondo et al., 2008). We demonstrate that intranasal IL-25 stimulates lung NH cells, resulting in Th2 cytokine production and eosinophil infiltration. IL-33 is also critical for the stimulation of purified lung NH cells, although it requires an additional cytokine, IL-2, IL-7 or TSLP, for efficient stimulation of lung NH cells *in vitro*. In contrast, IL-25 on its own or in combination with other cytokines does not stimulate purified lung NH cells while it enhances IL-13 production by lung NH cells stimulated by IL-33 plus IL-7. On the other hand, RAG-deficient mouse lung explants are stimulated by IL-25 alone, but not IL-33. Baseline production of IL-33 in the explant cultures explains why exogenous IL-33 does not stimulate lung explants and why lung explants produce low levels of IL-5 without additional cytokines, as IL-33 neutralization greatly decreases IL-5 and IL-13 levels. However, how IL-25 alone stimulates mouse lung explants or lung NH cells *in vivo* is still unknown. It is possible that IL-25 promotes the production of IL-7 or TSLP by stromal cells, which in combination with IL-33, stimulates lung NH cells in the explants cultures. Alternatively, the lung microenvironment may provide cell surface ligands that participate in lung NH cell stimulation. Lung NH cells express the T cell co-stimulatory receptor ICOS and also express the transcript for 4-1BB (data not shown), but their functional significance is currently unknown.

The phenotype and the function of lung NH cells are similar to those of recently discovered innate helper cells, termed multipotent progenitor type 2 (MMP^{type2}), Natural Helper cells (Moro et al., 2010), Nuocytes and innate type 2 helper cells (Saenz et al., 2010a).

MPP^{type2} cells were detected by the expression of GFP in IL-4-eGFP reporter mice stimulated with IL-25 (Saenz et al., 2010b). They are Lin⁻Sca-1⁺c-Kit⁺, but unlike lung NH cells, they do not express CD127 (Saenz et al., 2010a). Furthermore, *Il4* transcript is absent in unstimulated lung NH cells and no IL-4 is secreted from cytokine activated lung NH cells, although the most striking difference is that MPP^{typeII} have progenitor capacity and can differentiate into myeloid cells, whereas no progenitor activity is detected for lung NH cells. As such MPP^{type2} cells likely constitute an entirely separate lineage. Innate type 2 helper cells were also identified in IL-4-eGFP mice and were found in naïve mouse mesenteric LN, spleen and liver. They are also Lin⁻, but Sca-1⁻, CD122^{low}, heterogeneous for c-Kit expression, and express high baseline *Il4* transcripts, unlike lung NH cells (Price et al., 2010). It should be noted that lung NH cells do not produce detectable levels of IL-4 upon stimulation with cytokine combinations or papain treated lung explants cultures. Nuocytes were identified in the mesenteric LN and spleen of IL-13-eGFP mice upon induction by IL-25 or IL-33 administration or helminth infection (Neill et al., 2010). The phenotype of Nuocytes (Lin⁻Sca-1⁺c-Kit⁺CD127⁺ICOS⁺) is similar to that of lung NH cells. Functionally, Nuocytes produce IL-5 and IL-13, but differ from lung NH cells in their secretion of substantial amounts of IL-6. Natural Helper cells found in fat associated lymphoid cluster (FALC) in the mesentery are Lin⁻Sca-1⁺c-Kit⁺CD25⁺CD127⁺ and also produce IL-6 in addition to IL-5 and IL-13 when stimulated (Moro et al., 2010). Thus, lung NH cells, Nuocytes and FALC Natural Helper cells are similar to each other and they likely belong to the same innate lymphocyte lineage, although differences in cytokine production capacity and some cell-surface markers are evident. Most notably, IL-6 is not produced by lung NH cells while IL-17A is. It is possible that the differences are partly due to different ways of identifying those cells. MPP^{type2}, Nuocytes and innate type 2 helper cells were identified by

the reporter eGFP expression upon stimulation or helminth infection, and thus likely are activated cells and might have migrated into the affected tissue, whereas FALC Natural Helper cells and lung NH cells were identified in naïve mice and likely are unstimulated and tissue resident. It is also possible that they may represent different stages of development in the same cell lineage. Alternatively, their phenotypes and functions may be influenced by the microenvironment, as they are located in different anatomical sites.

The recently described Lin⁻ST2⁺Sca-1⁺c-Kit⁺ cells, also termed Natural Helper cells, in BALB/c mouse lungs, have been shown to play a role in influenza virus-induced airway hyper-reactivity (Chang et al., 2011). Although Lin⁻ST2⁺Sca-1⁺c-Kit⁺ cells may partially overlap with lung NH cells in our study, significant differences in phenotype and function are also apparent. Most strikingly, Lin⁻ST2⁺Sca-1⁺c-Kit⁺ cells are far less efficient in Th2 cytokine production than lung NH cells. Purified Lin⁻ST2⁺Sca-1⁺c-Kit⁺ cells (4×10^4 cells per well) stimulated with IL-33 plus IL-2 produce less than 500 pg/ml IL-13 and less than 125 pg/ml IL-5 whereas purified lung NH cells (10^3 cells per well) stimulated in the same way produce almost 4 ng/ml IL-13 and >2 ng/ml IL-5. In fact, it is unclear whether Lin⁻ST2⁺c-Kit⁺Sca-1⁺ cells in BALB/c mouse lungs are the major source of Th2 cytokines upon influenza virus infection as lung macrophages also produce significant levels of IL-13, with at least 12,500 IL-13⁺ macrophages per lung, compared to 200 Lin⁻ST2⁺Sca-1⁺c-Kit⁺ cells. The inability to produce a significant amount of IL-5 likely explains why lung Lin⁻ST2⁺Sca-1⁺c-Kit⁺ cells do not induce eosinophilic lung inflammation, even upon adoptive transplantation of *in vivo* expanded cells at 2000 times more than naïve cell numbers per animal. Eosinophilic inflammation induced by IL-5 is a hallmark Th2 response, and the lack of eosinophilia in influenza virus infection suggests that Lin⁻ST2⁺Sca-1⁺c-Kit⁺ cells are unlikely to be involved in Th2 mediated lung inflammation. Furthermore, viral infection did

not appear to stimulate IL-13 production from Lin⁻ST2⁺Sca-1⁺c-Kit⁺ cells as artificial stimulation with PMA plus ionomycin was required. It is possible that viral infection may induce macrophage IL-33 production and prime Lin⁻ST2⁺Sca-1⁺c-Kit⁺ cells in BALB/c mice. In our study, lung NH cells are the main, if not the only, source of IL-5 and IL-13 in papain-treated *Rag1*^{-/-} mouse lungs as indicated by intracellular cytokine staining as well as depletion of lung NH cells. Depletion of Lin⁻ST2⁺Sca-1⁺c-Kit⁺ by anti-CD90.2 injection results in significant decrease in virally induced airway hyper-reactivity in *Rag2*^{-/-} mice, but the effect is complicated by the presence of other CD90-positive cells in the lung, most notably NK cells (Koo et al., 1980), which respond to viral infections (Mandelboim et al., 2001). As detailed phenotypic analysis of Lin⁻ST2⁺c-kit⁺Sca-1⁺ population is lacking, it is difficult to directly compare the two populations. Nevertheless, the inefficient Th2 cytokine production by Lin⁻ST2⁺Sca-1⁺c-Kit⁺ cells clearly separates them from lung NH cells and other innate Th2 producing lymphocytes.

The gene expression profile of lung NH cells is very different from those of lung macrophages and DCs and indicates their distinct lymphoid origin. Interestingly, lung NH cells do not express the *Rorc* gene encoding ROR γ , a member of the ROR family of nuclear hormone receptors, known to be important for Th17 cells (Ivanov et al., 2006). The lack of *Rorc* expression also separates lung NH cells from another family of innate lymphocytes that includes LTi-like cells and IL-22-producing NK-like cells (Sawa et al., 2010). Those innate lymphocytes express ROR γ t, an isoform of ROR γ and produce IL-22.

The lung is a unique immune site as it is constantly exposed to potential pathogens. Innate lymphocytes that are capable of rapidly responding to infections are likely important for the lung immune system. Lung NH cells comprise a distinct population of innate lymphocytes which rapidly respond to lung epithelium-derived cytokines. Thus, innate

lymphocytes in the lung can be divided into two functionally distinct populations, namely cytotoxic NK cells and cytokine producing NH cells, similar to cytotoxic CD8 T cells and helper CD4 T cells in the adaptive immune system.

Chapter 3 Retinoic acid receptor-related orphan nuclear receptor alpha is required for Natural Helper cell development and allergic inflammation

3.1 Introduction

Natural Helper (NH) cells, also termed nuocytes (Neill et al., 2010), multipotent progenitor type 2 (Saenz et al., 2010b), type 2 innate lymphoid cells (ILCs) (Mjosberg et al., 2011) and innate helper type 2 (Ih2) cells (Price et al., 2010), are a novel type of innate lymphocyte in mucosal tissues capable of producing large amounts of Th2 cytokines. NH cells are activated by stroma-derived IL-33, IL-25 or TSLP and rapidly produce IL-5 and IL-13 (Halim et al., 2012a), and they have been implicated in the expulsion of helminths from the gut (Neill et al., 2010; Price et al., 2010; Saenz et al., 2010b), activation of B1 B cells in the peritoneum (Moro et al., 2010), airway hyper-reactivity and tissue repair in the lungs following influenza infection (Chang et al., 2011; Monticelli et al., 2011) and protease allergen induced lung inflammation (Halim et al., 2012a). While the precise relationship between NH cells in the lung and gut-associated lymphoid tissues is still unclear, all NH cells are thought to belong to a larger family of innate lymphocytes, which includes natural killer (NK) cells and ILCs expressing retinoic acid receptor-related orphan nuclear receptor (ROR) γ t (Spits and Di Santo, 2011; Spits and Cupedo, 2012). Although NH cells and ROR γ t⁺ ILCs are similar in cell surface marker expression, they significantly differ in their functions. The former produce Th2 cytokines while the latter produce IL-22 and IL-17.

A version of Chapter 3 has been published: Halim, T.Y.F., MacLaren A., Romanish, M.T., Gold, M.J., McNagny K.M., and Takei F. (2012) Retinoic acid receptor-related orphan nuclear receptor alpha is required for Natural Helper cell development and allergic inflammation. *Immunity* 37(3):463-474, with permission from Elsevier.

The development of NH cells, ROR γ ⁺ ILCs and NK cells is dependent on the transcription factor Id2 (Monticelli et al., 2011; Moro et al., 2010) whereas ROR γ ⁺ ILC development is also dependent on ROR γ t encoded by *Rorct* (Eberl et al., 2004; Sanos et al., 2009; Sawa et al., 2010). As we previously found that lung NH cells from naïve C57BL/6 mice express a high level of *Rora*, which encodes another member of the ROR family of transcription factors, namely ROR α but not *Rorc* (Halim et al., 2012a), we now have examined NH cells and ROR γ ⁺ ILCs in various tissues of ROR α -deficient and ROR γ t-deficient mice. We report here that ROR α -deficient mice have almost no NH cells in the lung or small and large intestines but they have normal level of ROR γ ⁺ ILCs in these tissues. Conversely, ROR γ t-deficient mice lack ROR γ ⁺ ILCs but have normal NH cells. We have also identified immature NH (iNH) cells in the bone marrow (BM) that develop into mature NH cells in the lung and the gut. NH cell-deficient mice have Th2 cells but do not develop allergic lung inflammation in response to protease allergen stimulation.

3.2 Materials and methods

3.2.1 Mice

C57BL/6, C57BL/6.Pep3b, NOD/SCID and NOD/SCID/*Il2rg*^{-/-} mice were maintained in the BCCRC pathogen free animal facility. B6.129P2(Cg)-*Rorc*^{tm2Litt}/J and B6.Cg-*Rora*^{sg}/J mice were purchased from The Jackson Laboratories. B6.*Rag2*^{-/-}/*Il2rg*^{-/-} mice were purchased from Taconic Farms. Mice were used at 4-8 weeks of age. All animal use was approved by the animal care committee of the University of British Columbia, and animals were maintained and euthanized under humane conditions in accordance with the guidelines of the Canadian Council on Animal Care.

3.2.2 Genotyping and qPCR

Pups from *Rora*^{sg/+} breeders were genotyped using DNA obtained from ear-notches before experiments. Primer sequences and PCR protocol were obtained from The Jackson Laboratories online database. Prior to performing relative quantification of *Rora* in the described NHC, we consulted the BioGPS database to gain an appreciation for potential tissues to use as positive controls; using RT-PCR we confirmed expression of *Rora* in primary B6 liver. For subsequent qRT-PCR experiments, RNA was isolated from FACS-purified B6 NH cells, expanded *in vitro* with IL-25 and IL-33 for 3 days, CD4⁺ T-cells isolated from B6 spleen using EasySep™ negative selection kit (StemCell) or primary B6 liver using the RNeasy Mini Kit (QIAGEN), treated by the Turbo DNase-free kit (Ambion), and reverse transcribed using Superscript III (Invitrogen); all procedures were performed as indicated by the manufacturer. Necessarily, the primer pairs for *Rora* (RORa-F: gagctccagcagataacgtg; RORa-R: gcaaactccaccacatactgg) and β -actin (B-actin-F: aaggccaaccgtgaaaagat; B-actin-R: gtggtacgaccagaggcatatc) were first found to amplify equally efficiently. The comparative C_T method was employed to determine *Rora* expression across the indicated cell types/tissues using POWER SYBR Green Master Mix (ABI) in an ABI 7500 Real Time System (ABI) under default reaction conditions.

3.2.3 Bone marrow transplantation

B6.*Rag2*^{-/-}*Il2rg*^{-/-} mice were sub-lethally irradiated (350 Rads) followed by intravenous transplantation of 10⁷ whole bone marrow cells from 4 week old WT or *Rora*^{sg/sg} mice. B6.Pep3b mice were lethally irradiated (1000 Rads) followed by transplantation of 10⁷ whole bone marrow cells from 4 week old WT or *Rora*^{sg/sg} mice. Mice were given Ciprofloxacin/HCL for 4 weeks, and used for analysis at 8-16 weeks post transplant.

3.2.4 Antibodies, reagents, FACS sorting and analysis

FITC-conjugated anti-CD3 ϵ , CD19, B220, NK1.1, Mac-1, Gr-1, Ter119, CD45.2, PE-conjugated anti-CD3, CD127, ROR γ t, PE.Cy5-conjugated CD127, PerCP-Cy5.5 conjugated anti-CD19, CD25, NK1.1, CD3, PE.Cy7-conjugated Sca-1, DX5, APC-conjugated anti-CD117, CD25, Fc ϵ R1 α , APC-eFluor $^{\text{®}}$ 780-conjugated B220, Alexa Fluor $^{\text{®}}$ 700-conjugated CD45.2, CD11c, eFluor $^{\text{®}}$ 450-conjugated CD3 ϵ , CD19, B220, NK1.1, Gr-1, CD11b, Ter119, NKp46, eFluor $^{\text{®}}$ 605NC-conjugated CD4 and eFluor $^{\text{®}}$ 650NC-conjugated Thy1.2 were purchased from eBioscience. FITC-conjugated 7/4 was purchased from Abcam. FITC-conjugated CD69, CD127, PE-conjugated anti-NKp46, CD27, CXCR4, CD122, Flt3, ICOS, IL-13, Siglec-F, APC-conjugated IL-5 and BD Horizon V500-conjugated CD45 was purchased from BD Bioscience. FITC-conjugated anti-T1/ST2 was purchased from MD Bioproducts. Propidium Iodide (PI), eFluor $^{\text{®}}$ 780 (eBioscience) or DAPI reagents were used to exclude non-viable cells. IL-2, 4, 7, 23, 25, 33 and TSLP were purchased from eBioscience, Papain, PMA and ionomycin were purchased from Sigma Aldrich. BD Fortessa, BD Caliber (Cytex 6 color upgrade) and Canto II were used for phenotypic analysis; BD FACS Aria II was used for cell sorting and phenotypic analysis. Flowjo v. 8.6 was used for data analysis.

3.2.5 Primary leukocyte preparation

Cell suspensions were prepared from lung, spleen, MLN or BM as described (Veinotte et al., 2008). Small and large intestines were dissected and flushed with cold PBS, cut longitudinally and washed with cold PBS. BM or washed intestines were cut into small pieces with a razor and digested for 40 minutes in MEM, 10% FBS, penicillin and streptomycin (P/S), 50 mM 2-mercaptoethanol (2ME), Collagenase IV (Invitrogen) and

DNase (Sigma) at 37°C. Digested tissue was pushed through a 70 µm strainer, followed by Percoll™ (GE Healthcare) gradient enrichment of leukocytes.

3.2.6 Isolation of NH, iNH, CLP and LMPP cells

Single cells were incubated with 2.4G2 to block Fc receptors and then stained with FITC-conjugated lineage marker mAbs (CD3, CD19, B220, NK1.1, Mac-1, GR-1, and Ter119), PE-conjugated CD127, PerCP-Cy5.5-conjugated CD25, PE.Cy7-conjugated Sca-1, and APC-conjugated CD117, Alexa 700-conjugated CD45.2 and purified by FACS. BM was stained with FITC-conjugated T1/ST2, PE-conjugated CD127, PerCP-Cy5.5-conjugated CD25, PE.Cy7-conjugated Sca-1, and APC-conjugated CD117, Alexa 700-conjugated CD45.2, eFluor 450-conjugated lineage marker mAbs (CD3, CD19, B220, NK1.1, Mac-1, GR-1, and Ter119) and purified by FACS. 4,500 CLP or iNH cells were injected into non-irradiated NSG mice via tail vein. For LMPP, CLP and iNH cell isolation BM was stained with FITC-conjugated CD127, PE-conjugated Flt3, PerCP-Cy5.5-conjugated CD25, PE.Cy7-conjugated Sca-1, and APC-conjugated CD117, APC-eFluor780-conjugated B220, eFluor 450-conjugated lineage marker mAbs (CD3, CD19, NK1.1, Mac-1, GR-1, and Ter119), V500-conjugated CD45.2 and purified by FACS. 2,500 LMPP, CLP or iNH cells were injected into non-irradiated NSG mice via tail vein.

3.2.7 Cytokine production assay

FACS purified cells were cultured in 200 µl RPMI-1640 media containing 10% FBS, P/S, 2 ME at 37°C. Cells were stimulated with IL-33 (10 ng/ml), PMA (30 ng/ml) and ionomycin (500 ng/ml), IL-23 (10 ng/ml), IL-7 (10 ng/ml), TSLP (10 ng/ml), IL-33 (10 ng/ml).

3.2.8 *In vitro* CD4⁺ T-cell stimulation

Spleen CD4⁺ T-cells were enriched using negative selection by EasySep™ (StemCell) and stimulated as described (McKenzie et al., 1998).

3.2.9 Intestine explant culture

Mice were sacrificed by CO₂ asphyxiation. Intestines were dissected, flushed with cold PBS, opened longitudinally and washed in cold PBS. Explants were prepared using a 5mm biopsy punch. Two explants were placed in 0.5 ml RPMI1640, 10% FCS, 2ME, P/S, and stimulated with IL-25 (10 ng/ml) or IL-23 (10 ng/ml).

3.2.10 Intracellular staining

Intracellular staining for RORγt was performed using the Foxp3 intracellular staining kit (eBioscience) according to the manufacturer's protocol. Intracellular staining for IL-5 was performed using the Cytofix/Cytoperm kit (BD Biosciences). Dead cells were stained with eFluor® 780 (eBioscience) fixable viability dye before fixation/permeabilization and excluded during analysis.

3.2.11 ELISA assay

IL-5, IL-13, IL-22 (eBioscience) ELISAs were performed according to the manufacturer's protocol.

3.2.12 RNA isolation and microarray

Total RNA was isolated from FACS purified un-stimulated cells by Trizol (Invitrogen). Agilent Bioanalyzer 2100, RNA amplification, and microarray services were performed by McGill University and Génome Québec Innovation Centre using the Affymetrix Mouse Gene 1.0 arrays. All data analysis was performed with FlexArray 1.5

(Genome Quebec). Microarray data sets for other cells were obtained from data assembled by the ImmGen consortium (Heng et al., 2008).

3.2.13 *In vivo* papain stimulation

Mice were anesthetized by isoflurane inhalation, followed by intranasal injection of papain or heat-inactivated papain (10 µg) in 40 µl of PBS on d 0-2. Mice were sacrificed on d 3 and lungs and BAL (1 ml PBS) were collected or airways were instilled with 50:50 Tissue-Tek® O.C.T. Compound/PBS (Adwin Scientific) and fixed in formalin. Lung tissue was processed as described previously; lung and BAL cells were then counted and identified by FACS. Fixed tissues were embedded in paraffin and processed for H&E or PAS (+/- diastase) staining by the Centre for Translational and Applied Genomics (Vancouver, Canada).

3.2.14 Statistics

Data were analyzed using GraphPad Prism 5 (GraphPad Software). A Student's t test was used to determine statistical significance between groups, with $p \leq 0.05$ being considered significant. The statistical analysis of microarray results was carried out using FlexArray (Genome Quebec).

3.3 Results

3.3.1 NH cells express *Rora* and can be distinguished from ROR γ t⁺ ILCs by Sca-1 and c-Kit expression.

As we previously reported (Halim et al., 2012a), NH cells in naïve C57BL/6 (B6) mouse lungs are readily identified by their distinct pattern of cell surface marker expression: Lineage marker-negative (Lin⁻) CD127⁺CD25⁺Sca-1^{hi}c-Kit^{-low} (Figure 14A, top). They expressed the IL-33 receptor T1/ST2 chain but not the chemokine receptor CCR6, which is known to be expressed on ROR γ t⁺ ILCs. In the small intestine (S. Int.), large intestine (L. Int.) and MLN, Lin⁻CD127⁺CD25⁺ cells could be divided into two clearly distinguishable populations, one Sca-1⁻c-Kit⁺ and the other Sca-1^{hi}c-Kit^{low}. The former expressed CCR6 but not T1/ST2 while the latter was CCR6⁻T1/ST2⁺, with the only exception being those in the small intestine, which did not express T1/ST2 (Figure 14A, second row). While both Lin⁻CD127⁺CD25⁺Sca-1⁻c-Kit⁺ and CD127⁺CD25⁺Sca-1^{hi}c-Kit^{-low} cells (gated by blue and red boxes, respectively, in Figure 14A) were found in the intestine and MLNs in comparable numbers, the former population was not detected in the lung (Figure 14A,B). We purified the two cell populations from the small intestine and stimulated them with IL-33 plus TSLP or IL-23. The Sca-1^{hi}c-Kit^{-low} subset was very similar to lung NH cells in our previous study (Halim et al., 2012a) and produced IL-5 and IL-13 in response to IL-33 plus TSLP but did not produce significant amount of IL-22 in response to IL-23 (Figure 14C, red bars). Therefore, this population likely consisted of NH cells. In contrast, the Sca-1⁻c-Kit⁺ subset produced IL-22 in response to IL-23 but did not produce IL-5 or IL-13 upon stimulation with IL-33 plus TSLP (Figure 14C, blue bars), indicating that this population likely contained ROR γ t⁺ ILCs but not NH cells. Lung NH cells did not produce IL-22 (Appendix 8A). Intracellular staining confirmed that all Lin⁻CD127⁺CD25⁺Sca-1⁻c-Kit⁺ cells in the small

intestine were $\text{ROR}\gamma\text{t}^+$ and $\text{CD127}^+\text{CD25}^+\text{Sca-1}^{\text{hi}}\text{c-Kit}^{\text{low}}$ cells were $\text{ROR}\gamma\text{t}^-$ (Figure 14D). No $\text{ROR}\gamma\text{t}^+$ $\text{Lin}^-\text{CD25}^+$ cells were found in naïve mouse lungs. Thus, normal mouse lungs seemed to have no detectable $\text{ROR}\gamma\text{t}^+$ ILCs. This is consistent with our previous microarray analysis of global gene expression in lung NH cells, which showed no detectable *Rorc* expression in lung NH cells (Halim et al., 2012a) (Appendix 8B). Instead, they expressed a high level of *Rora*, which encodes $\text{ROR}\alpha$, another member of the ROR family of nuclear receptors. The expression of *Rora* in both lung and gut NH cells were confirmed by qPCR (Figure 14E).

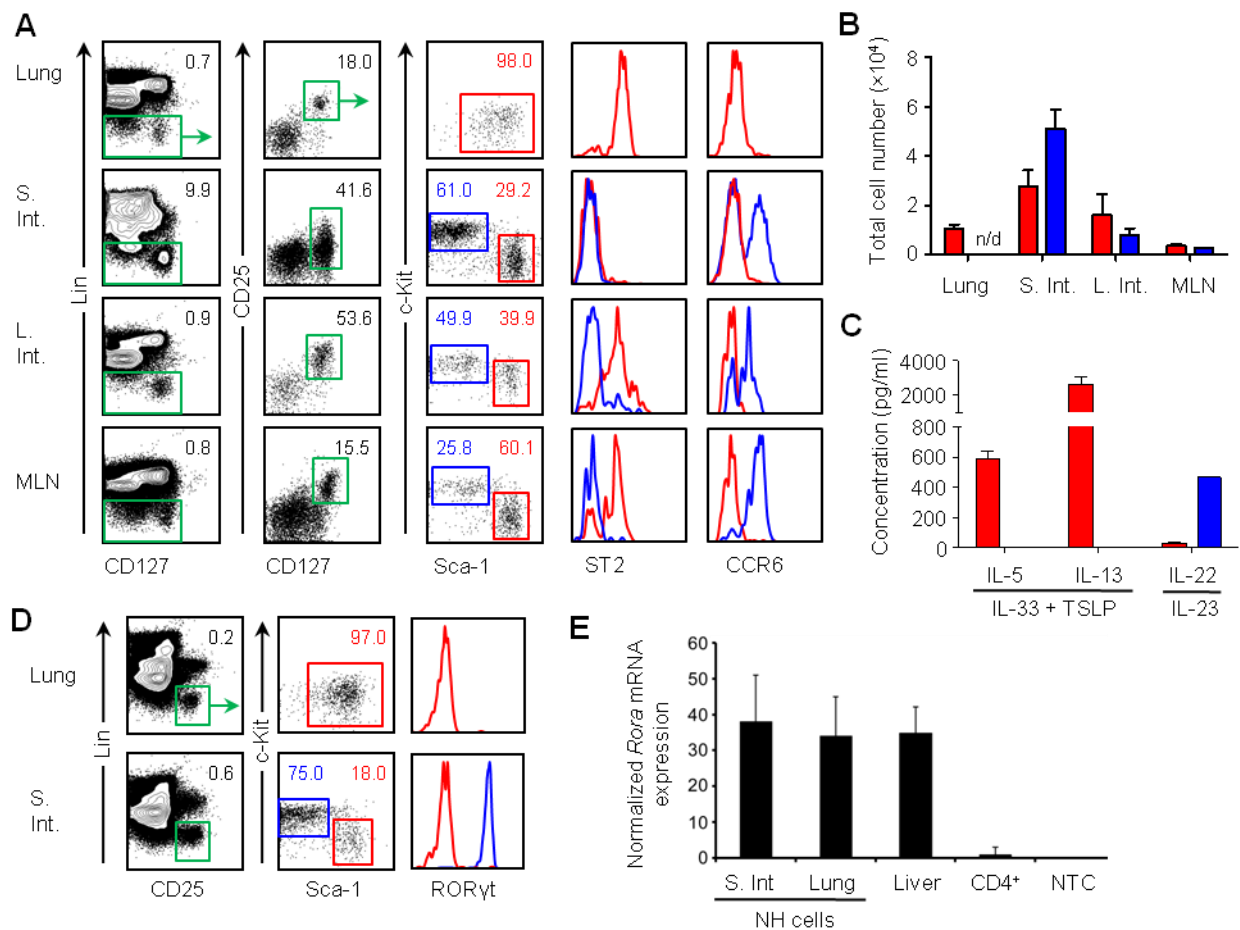


Figure 14 *Rora* and *Rorc* expressing innate lymphocyte subsets in naïve WT mice.

(A) Cells from lung, small intestine (S. Int.), large intestine (L. Int.) and mesenteric lymph node (MLN) were analyzed by FACS. Live (PI) leukocytes (CD45^+) were first gated, Lineage (Lin) negative cells were gated (green box) and analyzed for CD127 and CD25

expression. CD25⁺CD127⁺ were then gated (green box) and analyzed for Sca-1 and c-Kit expression. Sca-1⁺c-Kit^{-low} cells (red) and Sca-1⁺c-Kit⁺ cells (blue) were gated and analyzed for CCR6 and T1/ST2 expression. Red and blue histograms correspond to the cells gated by the boxes in the same colors in the plots.

(B) Absolute numbers (per mouse) of Lin⁻CD127⁺CD25⁺Sca-1⁺c-Kit^{-low} cells (red) and Lin⁻CD127⁺CD25⁺Sca-1⁺c-Kit⁺ cells (blue) in indicated tissues were calculated from the total number of CD45⁺ live cells and the frequencies of individual cell populations determined in (A).

(C) Lin⁻CD127⁺CD25⁺Sca-1⁺c-Kit^{-low} cells (red) and Lin⁻CD127⁺CD25⁺Sca-1⁺c-Kit⁺ cells (blue) were FACS purified from small intestine and stimulated *in vitro* with IL-33 plus TSLP or IL-23 plus IL-7 for 3 days and the indicated cytokines in culture supernatant were analyzed by ELISA.

(D) Lin⁻CD25⁺Sca-1⁺c-Kit^{-low} NH cells (red) and/or Lin⁻CD25⁺Sca-1⁺c-Kit⁺ ILC (blue) in the indicated tissues were stained for intracellular ROR γ t. All cells were first gated for live (eFluor®780⁻) leukocytes (CD45⁺).

(E) NH cells (Lin⁻CD127⁺CD25⁺Sca-1⁺c-Kit^{-low} cells) were purified from small intestine (gut) and lung, RNA was extracted, converted to cDNA and subjected to quantitative PCR analysis for *Rora* mRNA expression by qPCR analysis. Relative expression values are normalized to endogenous β -actin levels, and shown relative to *Rora* expression in CD4⁺ T cells. No template control (NTC) was used. Bars represent the mean of three independent experiments \pm SD.

Data are representative of at least three independent experiments (mean and SEM in B, C). (See also Appendix 8)

3.3.2 ROR α -deficient mice do not have functional NH cells.

The *staggerer* mutation (*Rora*^{sg/sg}) deletes the *Rora* gene. To test the effects of ROR α -deficiency, we compared NH cells, ROR γ t⁺ ILCs and other lymphocytes in *Rora*^{sg/sg}, *Rorct*^{-/-} and wild type (WT) B6 mice. Lin⁻CD127⁺CD25⁺Sca-1^{hi}c-Kit^{-low} NH cells were greatly reduced in *Rora*^{sg/sg} mouse lungs, small and large intestines as compared to WT or *Rorct*^{-/-} mice (Figure 15A). Conversely, ROR γ t⁺ ILCs (Lin⁻CD127⁺CD25⁺Sca-1⁺c-Kit⁺) were undetectable in *Rorct*^{-/-} mice, as expected (Spits and Di Santo, 2011), but they had a normal frequency of NH cells. The absolute number of NH cells in *Rora*^{sg/sg} mice was severely reduced to almost non-detectable levels in all tissues examined (Figure 15B). Heterozygous *Rora*^{sg/+} mice had normal NH cell numbers (Appendix 9A and B). The number of ROR γ t⁺

ILCs was also moderately reduced in the small intestine, but not in the large intestine, of *Rora*^{sg/sg} mice as compared to WT mice, whereas they were almost undetectable in *Rorct*^{-/-} mouse small and large intestines (Figure 15C). It should be noted that *Rora*^{sg/sg} mice in this analysis were only 3 weeks old and significantly smaller than WT and *Rorct*^{-/-} mice. These data further confirm the gating strategy to identify NH cells and RORγt⁺ ILCs in Figure 1, and highlight the importance of using Sca-1 and c-Kit to differentiate between the two innate lymphocyte populations in the gut.

The lungs of *Rora*^{sg/sg} mice have a distinct Lin⁻CD127⁺CD25⁻ population, possibly representing NH cells with a slightly changed phenotype. However, these cells did not produce Th2 cytokines when purified by FACS and stimulated *in vitro* (data not shown). To further exclude the possibility of functional but phenotypically different NH cells being present in *Rora*^{sg/sg} mice, we stimulated organ explants from WT and *Rora*^{sg/sg} mouse small intestines with IL-25 (Figure 2D). Explant cultures prepared from WT mice produced significantly more IL-5 in response to IL-25 than those from *Rora*^{sg/sg} mice, which produced virtually none. When stimulated with IL-23, WT and *Rora*^{sg/sg} explants produced comparable amounts of IL-22 (Appendix 9C). We concluded that *Rora*^{sg/sg} mice do not have functional NH cells but have normal RORγt⁺ ILCs.

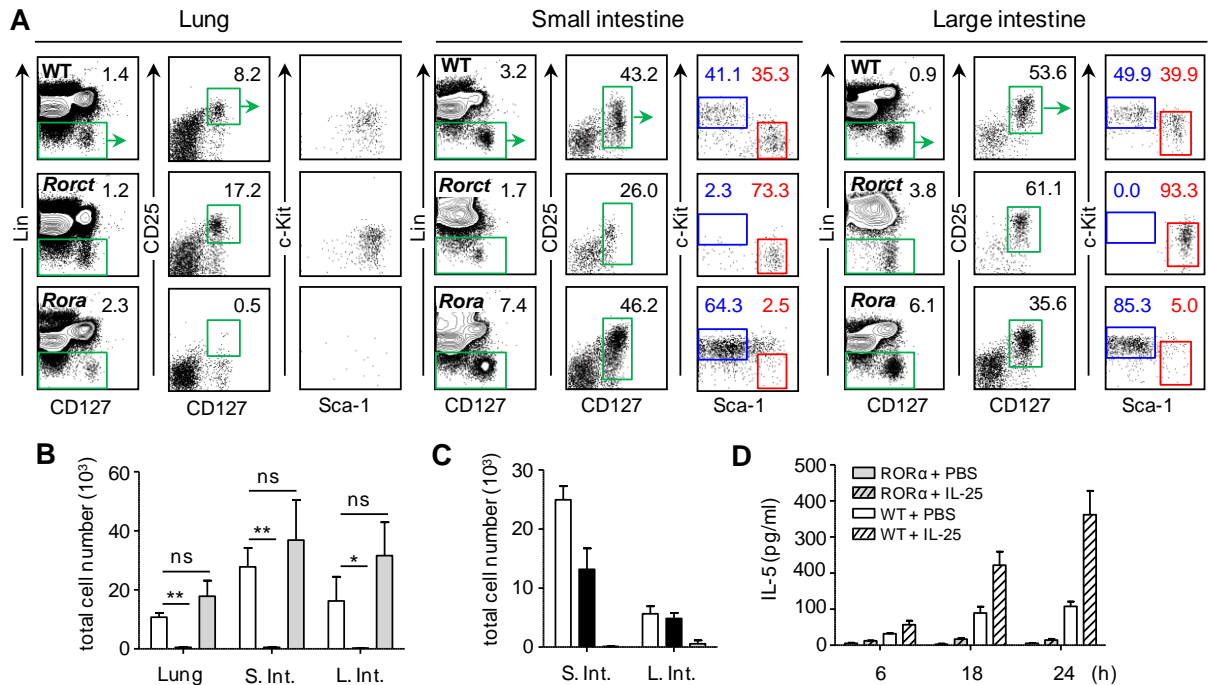


Figure 15 *Rora*^{sg/sg} mice are deficient in NH cells but not ILC.

(A) Cells were isolated from the lung, small intestine and large intestine of WT, *Rora*^{sg/sg}, *Rorct*^{-/-} mice and analyzed by FACS as in Figure 1. Lin⁻CD127⁺CD25⁺ in the indicated tissues were gated (green boxes) and NH cells (red) and RORγt⁺ ILCs (blue) were identified by Sca-1⁺c-Kit^{low} and Sca-1⁺c-Kit⁺, respectively. Numbers show the percentages of cells in the gates. Live (PI⁻) CD45⁺ leukocytes were analyzed.

(B) Total number (per mouse) of NH cells in indicated tissues of WT (white), *Rora*^{sg/sg} (black) and *Rorct*^{-/-} (grey) mice was calculated from their percentages among CD45⁺ cells and the total numbers of CD45⁺ cells in each tissue..

(C) Total numbers of RORγt⁺ ILCs per mouse in indicated tissues were calculated as in B.

(D) Small intestine explants cultures from indicated mouse strains were stimulated with PBS (ctrl) or IL-25 and analyzed for cytokine production at the indicated time points.

*p < 0.05, **p < 0.001 (two-tailed Student's t-test). Data are representative of at least three independent experiments (mean and SEM in B-D) (See also Appendix 9)

3.3.3 *Rora*^{sg/sg} bone-marrow transplanted mice are NH cell deficient, but have functional Th2 cells and RORγt⁺ ILCs.

RORα plays a critical role in the development of Purkinje cells in the mouse cerebellum (Gold et al., 2003) and cones in the retina (Fujieda et al., 2009). RORα-deficient

homozygous *staggerer* mice (*Rora*^{sg/sg}) have severe neurological defects, and do not survive long past weaning. *Rora*^{sg/sg} mice also have a runty phenotype, exhibit significantly smaller spleens and thymi and reduced numbers of lymphocytes (Bakalian et al., 1992). To determine whether the NH cell-deficiency in *Rora*^{sg/sg} mice is due to the runty phenotype of the mice or intrinsic effects of ROR α on NH cell development, we transplanted *Rora*^{sg/sg} or WT whole BM into sub-lethally irradiated lymphocyte-deficient *Rag2*^{-/-}*Il2rg*^{-/-} (RGC) mice and analyzed lymphocytes in the mice after 8-16 weeks. NH (Lin⁻CD127⁺CD25⁺Sca-1^{hi}c-Kit^{-/low}) cells were readily detected in the lung, small intestine and large intestine of RGC mice receiving WT bone marrow transplantation (WT BMT mice) (Figure 16A, top row). ROR γ t⁺ ILCs (CD127⁺CD25⁺Sca-1^c-Kit⁺) were also detected in the small and large intestine, but not in the lung, of those mice. On the other hand, very few, if any, NH cells were found in the intestine and lung of RGC mice injected with *Rora*^{sg/sg} BM (*Rora*^{sg/sg} BMT mice) (Figure 16A, middle row). RGC mice without BMT (Figure 16A, bottom row) did not have NH cells or other lymphocytes. The absolute numbers of NH cells in all tissues examined were significantly lower in *Rora*^{sg/sg} BMT mice than WT BMT mice (Figure 16B), while the absolute numbers of ROR γ t⁺ ILCs were not significantly different between those mice (Figure 16C). The two groups of mice also had comparable numbers of CD4 T, CD8 T, NKT, NK and B cells in the spleen, indicating that ROR α -deficiency had no significant effect on the development of other lymphocytes (Figure 16D). We also isolated spleen CD4⁺ T cells from these mice and stimulated them to induce Th2 differentiation. *Rora*^{sg/sg} BM-derived CD4 T cells produced the same amounts of IL-5 and IL-13 as those from WT BM-derived CD4 T cells (Figure 16E), indicating that ROR α -deficiency has no significant effects on Th2 cell differentiation.

We also transplanted ROR α -deficient BM into lethally irradiated C57BL/6-Pep3b mice and analyzed the development of all leukocytes. There was no difference in other donor-derived (CD45.2⁺) leukocyte populations between mice receiving WT BMT and ROR α -deficient BMT (Appendix 10). These data demonstrate that ROR α is critical for the development of NH cells, but not for other lymphocytes.

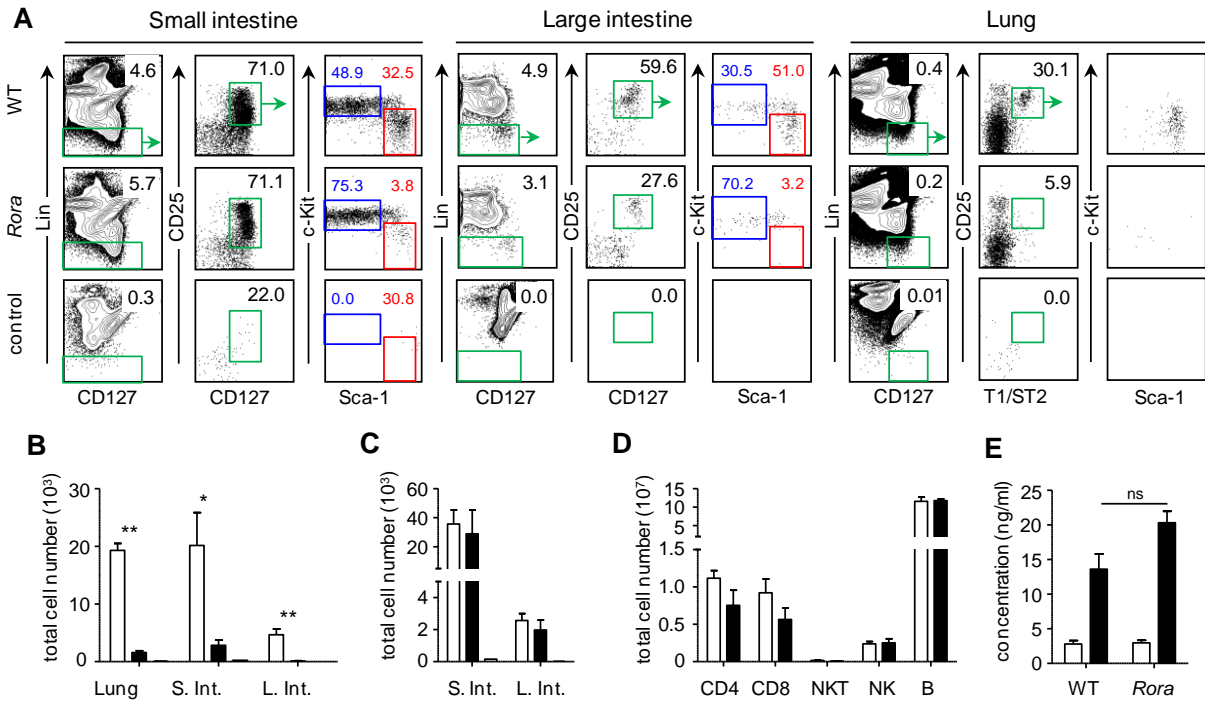


Figure 16 *Rora* deficiency affects NH cell development.

(A) *Rag2*^{-/-}*Il2rg*^{-/-} (RGC) mice (control) were reconstituted with *Rora*^{sg/sg} or WT bone marrow, followed by FACS analysis for Lin⁻CD127⁺CD25⁺Sca-1⁻c-Kit^{low} NH cells (red) and Lin⁻CD127⁺CD25⁺Sca-1⁻c-Kit⁺ ILC (blue) in the indicated tissues. Numbers show the percentages of cells in the gates. Live (PI⁻) CD45⁺ leukocytes were analyzed.

(B, C) Absolute numbers (per mouse) of NH cells (B) and ROR γ ⁺ ILCs (C) in WT (white), *Rora*^{sg/sg} (black) BMT mice or RGC control (grey) were calculated in the indicated tissues.

(D) Other leukocyte subsets in WT (white) or *Rora*^{sg/sg} (black) BMT mice were identified by flow cytometry and absolute numbers in the spleen were calculated.

(E) CD4⁺ T-cells were purified from the spleens of RGC mice reconstituted with WT or *Rora*^{sg/sg} BM and stimulated under Th2-inducing conditions for 5 days. On day 5, one million cells were stimulated for 24 hours and supernatant was analyzed for IL-5 (white bars) or IL-13 (black bars) production.

*p < 0.05, **p < 0.001 (two-tailed Student's t-test). Data are representative of at least three independent experiments (mean and SEM in B-E). (See also Appendix 10)

3.3.4 Immature NH cells in the bone-marrow develop into mature NH cells in mucosal tissues.

As the above results showed that NH cell development is ROR α -dependent, we sought ROR α -dependent NH cell progenitors in the BM. FACS analysis of BM cells from 3-week old WT and *Rora*^{sg/sg} mice showed that the latter BM had a much smaller population of Lin⁻Sca-1⁺c-Kit⁻ (LSK⁻) cells than the former (Figure 17A). As *Rora*^{sg/sg} mice live for ~3 weeks and they were significantly smaller than WT mice, we then analyzed BM cells of RGC mice with WT and *Rora*^{sg/sg} BMT. WT and *Rora*^{sg/sg} BMT mice did not significantly differ in the size of the LSK⁻ cell population. However, the LSK⁻ population was heterogeneous and could be divided into CD127⁻CD25⁻, CD127⁺CD25⁻ and CD127⁺CD25⁺ subsets (Figure 17B). In BM of WT BMT mice, the first two subsets were mostly T1/ST2⁻ whereas the third subset was mostly T1/ST2⁺, thus closely resembling mature NH cells, but also contained a small T1/ST2⁻ population. In BM of *Rora*^{sg/sg} BMT mice, the CD127⁺CD25⁺ subset was significantly smaller than that of WT BMT mice and the majority of them did not express T1/ST2. To further characterize Lin⁻Sca-1⁺c-Kit⁻CD127⁺CD25⁺T1/ST2⁺ cells, they were compared with common lymphoid progenitors (CLPs) identified by Lin⁻CD127⁺Sca-1^{low}c-Kit^{low} (Kondo et al., 1997) in WT mouse BM (Figure 17C). Lin⁻Sca-1⁺c-Kit⁻CD127⁺CD25⁺ cells and CLPs were readily distinguished by the expression levels of Sca-1 and c-Kit (Figure 17C, bottom), and CLPs did not express CD25 or T1/ST2. When purified and stimulated by phorbol ester plus ionomycin, Lin⁻Sca-1⁺c-Kit⁻CD127⁺CD25⁺T1/ST2⁺ BM cells produced much lower amounts of Th2-cytokines than lung or small intestine NH cells (Figure 17D), indicating their functional immaturity, and we term them immature NH (iNH) cells. *Rora*^{sg/sg} BMT mice had significantly less iNH cells than WT BMT mice, but they had similar frequencies of CLPs (Figure 17E). When compared to mature lung NH cells

from naïve WT mice, BM iNH cells expressed lower levels of CD69, CXCR4 and CD122, but higher levels of CD27 (Figure 17F). Intracellular staining showed that the fraction of IL-5⁺ cells was similar between BM iNH and lung NH cells (Figure 17G). Purified BM iNH cells and lung NH cells were cultured with IL-33 (10 ng/ml) + IL-25 (10 ng/ml) or IL-33 + TSLP (10 ng/ml) followed by cell count and phenotypic analysis (Appendix 11A and B). While lung NH cells survived in IL-33 + IL-25, no iNH cells could be detected after 7 days in culture. Conversely, BM iNH cells expanded significantly more *in vitro* when stimulated with IL-33 and TSLP than lung NH cells.

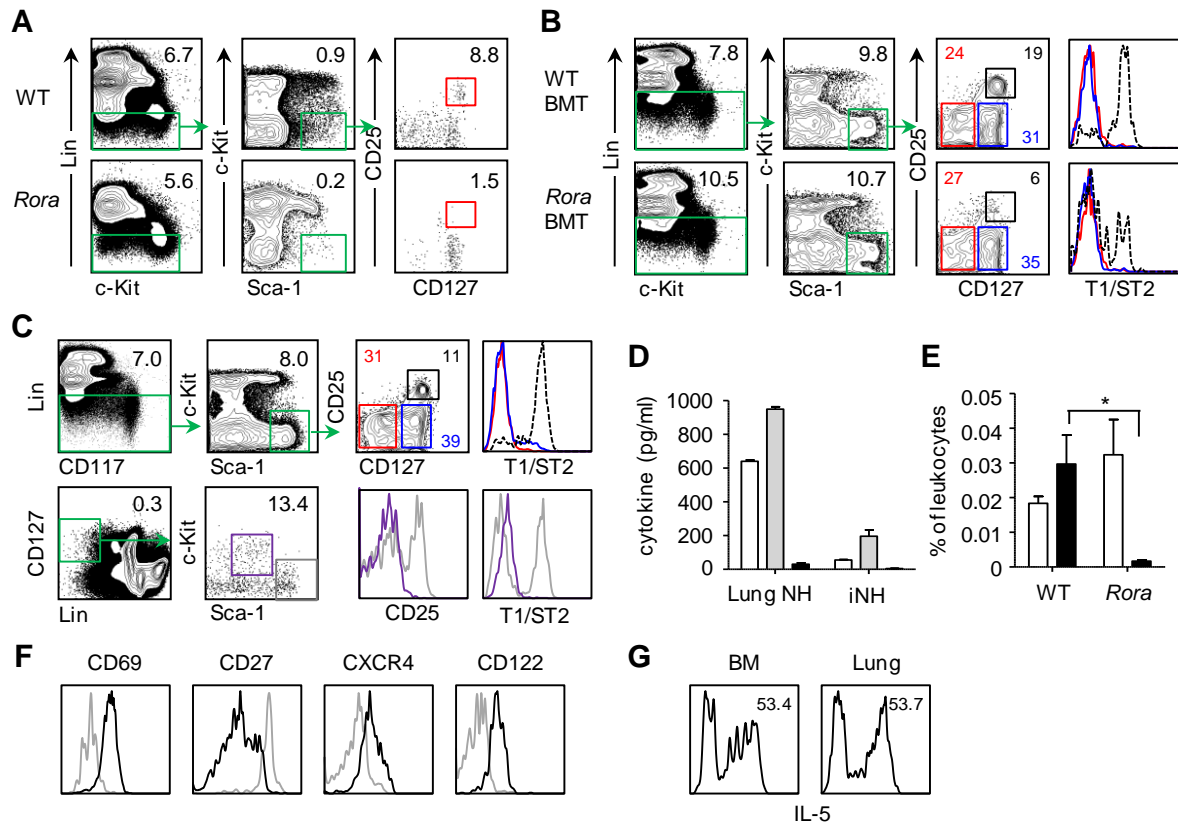


Figure 17 Lin⁺Sca-1^{hi}c-Kit⁺ (LSK⁺) cells contain *Rora*-dependent CD127⁺CD25⁺T1/ST2⁺ immature NH cells.

(A) BM cells from WT and *Rora*^{sg/sg} littermates were analyzed for Lin⁺Sca-1⁺c-Kit⁺ (LSK⁺) cells (gated by green box) and CD25⁺CD127⁺LSK⁺ cells (gated by red box). Numbers show the percentages of gated cells.

(B) BM LSK⁻ cells of WT and *Rora*^{sg/sg} BMT mice were gated (shown in green boxes), divided into CD127⁺CD25⁺ (black box), CD127⁺CD25⁻ (blue box) and CD127⁻CD25⁻ (red box) subsets, and the expression of T1/ST2 in each subset is shown by histograms. The colors of the histograms correspond to the subsets shown by the gates in the dot plots. Numbers show the percentages of gated cells.

(C) LSK⁻ cells in WT mouse BM were divided into subsets and analyzed for T1/ST2 expression as in (B) (top). Lin⁻CD127⁺Sca-1^{lo}c-Kit^{lo} common lymphoid progenitors (CLPs) (bottom, purple gates) and LSK⁻ cells (grey gates) in WT mouse BM were identified and analyzed for the expression of CD25 and T1/ST2. The colors of the histograms correspond to the gates in the dot plots. Numbers show the percentages of gated cells.

(D) BM LSK⁻CD127⁺CD25⁺T1/ST2⁺ (iNH) cells and mature lung NH cells (Lin⁻CD127⁺CD25⁺Sca-1⁺c-Kit^{-low}) were purified and stimulated for 72 hours with PMA plus ionomycin and IL-5 (white), IL-13 (grey) or IL-22 (black) production was measured by ELISA.

(E) RGC mice received *Rora*^{sg/sg} BMT and WT BMT, and iNH cells (black) or CLPs (white) in the BM were analyzed by flow cytometer.

(F) Lung NH cells (black) and BM iNH cells (grey) from normal B6 mice were identified as in (A) and (C) and the expression of CD69, CD27, CXCR4 and CD122 was compared..

(G) BM and Lung leukocytes were stimulated for 4 hr with PMA and ionomycin in the presence of Brefeldin A, followed by cell surface staining and intracellular staining for IL-5. CD45⁺Lin⁻CD127⁺CD25⁺Sca-1⁺ cells were gated and the percent of IL-5⁺ cells was measured.

For all the FACS analysis, Live (PI⁻ or eFluor780⁻), CD45⁺ leukocytes were first gated. *p < 0.05 (two-tailed Student's t-test). Data are representative of three independent experiments (mean and SEM in D and E) (See also Appendix 11)

To test whether BM iNH cells develop into mature NH cells, iNH cells were purified and transplanted into Nod/Scid/*Il2rg*^{-/-} (NSG) mice. We also purified Lin⁻Sca-1^{low}c-Kit^{low}CD127⁺ CLPs, CD127⁻CD25⁻ and CD127⁺CD25⁻ LSK⁻ cells and injected them into NSG (4,500 cells/mouse) mice for comparison. Three weeks after the injection, donor derived CD45.2⁺ NH cells were detected in the small intestine and lung of the mice injected with iNH cells whereas they were barely detectable in those injected with BM CLPs (Figure 18A). No NH cells were detected in mice injected with CD127⁻CD25⁻ and CD127⁺CD25⁻ LSK⁻ cells (data not shown). While iNH cell-derived NH cells were detected in significant numbers in the small intestine (Figure 18B) and the lung (Figure 18C and D), only very

small numbers (~20-100 fold less) of CLP-derived NH cells were detected. It should be noted that purified mature lung NH cells repopulate the lung only for a short term and could not be detected after 3 weeks in the injected mice (Halim et al., 2012a). To determine if lung leukocyte isolation conditions adversely affects cells, we treated BM similar to lung tissue, which did not significantly affect NH cell repopulation (Appendix 12A and B). We also analyzed donor-derived lymphocytes in the spleen (Figure 18E). As expected, the large majority of CLP-derived cells were B cells while small numbers of CD4⁺T cells, CD8⁺T cells and NK cells were also detected in the spleen (Figure 18E, black bars). Only very small number of CD8 T cells and no other donor-derived lymphocytes were detected in the spleen of iNH cell-injected mice (Figure 18E, white bars). CD127⁻CD25⁻ LSK⁻ BM cells developed into CD4⁺ and CD8⁺ T cells (Figure 18E, blue bars) whereas CD127⁺CD25⁻ LSK⁻ cells were similar to CLPs and developed into B, T and NK cells (Figure 18E, red bars), although they had less B cell potential and more T cell potential than CLPs. To further investigate the repopulation dynamics of BM derived progenitors, we also purified lymphoid primed multipotent progenitors (LMPP) as they were reported to have greater NH cell potential than CLP (Yang et al., 2011). Lin⁻Sca-1⁺c-Kit^{hi}Flt3⁺ LMPP, Lin⁻Sca-1^{low}c-Kit^{low}Flt3⁺D127⁺ CLP and iNH cells (Appendix 12C) were purified from WT BM and injected into NSG mice (2,500 cells/mouse), followed by analysis of the lung (Appendix 12D) and small intestine (Appendix 12E) for NH cell reconstitution. As expected, LMPP produced slightly higher numbers of NH cells in both tissues than CLP. Significantly greater numbers of NH cells were derived from iNH cells in both tissues, while iNH cells have significantly less capacity to differentiate into other lymphoid lineages compared to LMPP and CLP (Appendix 12F). Besides B and NK cells, low numbers (less than 5000 cells) of T and NKT cells were detected in CLP and LMPP injected spleens after 3 weeks.

The BM of NSG mice transplanted with LMPP, CLP and iNH cells was also analyzed after 3 weeks for donor-derived iNH cells (Figure 18F). A minor fraction of LMPP or CLP derived cells in the BM of recipients was iNH cells after 3 weeks, whereas the majority of iNH cell-derived cells were iNH cells. The absolute number of iNH cells derived from CLP was significantly lower than that of LMPP, whereas significantly more iNH cells were recovered in the BM of NSG mice injected with iNH cells than those with CLP and LMPP (Figure 18G).

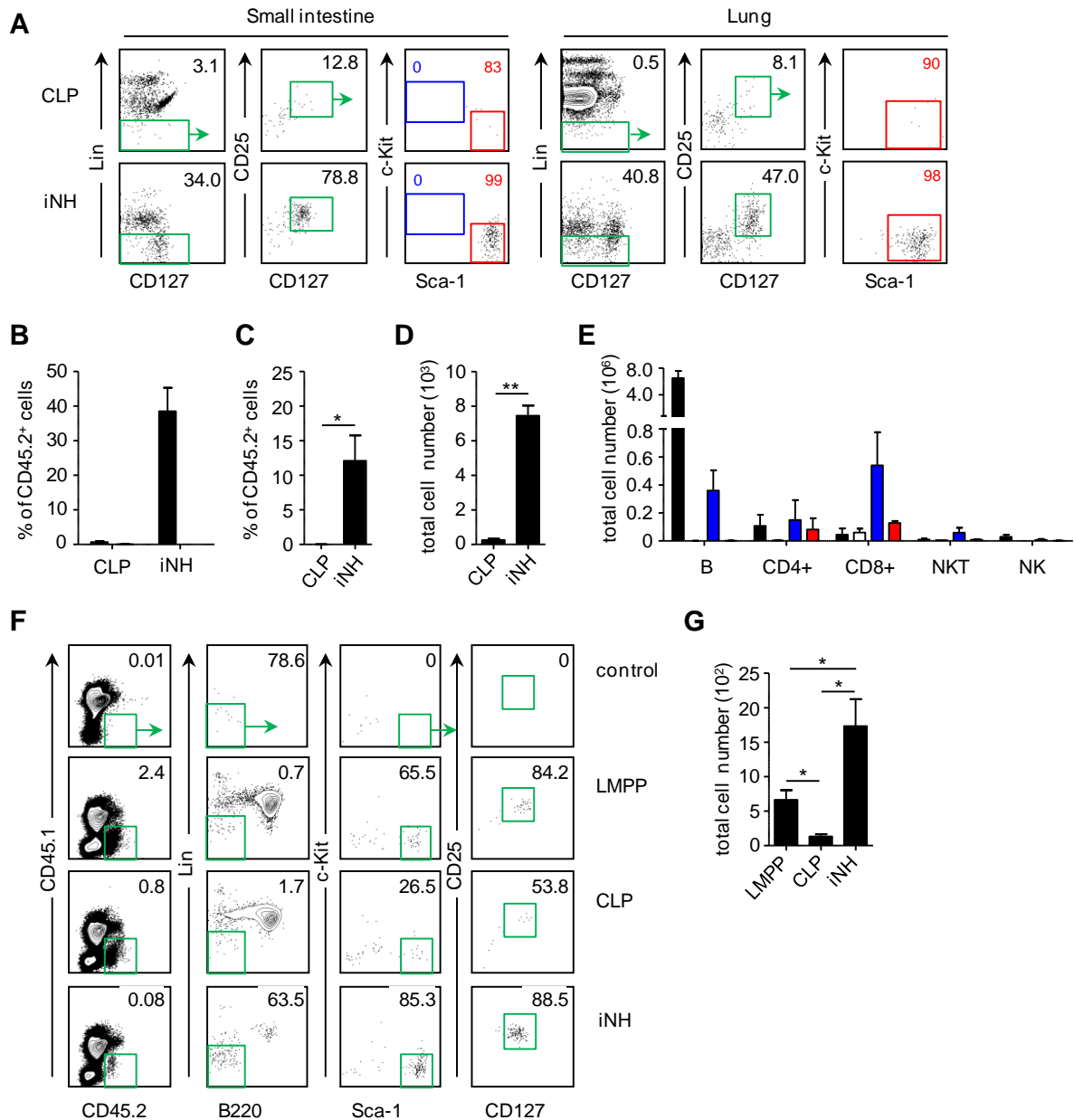


Figure 18 iNH cells are more NH cell lineage restricted and efficient than LMPP or CLP at generating NH cells

(A) CLPs and iNH cells were purified by cell sorting from WT B6 mouse BM, and 4,500 cells per mouse were transplanted into 1 Nod/Scid/*Il2rg*^{-/-} (NSG) mice. Mice were analyzed for donor-derived NH cells (red) and RORγt⁺ ILCs in the small intestine and lung after 3 weeks. Numbers are the percentages of gated cells among live (DAPI), CD45.2⁺ donor leukocytes.

The percentages of donor-derived NH cells in the small intestine (B) and lung (C) in multiple experiments are shown.

(D) Absolute numbers of donor-derived mature NH cells in the lung were calculated.

(E) Donor-derived lymphocytes in the spleen of NSG mice injected with iNH (white), CLP (black), LSK⁻CD127⁺CD25⁺T1/ST2⁻ (blue) and LSK⁻CD127⁻CD25⁺T1/ST2⁻ (red) cells were identified by flow cytometer and quantified.

(F) The BM of NSG mice injected with nothing (control), LMPP, CLP or iNH cells (2,500 cells per mouse) was analyzed 3 weeks after adoptive transplant for iNH cells. Numbers show the percentages of gated cells. Live (PI⁻) cells were first gated.

(G) The absolute number of donor derived iNH cells in the BM (left femur and tibia) of the transplanted mice in (F) was calculated.

*p < 0.05 **p < 0.001 (two-tailed Student's t-test). Data are representative of three independent experiments (mean and SEM in B, C, D, E, and G) (See also Appendix 12)

3.3.5 NH cell-deficient mice have defective inflammatory responses to allergens.

The *in vivo* function of NH cells as a source of innate Th2-cytokines has been established primarily through adoptive transfer of *in vitro* expanded NH cells into lymphodeficient RGC or *Il17rb*^{-/-} mice (Halim et al., 2012a; Moro et al., 2010; Neill et al., 2010; Saenz et al., 2010b) or selective depletion of NH cells from T/NKT/B-cell deficient RAG-knockout mice (Chang et al., 2011; Halim et al., 2012a; Monticelli et al., 2011). However, the importance of NH cells in the presence of the adaptive immune system is still unclear. Therefore, we tested the effects of intranasal administration of protease allergen papain on RGC mice receiving *Rora*^{sg/sg} BMT, which are NH cell deficient but have normal T cells. As in our previous study (Halim et al., 2012a), daily intranasal administration of papain induced severe and acute eosinophilic lung inflammation in control WT BMT mice. Eosinophils were detected in the lung lavage (Figure 19A) and lung tissue (Figure 19B) of WT BMT mice treated with papain, but not heat-inactivated papain. In contrast, eosinophil infiltration was almost undetectable in *Rora*^{sg/sg} BMT mice. WT BMT and *Rora*^{sg/sg} BMT mice did not significantly differ in papain-induced neutrophil infiltration into lung lavage (Figure 19C). They also had the same numbers of other leukocytes, including CD4 T cells, NK cells and B cells, in the lung, and papain-treatment did not significantly change the

leukocyte numbers other than eosinophils (Figure 19D). Papain-induced mucus hyperproduction was also significantly less in *Rora*^{sg/sg} BMT mice than WT BMT mice (Figure 19E). We also tested IL-25-induced peritoneal inflammation. Intraperitoneal injection of IL-25 induced eosinophil infiltration into the peritoneal cavity and mucus production in the small intestine of WT BMT mice while those inflammatory responses were greatly reduced in *Rora*^{sg/sg} BMT mice (Appendix 14). Comprehensive analysis of leukocytes in the peritoneal lavage showed no significant difference in macrophages (Figure 19F), neutrophils, dendritic cells, basophils (Figure 19G), B cells, NK, NKT and T cell subsets (Figure 19I) between WT and *Rora*^{sg/sg} BMT mice treated with IL-25 (see also Appendix 14). These results indicate that even in the presence of intact Th2 cells, NH cells are required for allergen-induced acute eosinophilic inflammation.

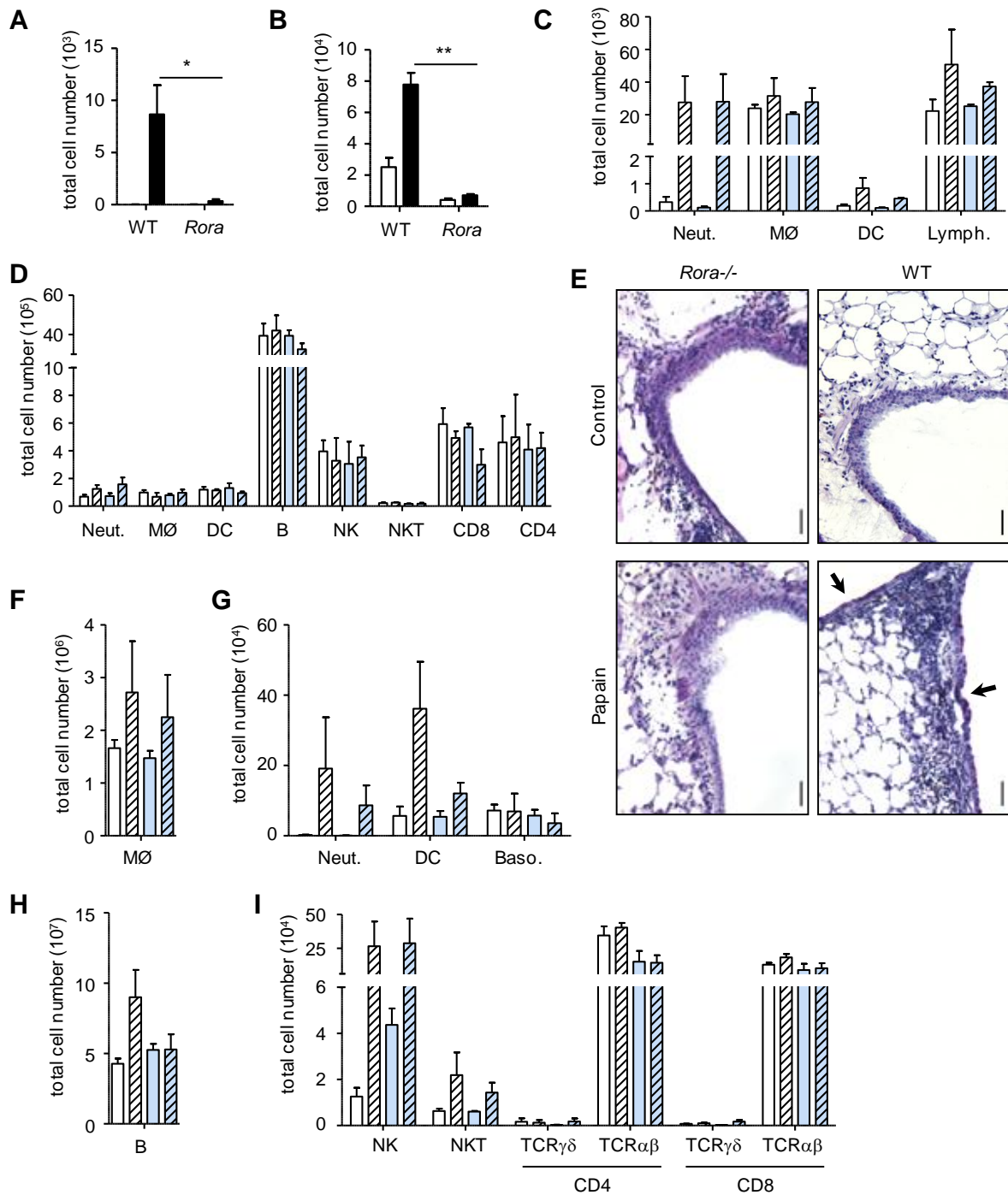


Figure 19 NH cell deficient *Rora*^{sg/sg} BM chimeras have an impaired innate Th2-response.

(A) *Rag2*^{-/-}*Il2rg*^{-/-} (RGC) mice reconstituted with *Rora*^{sg/sg} (*Rora*) or WT BM received three consecutive daily intranasal administration of the protease allergen papain (black bars) or heat-inactivated papain (white bars), and bronchioalveolar lavage was prepared on day 4. Eosinophils in the lavage were identified by FACS and quantified.

(B) Eosinophils in the lung tissues of the mice in (A) were identified by flow cytometer and quantified. White bars show those in mice treated with heat inactivated papain and black bars papain treated.

(C) Indicated leukocytes in bronchioalveolar lavage prepared from WT (white) or *Rora*^{sg/sg} (blue) bone marrow transplanted mice as in (A) were identified by flow cytometer. Results with control mice treated by heat inactivated papain (no stripes) and those with papain treated mice (stripes) are shown.

(D) Indicated leukocytes in the lung tissues of WT (white) or *Rora*^{sg/sg} (blue) bone marrow transplanted mice as in (A) were analyzed and quantified by flow cytometer. Results with control mice treated by heat inactivated papain (no stripes) and those with papain treated mice (stripes) are shown.

(E) RGC mice reconstituted with *Rora*^{sg/sg} (*Rora*) or WT BM were treated with papain as in (A) and mucus production in the lung was analyzed by PAS staining. Black arrows show mucus. Scale bar represents 50 μ m.

(F-I) RGC mice reconstituted with *Rora*^{sg/sg} or WT bone marrow were challenged by three daily intraperitoneal administration of IL-25 or PBS control. Macrophages (F), Neutrophils, DCs, basophils (G) and B cells (H) and other indicated lymphocytes (I) were identified in the peritoneal lavage by FACS in WT (white) or *Rora*^{sg/sg} (blue) bone marrow transplanted mice treated with control (no stripes) or IL-25 (stripes).

* $p < 0.05$, ** $p < 0.001$ (two-tailed Student's t-test). Data are representative of three independent experiments (mean and SEM in A-D and F-I). (See also Appendix 13 and 14).

3.4 Discussion

NH cells and ROR γ t⁺ ILCs represent two populations of innate lymphocytes whose primary function is to produce cytokines. NH cells are stimulated by combinations of IL-33, IL-25, TSLP, IL-7 (Halim et al., 2012a; Moro et al., 2010; Neill et al., 2010; Saenz et al., 2010b) and produce IL-5 and IL-13 whereas ROR γ t⁺ ILCs are stimulated by IL-23 and produce IL-22 and IL-17A. While both share the phenotype of Lin⁻CD127⁺CD25⁺, the lineage relationship between the two innate lymphocyte populations has been unclear. In the current study, innate lymphocytes (Lin⁻CD127⁺CD25⁺) have been divided into two distinct subsets, namely Sca-1⁺c-Kit^{-low} NH cells and Sca-1⁻c-Kit⁺ ROR γ t⁺ ILCs. This allows simultaneous analysis of the two innate lymphocyte populations in multiple tissues, including the lung, small and large intestine and MLN. While both populations are found in the

intestine and MLN, naïve mouse lungs have NH cells but not $\text{ROR}\gamma^+$ ILCs. Our analysis of mutant mice deficient for $\text{ROR}\alpha$ or $\text{ROR}\gamma$, two members of the ROR family of transcription factors, has shown that they differentially regulate the development of the two innate lymphocyte populations in all tissues examined. $\text{ROR}\alpha$ is critical for NH cells but not $\text{ROR}\gamma^+$ ILCs whereas $\text{ROR}\gamma$ is required for $\text{ROR}\gamma^+$ ILCs but not for NH cells, as previously reported (Eberl et al., 2004; Sanos et al., 2009; Sawa et al., 2010). In addition, we have identified a possible NH cell-committed progenitor (iNH cells), that is distinct from CLPs. These iNH cells have the capacity to develop into mature NH cells but not $\text{ROR}\gamma^+$ ILCs. In contrast to Wong et al. we find that CLPs do not efficiently develop into NH cells or $\text{ROR}\gamma^+$ ILCs (Wong et al., 2012).

Our finding with $\text{ROR}\alpha$ -deficient mice is consistent with a very recent report by Wong et al. who have also shown that $\text{ROR}\alpha$ is critical for nuocyte development (Wong et al., 2012). Nuocytes in their study, identified in the MLN by $\text{Lin}^- \text{ICOS}^+ \text{ST2}^+$, produced IL-5 and IL-13 upon stimulation and are therefore likely to be identical to NH cells in the MLN observed in our study. We have shown that $\text{ROR}\alpha$ -deficient, but not $\text{ROR}\gamma$ -deficient, mice have very few NH cells in the lung, small intestine and large intestine. We have also found that NH cells in the small intestine of naïve WT mice do not express T1/ST2, which is often used as a marker for NH cells. We have not been able to detect a significant number of NH cells or $\text{ROR}\gamma^+$ ILCs in the lung and intestine of NSG mice injected with BM CLPs. Instead, we have found that NH cells are generated much more efficiently from NH-like cells termed iNH cells, which are among the LSK^- BM cells. LSK^- cells have been known to have no long-term repopulation capacity, are phenotypically and functionally heterogeneous, and contain early-lymphoid committed progenitors (Kumar et al., 2008). While iNH cells resemble mature NH cells, their cell surface expression of CD27 is higher than lung NH cells.

CD27 is found on hematopoietic stem cells and lymphoid progenitors, and its expression is known to decrease during the maturation of other innate lymphocytes (Gascoyne et al., 2009). Conversely, iNH cells express lower levels of CD69, CXCR4 and CD122 compared to mature lung NH cells in naïve mice. Furthermore, on a per cell basis, iNH cells produce much smaller amounts of Th2 cytokines upon stimulation by PMA plus ionomycin and differ from mature lung NH cells in their response to different cytokine stimulation *in vitro*. When injected into non-irradiated NSG mice, iNH cells amplify and are found in the bone marrow, and become NH cells in the lung and the intestine. It should be noted that mature NH cells isolated from the lung and injected into NSG mice do not expand or persist in the mice (data not shown). Interestingly, a subset of iNH cells in the BM seems to be ROR α -independent as we detect a small number of iNH cells in the BM of RGC mice injected with *Rora*^{sg/sg} BM cells. They might be progenitors for iNH cells that require ROR α for further differentiation into iNH cells.

CLPs in our study are defined by Lin⁻CD127⁺ expressing intermediate levels of Sca-1 and c-Kit (Kondo et al., 1997) and approximately 70% of this population expresses Flt3. When injected into non-irradiated NSG mice, they efficiently develop into splenic T, B and NK cells and a very small number of NH cells. Wong et al. isolated Lin⁻CD127⁺Flt3⁺ BM cells as CLPs and induced their differentiation into nuocytes *in vitro* (Wong et al., 2012). When the same CLP population was injected into irradiated CD45-congenic mice, donor-derived nuocytes were not detected in the MLN unless IL-25 was injected. Thus, CLPs may have residual potential for NH cell differentiation, but they do not seem to be the main source of NH cells *in vivo*. Recent work by the Bhandoola laboratory also showed that CLPs have only limited NH cell potential while more immature Lin⁻Sca-1⁺c-Kit^{hi}Flt3⁺ lymphoid primed multipotent progenitors (LMPP) more efficiently develop into NH cells in the lung

(Yang et al., 2011). Our results confirm that LMPP are indeed more efficient than Lin⁻ CD127⁺Flt3⁺ CLP at generating NH cells, and we furthermore show that iNH cells have significantly more robust potential for NH cell differentiation than either CLP or LMPP. We also show that while LMPP give rise to significantly more iNH cells in the BM after transplantation than CLP, the number of iNH cells that expand after adoptive transfer is also significantly more than both CLP and LMPP. Furthermore, CLP and LMPP by definition are not committed to a single lineage, as seen by the small fraction of iNH cells generated in the BM and the presence of other lymphocytes detected in the spleen, while injected iNH cells appear to be highly restricted to a NH cell fate. As such, it appears likely that CLPs, as currently defined, are heterogeneous with a minor fraction retaining NH cell potential. While LMPPs are likely located upstream of CLPs and iNH cells, most iNH cells probably do not develop from CLPs.

Rora is highly expressed in Th17 cells, which also express *Rorct* (Ivanov et al., 2006; Yang et al., 2008). *Rora*^{sg/sg} mouse spleen CD4 T cells show significantly lower Th17 responses than those of WT mice (Yang et al., 2008). However, *Rora*^{sg/sg} mice are much smaller and have much fewer lymphocytes in general, and they do not live much longer than 3 weeks after birth. Transplantation of BM cells from *Rora*^{sg/sg} RORγt-deficient and double deficient mice into RAG-deficient mice showed that RORα-deficiency has only a minor effect on Th17 cell differentiation. While RORγt is more critical for Th17 cells, deficiency of both RORα and RORγt almost completely inhibited Th17 differentiation. Unlike Th17 cells, NH cells do not express RORγt, and RORα-deficiency alone is sufficient to impair NH cell development as demonstrated by the lack of NH cells in the lung and the intestine of RGC mice receiving *Rora*^{sg/sg} BMT. Importantly, no other defects are detected in these mice, and other Th2 responses appear normal. Nevertheless, these mice do not mount an eosinophilic

lung inflammatory response to the protease allergen papain, which is mediated by Th2 cytokines. Therefore, the data suggest that NH cells are critical for acute allergic inflammation even in the presence of an otherwise intact Th2 cell response. Interestingly, *Rora*^{sg/sg} mice also have an attenuated Th2 response to OVA-induced airway inflammation (Jaradat et al., 2006). In humans, *RORA* has been found to be one of several asthma-associated genes (Moffatt et al., 2010). Previous studies have shown that NH cells are a critical source of Th2 cytokines in RAG-deficient mice, but the *in vivo* role of NH cells in normal mice is still unclear. Further studies of NH cell-deficient mice generated by *Rora*^{sg/sg} BMT into RGC mice will likely reveal the importance of NH cells in allergic diseases including asthma in the presence of intact adaptive immune system.

Chapter 4 General summary and discussion

4.1 Summary

The immune system is designed to detect and destroy invading pathogens. It accomplishes this difficult task through the combined effect of numerous defensive mechanisms. Recent advances in understanding the innate immune system have identified novel cell types that produce important cytokines. My work has added to our understanding of ILCs and the role of lung NH cells in mediating acute Th2-type lung inflammation.

In Chapter 2, I focused on characterizing Lung NH cells and their role in mediating acute allergic lung inflammation in response to protease allergens. Briefly, I discovered NH cells in the lungs of naïve B6 mice. Using different mutant mice and gene expression microarray analyses, I determined that lung NH cells likely constitute a distinct lineage of innate lymphocytes. By means of *in vitro* cell and tissue explant culture, I demonstrated that IL-33 plus co-stimulation plays a critical role in NH cell activation. Lastly, I implicated NH cells in mediating protease-allergen induced acute Th2-type lung inflammation. (Figure 20)

In Chapter 3, I delineated the development of NH cells from a BM derived precursor, and demonstrated the role of *Rora* in NH cell development. Briefly, using flow-cytometry to distinguish accurately between different ILC populations in mucosal tissue, I showed that *Rora*-knockout mice lack NH cells while *Rorc*⁺ ILC are unaffected. Functional studies with *Rora*-knockout BMT mice provide definitive proof of NH cell involvement in instigating protease mediated acute lung inflammation. Furthermore, comparison of WT, ROR α -knockout BM and BMT mice revealed the presence of a novel iNH cell. I demonstrated that iNH cells are functionally immature, phenotypically distinct from mature lung NH cells and

have efficient repopulation capacity. Additionally, I showed that iNH cells are highly lineage-restricted and likely derive primarily from upstream LMPP in the BM. (Figure 21)

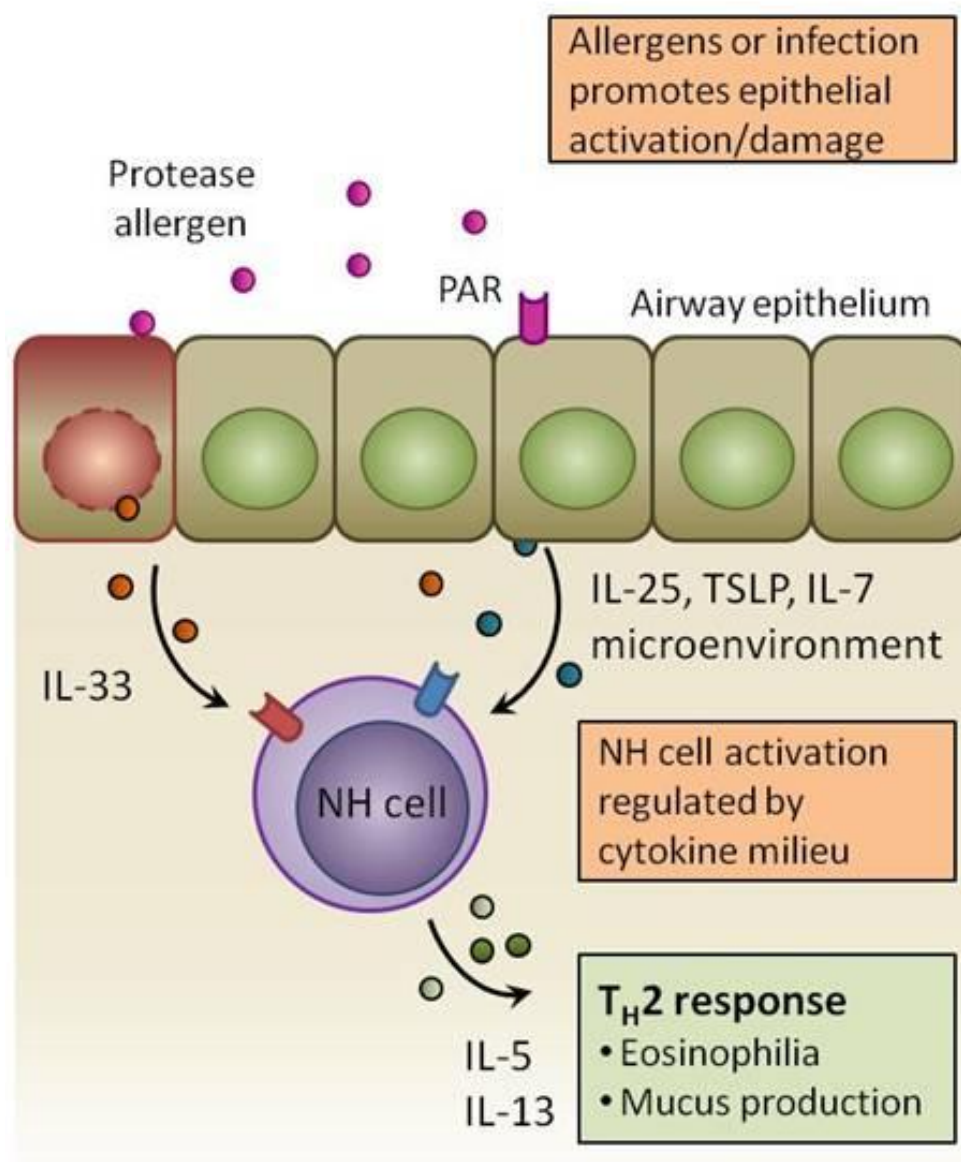


Figure 20 Model for lung NH cell function and activation.

Protease allergens damage or activate the airway epithelium, inducing the release of IL-33 or production of stroma-derived IL-25 or TSLP. NH cells present in naïve lungs are poised to detect these cytokines and rapidly respond by production of IL-5 and IL-13, which are the inducers of Th2-type acute lung inflammation.

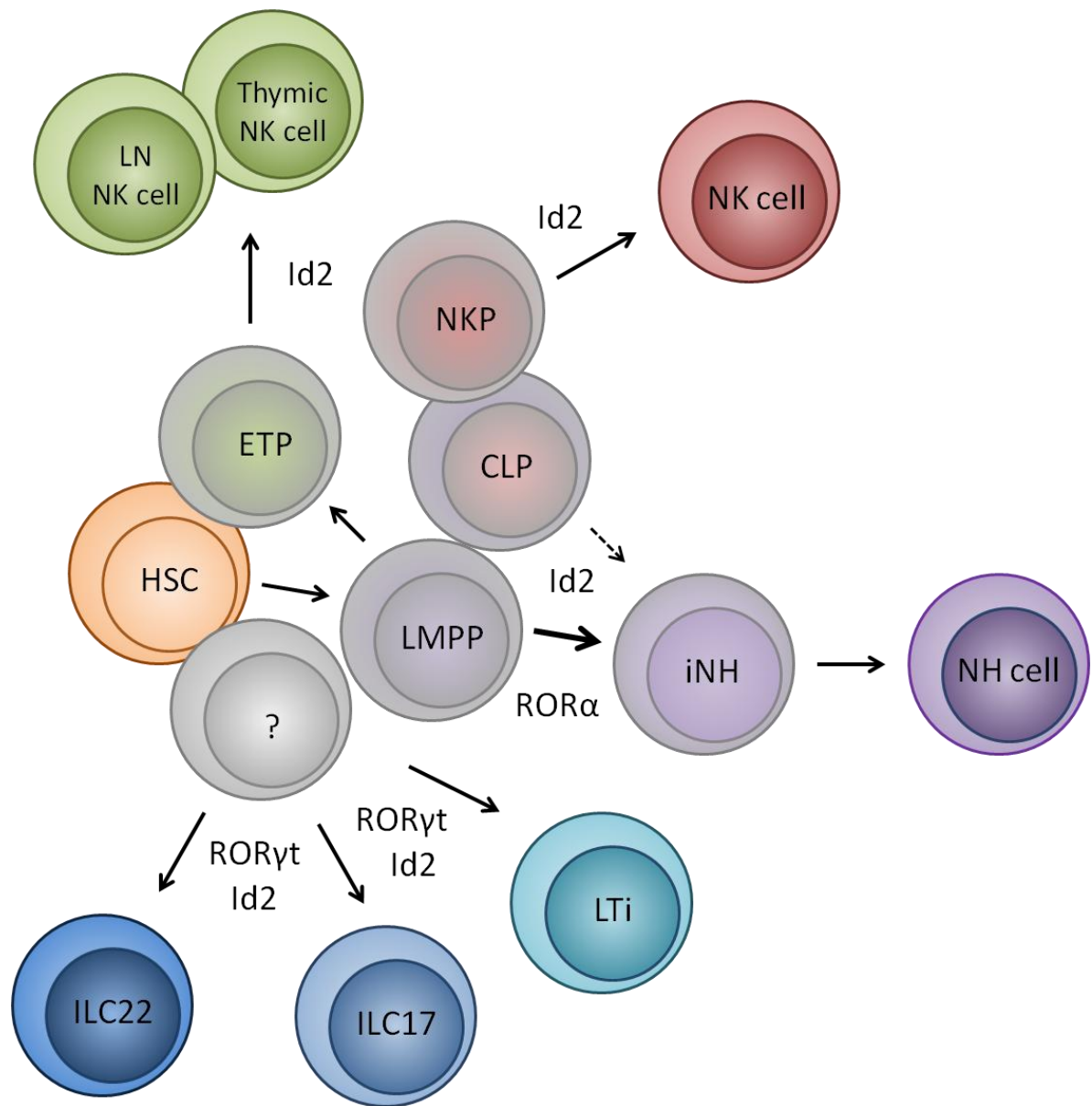


Figure 21 *Rora* in NH cell development.

The development of NH cells occurs in the BM from iNH cells derived primarily from LMPP. While *Id2* is required for all innate lymphocytes, *RORγt* is critical for ILC22, ILC17 and LTi development. The transcription factor *RORα* is important for NH cell development.

4.2 Significance of the work

The discovery of lung NH cells marks an important milestone in the fields of immunology and medicine. Early observations of innate Th2-type responses were noted in RAG-deficient animals and attributed to a poorly defined non-T-non-B cell type. The discovery of innate Th2-cytokine producing cells in the gut reinvigorated interest due to their important physiological role in clearing parasites. The Th2-type cytokine profile of these innate lymphocytes suggests a connection with allergies and asthma. While Th2-cells remain the most abundant Th2-cytokine source in chronic disease such as asthma, the role of lung NH cells in initiating acute inflammation or driving Th2-skewing is highly intriguing. If lung NH cells are indeed located at the start of a Th2 “domino effect”, their manipulation by drugs or other means could represent a breakthrough in asthma treatment.

The identification of *Rora* as an important gene for NH cell development constitutes a groundbreaking finding. *Rora* appears to be a master regulator for NH cell-lineage selection, akin to *Rorct* in *Rorct*⁺ ILCs. This discovery paves the way for future studies looking at the function, expression pattern and regulation of *Rora* in lymphopoiesis. Furthermore, the development of *Rora*-knockout BMT mice provides a model that is deficient in NH cells but has normal Th2 cells.

Our understanding of lymphopoiesis is rapidly evolving with advances in single-cell analysis, imaging technology, and development of genetically-modified model organisms. Entrenched ideas such as the “common lymphoid progenitor” are being challenged by ever increasing resolution of our analyses, new models of haematopoiesis, and the discovery of novel lymphocytes. To this effect, I demonstrate that LMPP are the major contributors to NH cell development through an iNH cell intermediate found in the BM.

4.3 Strength and limitations

While the discovery of lung NH cells in mice constitutes an advance in immunology, we must keep in mind that significant differences exist between rodents and the human immune system. Analysis of human primary lung tissue by Mjosberg et al. reveals the presence of a similar Th2-cytokine producing ILC (Mjosberg et al., 2011). Further study of these cells, possibly using humanized-immune-system (HIS) mice, is required to reveal the role of NH cells in human lung immune function. Similarly, although the presence of a BM derived iNH cell in mice is interesting, the development of NH cells in humans is unknown. The dependence of NH cell development on *Rora* is of great interest, and similar studies should be conducted in humans. Technically, limitations of my work include the lack of a unifying NH cell marker. Although a reliable FACS-staining protocol is described for naïve NH cells in mice, their reliable detection in inflamed tissue remains difficult. If no NH cell lineage-restricted surface marker is discovered, a solution might be to develop *Rora*-reporter mice.

Another limitation in our analysis of iNH cells is the adoptive transfer experiment. As we see engraftment and expansion of iNH cells in the BM, we assume that injected iNH home back to the BM, expand and subsequently seed peripheral tissues. This assumption is attractive but might be incorrect, as injected iNH could possibly also mature and expand in the body. Detailed tracing analysis of injected iNH cells shortly after transfer, or injections directly into marrow can be conducted to provide a more definitive answer.

4.4 Future directions

Future directions should include the logical progression towards applying these findings to humans. Firstly, *Rora* expression and function in human ILC2 should be analyzed. In mouse, the expression of *Rora* should be examined through the generation of reporter-mice and usable antibodies to ROR α . Lineage tracing using combined *Rora* and *Rorct* reporter mice may elucidate the upstream developmental stages of innate lymphoid development, an ILC lineage bifurcation point or a common ILC progenitor. ROR α function and gene-regulation are also of interest, which may be answered by means of ChIP-seq and IP-mass spectrometry analysis. ROR α as a drugable target for inflammatory disease is of great interest, and ROR α agonists and antagonists have been reported in the literature. The effect of these compounds on NH cells should be tested. Finally, the role of NH cells in Th2-skewing of CD4⁺ naïve Th0 cells is an interesting question. As the cellular source of innate Th2 cytokines in acute inflammation, the role of NH cells in creating a “Th2-milieu” should be examined.

References

- Bakalian, A., Kopmels, B., Messer, A., Fradelizi, D., Delhay-Bouchaud, N., Wollman, E., and Mariani, J. (1992). Peripheral macrophage abnormalities in mutant mice with spinocerebellar degeneration. *Res. Immunol.* 143, 129-139.
- Ballantyne, S.J., Barlow, J.L., Jolin, H.E., Nath, P., Williams, A.S., Chung, K.F., Sturton, G., Wong, S.H., and McKenzie, A.N. (2007). Blocking IL-25 prevents airway hyperresponsiveness in allergic asthma. *J. Allergy Clin. Immunol.* 120, 1324-1331.
- Becker-Andre, M., Andre, E., and DeLamarter, J.F. (1993). Identification of nuclear receptor mRNAs by RT-PCR amplification of conserved zinc-finger motif sequences. *Biochem. Biophys. Res. Commun.* 194, 1371-1379.
- Brigl, M., Bry, L., Kent, S.C., Gumperz, J.E., and Brenner, M.B. (2003). Mechanism of CD1d-restricted natural killer T cell activation during microbial infection. *Nat. Immunol.* 4, 1230-1237.
- Bryceson, Y.T., March, M.E., Ljunggren, H.G., and Long, E.O. (2006). Activation, coactivation, and costimulation of resting human natural killer cells. *Immunol. Rev.* 214, 73-91.
- Cerutti, A., Puga, I., and Cols, M. (2011). Innate control of B cell responses. *Trends Immunol.* 32, 202-211.
- Chang, Y.J., Kim, H.Y., Albacker, L.A., Baumgarth, N., McKenzie, A.N., Smith, D.E., Dekruyff, R.H., and Umetsu, D.T. (2011). Innate lymphoid cells mediate influenza-induced airway hyper-reactivity independently of adaptive immunity. *Nat. Immunol.*
- Chi, A.W., Bell, J.J., Zlotoff, D.A., and Bhandoola, A. (2009). Untangling the T branch of the hematopoiesis tree. *Curr. Opin. Immunol.* 21, 121-126.
- Cohn, L., Elias, J.A., and Chupp, G.L. (2004). Asthma: mechanisms of disease persistence and progression. *Annu. Rev. Immunol.* 22, 789-815.
- Crotty, S. (2011). Follicular helper CD4 T cells (TFH). *Annu. Rev. Immunol.* 29, 621-663.
- Cupedo, T., Crellin, N.K., Papazian, N., Rombouts, E.J., Weijer, K., Grogan, J.L., Fibbe, W.E., Cornelissen, J.J., and Spits, H. (2009). Human fetal lymphoid tissue-inducer cells are interleukin 17-producing precursors to RORC⁺ CD127⁺ natural killer-like cells. *Nat. Immunol.* 10, 66-74.
- Duerr, C.U., and Hornef, M.W. (2012). The mammalian intestinal epithelium as integral player in the establishment and maintenance of host-microbial homeostasis. *Semin. Immunol.* 24, 25-35.

- Eberl, G., Marmon, S., Sunshine, M.J., Rennert, P.D., Choi, Y., and Littman, D.R. (2004). An essential function for the nuclear receptor RORgamma(t) in the generation of fetal lymphoid tissue inducer cells. *Nat. Immunol.* 5, 64-73.
- Fathman, J.W., Bhattacharya, D., Inlay, M.A., Seita, J., Karsunky, H., and Weissman, I.L. (2011). Identification of the earliest natural killer cell-committed progenitor in murine bone marrow. *Blood* 118, 5439-5447.
- Flajnik, M.F., and Du Pasquier, L. (2004). Evolution of innate and adaptive immunity: can we draw a line? *Trends Immunol.* 25, 640-644.
- Fujieda, H., Bremner, R., Mears, A.J., and Sasaki, H. (2009). Retinoic acid receptor-related orphan receptor alpha regulates a subset of cone genes during mouse retinal development. *J. Neurochem.* 108, 91-101.
- Galli, S.J., and Tsai, M. (2012). IgE and mast cells in allergic disease. *Nat. Med.* 18, 693-704.
- Gascoyne, D.M., Long, E., Veiga-Fernandes, H., de Boer, J., Williams, O., Seddon, B., Coles, M., Kioussis, D., and Brady, H.J. (2009). The basic leucine zipper transcription factor E4BP4 is essential for natural killer cell development. *Nat. Immunol.* 10, 1118-1124.
- Giguere, V., Tini, M., Flock, G., Ong, E., Evans, R.M., and Otulakowski, G. (1994). Isoform-specific amino-terminal domains dictate DNA-binding properties of ROR alpha, a novel family of orphan hormone nuclear receptors. *Genes Dev.* 8, 538-553.
- Gold, D.A., Baek, S.H., Schork, N.J., Rose, D.W., Larsen, D.D., Sachs, B.D., Rosenfeld, M.G., and Hamilton, B.A. (2003). RORalpha coordinates reciprocal signaling in cerebellar development through sonic hedgehog and calcium-dependent pathways. *Neuron* 40, 1119-1131.
- Gregory, L.G., and Lloyd, C.M. (2011). Orchestrating house dust mite-associated allergy in the lung. *Trends Immunol.* 32, 402-411.
- Guo, J., Hawwari, A., Li, H., Sun, Z., Mahanta, S.K., Littman, D.R., Krangel, M.S., and He, Y.W. (2002). Regulation of the TCRalpha repertoire by the survival window of CD4(+)CD8(+) thymocytes. *Nat. Immunol.* 3, 469-476.
- Halim, T.Y., Krauss, R.H., Sun, A.C., and Takei, F. (2012a). Lung natural helper cells are a critical source of th2 cell-type cytokines in protease allergen-induced airway inflammation. *Immunity* 36, 451-463.
- Halim, T.Y., Maclaren, A., Romanish, M.T., Gold, M.J., McNagny, K.M., and Takei, F. (2012b). Retinoic-Acid-Receptor-Related Orphan Nuclear Receptor Alpha Is Required for Natural Helper Cell Development and Allergic Inflammation. *Immunity* 37, 463-474.
- Hamelmann, E., and Gelfand, E.W. (2001). IL-5-induced airway eosinophilia--the key to asthma? *Immunol. Rev.* 179, 182-191.

Heng, T.S., Painter, M.W., and Immunological Genome Project Consortium. (2008). The Immunological Genome Project: networks of gene expression in immune cells. *Nat. Immunol.* 9, 1091-1094.

Henjakovic, M., Martin, C., Hoymann, H.G., Sewald, K., Ressmeyer, A.R., Dassow, C., Pohlmann, G., Krug, N., Uhlig, S., and Braun, A. (2008). Ex vivo lung function measurements in precision-cut lung slices (PCLS) from chemical allergen-sensitized mice represent a suitable alternative to in vivo studies. *Toxicol. Sci.* 106, 444-453.

Hurst, S.D., Muchamuel, T., Gorman, D.M., Gilbert, J.M., Clifford, T., Kwan, S., Menon, S., Seymour, B., Jackson, C., Kung, T.T., *et al.* (2002). New IL-17 family members promote Th1 or Th2 responses in the lung: in vivo function of the novel cytokine IL-25. *J. Immunol.* 169, 443-453.

Ivanov, I.I., McKenzie, B.S., Zhou, L., Tadokoro, C.E., Lepelley, A., Lafaille, J.J., Cua, D.J., and Littman, D.R. (2006). The orphan nuclear receptor ROR γ directs the differentiation program of proinflammatory IL-17+ T helper cells. *Cell* 126, 1121-1133.

Jaradat, M., Stapleton, C., Tilley, S.L., Dixon, D., Erikson, C.J., McCaskill, J.G., Kang, H.S., Angers, M., Liao, G., Collins, J., Grissom, S., and Jetten, A.M. (2006). Modulatory role for retinoid-related orphan receptor alpha in allergen-induced lung inflammation. *Am. J. Respir. Crit. Care Med.* 174, 1299-1309.

Jetten, A.M. (2009). Retinoid-related orphan receptors (RORs): critical roles in development, immunity, circadian rhythm, and cellular metabolism. *Nucl. Recept. Signal.* 7, e003.

Journiac, N., Jolly, S., Jarvis, C., Gautheron, V., Rogard, M., Trembleau, A., Blondeau, J.P., Mariani, J., and Vernet-der Garabedian, B. (2009). The nuclear receptor ROR(alpha) exerts a bi-directional regulation of IL-6 in resting and reactive astrocytes. *Proc. Natl. Acad. Sci. U. S. A.* 106, 21365-21370.

Kaiko, G.E., and Foster, P.S. (2011). New insights into the generation of Th2 immunity and potential therapeutic targets for the treatment of asthma. *Curr. Opin. Allergy Clin. Immunol.* 11, 39-45.

Karre, K., Ljunggren, H.G., Piontek, G., and Kiessling, R. (1986). Selective rejection of H-2-deficient lymphoma variants suggests alternative immune defence strategy. *Nature* 319, 675-678.

Kiel, M.J., Yilmaz, O.H., Iwashita, T., Yilmaz, O.H., Terhorst, C., and Morrison, S.J. (2005). SLAM family receptors distinguish hematopoietic stem and progenitor cells and reveal endothelial niches for stem cells. *Cell* 121, 1109-1121.

Kim, H.Y., DeKruyff, R.H., and Umetsu, D.T. (2010). The many paths to asthma: phenotype shaped by innate and adaptive immunity. *Nat. Immunol.* 11, 577-584.

Kita, H. (2011). Eosinophils: multifaceted biological properties and roles in health and disease. *Immunol. Rev.* 242, 161-177.

Kondo, M., Weissman, I.L., and Akashi, K. (1997). Identification of clonogenic common lymphoid progenitors in mouse bone marrow. *Cell* 91, 661-672.

Kondo, Y., Yoshimoto, T., Yasuda, K., Futatsugi-Yumikura, S., Morimoto, M., Hayashi, N., Hoshino, T., Fujimoto, J., and Nakanishi, K. (2008). Administration of IL-33 induces airway hyperresponsiveness and goblet cell hyperplasia in the lungs in the absence of adaptive immune system. *Int. Immunol.* 20, 791-800.

Koo, G.C., Jacobson, J.B., Hammerling, G.J., and Hammerling, U. (1980). Antigenic profile of murine natural killer cells. *J. Immunol.* 125, 1003-1006.

Kool, M., Hammad, H., and Lambrecht, B.N. (2012). Cellular networks controlling Th2 polarization in allergy and immunity. *F1000 Biol. Rep.* 4, 6.

Kumar, R., Fossati, V., Israel, M., and Snoeck, H.W. (2008). Lin-Sca1+kit- bone marrow cells contain early lymphoid-committed precursors that are distinct from common lymphoid progenitors. *J. Immunol.* 181, 7507-7513.

Lloyd, C.M., and Hessel, E.M. (2010). Functions of T cells in asthma: more than just T(H)2 cells. *Nat. Rev. Immunol.* 10, 838-848.

Mandelboim, O., Lieberman, N., Lev, M., Paul, L., Arnon, T.I., Bushkin, Y., Davis, D.M., Strominger, J.L., Yewdell, J.W., and Porgador, A. (2001). Recognition of haemagglutinins on virus-infected cells by NKp46 activates lysis by human NK cells. *Nature* 409, 1055-1060.

Martin, F., and Kearney, J.F. (2000). B-cell subsets and the mature preimmune repertoire. Marginal zone and B1 B cells as part of a "natural immune memory". *Immunol. Rev.* 175, 70-79.

Matsui, T., Sashihara, S., Oh, Y., and Waxman, S.G. (1995). An orphan nuclear receptor, mROR alpha, and its spatial expression in adult mouse brain. *Brain Res. Mol. Brain Res.* 33, 217-226.

Mauri, C., and Ehrenstein, M.R. (2008). The 'short' history of regulatory B cells. *Trends Immunol.* 29, 34-40.

McKenzie, G.J., Emson, C.L., Bell, S.E., Anderson, S., Fallon, P., Zurawski, G., Murray, R., Grencis, R., and McKenzie, A.N. (1998). Impaired development of Th2 cells in IL-13-deficient mice. *Immunity* 9, 423-432.

Mjosberg, J.M., Trifari, S., Crellin, N.K., Peters, C.P., van Drunen, C.M., Piet, B., Fokkens, W.J., Cupedo, T., and Spits, H. (2011). Human IL-25- and IL-33-responsive type 2 innate lymphoid cells are defined by expression of CCR4 and CD161. *Nat. Immunol.* 12, 1055-1062.

Moffatt, M.F., Gut, I.G., Demenais, F., Strachan, D.P., Bouzigon, E., Heath, S., von Mutius, E., Farrall, M., Lathrop, M., Cookson, W.O., and GABRIEL Consortium. (2010). A large-

scale, consortium-based genomewide association study of asthma. *N. Engl. J. Med.* 363, 1211-1221.

Mogensen, T.H. (2009). Pathogen recognition and inflammatory signaling in innate immune defenses. *Clin. Microbiol. Rev.* 22, 240-73, Table of Contents.

Monticelli, L.A., Sonnenberg, G.F., Abt, M.C., Alenghat, T., Ziegler, C.G., Doering, T.A., Angelosanto, J.M., Laidlaw, B.J., Yang, C.Y., Sathaliyawala, T., *et al.* (2011). Innate lymphoid cells promote lung-tissue homeostasis after infection with influenza virus. *Nat. Immunol.* 12, 1045-1054.

Moro, K., Yamada, T., Tanabe, M., Takeuchi, T., Ikawa, T., Kawamoto, H., Furusawa, J., Ohtani, M., Fujii, H., and Koyasu, S. (2010). Innate production of T(H)2 cytokines by adipose tissue-associated c-Kit(+)Sca-1(+) lymphoid cells. *Nature* 463, 540-544.

Moussion, C., Ortega, N., and Girard, J.P. (2008). The IL-1-like cytokine IL-33 is constitutively expressed in the nucleus of endothelial cells and epithelial cells in vivo: a novel 'alarmin'? *PLoS One* 3, e3331.

Murphy, K., Travers, P., and Walport, M. (2007). *Janeway's Immunobiology* (New York, US: Garland Science).

Neill, D.R., Wong, S.H., Bellosi, A., Flynn, R.J., Daly, M., Langford, T.K., Bucks, C., Kane, C.M., Fallon, P.G., Pannell, R., Jolin, H.E., and McKenzie, A.N. (2010). Nuocytes represent a new innate effector leukocyte that mediates type-2 immunity. *Nature* 464, 1367-1370.

Novey, H.S., Marchioli, L.E., Sokol, W.N., and Wells, I.D. (1979). Papain-induced asthma--physiological and immunological features. *J. Allergy Clin. Immunol.* 63, 98-103.

Oboki, K., Ohno, T., Kajiwara, N., Arae, K., Morita, H., Ishii, A., Nambu, A., Abe, T., Kiyonari, H., Matsumoto, K., *et al.* (2010). IL-33 is a crucial amplifier of innate rather than acquired immunity. *Proc. Natl. Acad. Sci. U. S. A.* 107, 18581-18586.

O'Shea, J.J., and Paul, W.E. (2010). Mechanisms underlying lineage commitment and plasticity of helper CD4+ T cells. *Science* 327, 1098-1102.

Paul, W.E., and Zhu, J. (2010). How are T(H)2-type immune responses initiated and amplified? *Nat. Rev. Immunol.* 10, 225-235.

Pichery, M., Mirey, E., Mercier, P., Lefrancais, E., Dujardin, A., Ortega, N., and Girard, J.P. (2012). Endogenous IL-33 Is Highly Expressed in Mouse Epithelial Barrier Tissues, Lymphoid Organs, Brain, Embryos, and Inflamed Tissues: In Situ Analysis Using a Novel IL-33-LacZ Gene Trap Reporter Strain. *J. Immunol.* 188, 3488-3495.

Price, A.E., Liang, H.E., Sullivan, B.M., Reinhardt, R.L., Eisle, C.J., Erle, D.J., and Locksley, R.M. (2010). Systemically dispersed innate IL-13-expressing cells in type 2 immunity. *Proc. Natl. Acad. Sci. U. S. A.* 107, 11489-11494.

- Rankin, L., and Belz, G.T. (2011). Diverse roles of inhibitor of differentiation 2 in adaptive immunity. *Clin. Dev. Immunol.* 2011, 281569.
- Reed, C.E., and Kita, H. (2004). The role of protease activation of inflammation in allergic respiratory diseases. *J. Allergy Clin. Immunol.* 114, 997-1008; quiz 1009.
- Saenz, S.A., Noti, M., and Artis, D. (2010a). Innate immune cell populations function as initiators and effectors in Th2 cytokine responses. *Trends Immunol.* 31, 407-413.
- Saenz, S.A., Siracusa, M.C., Perrigoue, J.G., Spencer, S.P., Urban, J.F., Jr, Tocker, J.E., Budelsky, A.L., Kleinschek, M.A., Kastelein, R.A., Kambayashi, T., Bhandoola, A., and Artis, D. (2010b). IL25 elicits a multipotent progenitor cell population that promotes T(H)2 cytokine responses. *Nature* 464, 1362-1366.
- Sakaguchi, S., Wing, K., and Miyara, M. (2007). Regulatory T cells - a brief history and perspective. *Eur. J. Immunol.* 37 Suppl 1, S116-23.
- Sanos, S.L., Bui, V.L., Mortha, A., Oberle, K., Heners, C., Johner, C., and Diefenbach, A. (2009). RORgammat and commensal microflora are required for the differentiation of mucosal interleukin 22-producing NKp46+ cells. *Nat. Immunol.* 10, 83-91.
- Sawa, S., Cherrier, M., Lochner, M., Satoh-Takayama, N., Fehling, H.J., Langa, F., Di Santo, J.P., and Eberl, G. (2010). Lineage relationship analysis of RORgammat+ innate lymphoid cells. *Science* 330, 665-669.
- Schmitz, J., Owyang, A., Oldham, E., Song, Y., Murphy, E., McClanahan, T.K., Zurawski, G., Moshrefi, M., Qin, J., Li, X., *et al.* (2005). IL-33, an interleukin-1-like cytokine that signals via the IL-1 receptor-related protein ST2 and induces T helper type 2-associated cytokines. *Immunity* 23, 479-490.
- Schneider, E., Petit-Bertron, A.F., Bricard, R., Levasseur, M., Ramadan, A., Girard, J.P., Herbelin, A., and Dy, M. (2009). IL-33 activates unprimed murine basophils directly in vitro and induces their in vivo expansion indirectly by promoting hematopoietic growth factor production. *J. Immunol.* 183, 3591-3597.
- Siracusa, M.C., Wojno, E.D., and Artis, D. (2012). Functional heterogeneity in the basophil cell lineage. *Adv. Immunol.* 115, 141-159.
- Spits, H., and Cupedo, T. (2012). Innate lymphoid cells: emerging insights in development, lineage relationships, and function. *Annu. Rev. Immunol.* 30, 647-675.
- Spits, H., and Di Santo, J.P. (2011). The expanding family of innate lymphoid cells: regulators and effectors of immunity and tissue remodeling. *Nat. Immunol.* 12, 21-27.
- Steinke, J.W., and Borish, L. (2001). Th2 cytokines and asthma. Interleukin-4: its role in the pathogenesis of asthma, and targeting it for asthma treatment with interleukin-4 receptor antagonists. *Respir. Res.* 2, 66-70.

Strickland, D.H., Upham, J.W., and Holt, P.G. (2010). Epithelial-dendritic cell interactions in allergic disorders. *Curr. Opin. Immunol.* 22, 789-794.

Sun, J.C., Beilke, J.N., and Lanier, L.L. (2009). Adaptive immune features of natural killer cells. *Nature* 457, 557-561.

Terashima, A., Watarai, H., Inoue, S., Sekine, E., Nakagawa, R., Hase, K., Iwamura, C., Nakajima, H., Nakayama, T., and Taniguchi, M. (2008). A novel subset of mouse NKT cells bearing the IL-17 receptor B responds to IL-25 and contributes to airway hyperreactivity. *J. Exp. Med.* 205, 2727-2733.

Thompson, P.J., Asokanathan, N., and Knight, D. and Stewart, G. A. (2001). Protease-activated receptors and the airway epithelium. *Clinical & Experimental Allergy Reviews* 1, 107-110.

Trenkner, E., and Hoffmann, M.K. (1986). Defective development of the thymus and immunological abnormalities in the neurological mouse mutation "staggerer". *J. Neurosci.* 6, 1733-1737.

Tsuji, M., Suzuki, K., Kitamura, H., Maruya, M., Kinoshita, K., Ivanov, I.I., Itoh, K., Littman, D.R., and Fagarasan, S. (2008). Requirement for lymphoid tissue-inducer cells in isolated follicle formation and T cell-independent immunoglobulin A generation in the gut. *Immunity* 29, 261-271.

Urbanek, P., Wang, Z.Q., Fetka, I., Wagner, E.F., and Busslinger, M. (1994). Complete block of early B cell differentiation and altered patterning of the posterior midbrain in mice lacking Pax5/BSAP. *Cell* 79, 901-912.

van Rijt, L.S., Kuipers, H., Vos, N., Hijdra, D., Hoogsteden, H.C., and Lambrecht, B.N. (2004). A rapid flow cytometric method for determining the cellular composition of bronchoalveolar lavage fluid cells in mouse models of asthma. *J. Immunol. Methods* 288, 111-121.

Veinotte, L.L., Halim, T.Y., and Takei, F. (2008). Unique subset of natural killer cells develops from progenitors in lymph node. *Blood* 111, 4201-4208.

Voehringer, D., Reese, T.A., Huang, X., Shinkai, K., and Locksley, R.M. (2006). Type 2 immunity is controlled by IL-4/IL-13 expression in hematopoietic non-eosinophil cells of the innate immune system. *J. Exp. Med.* 203, 1435-1446.

Wills-Karp, M. (2004). Interleukin-13 in asthma pathogenesis. *Immunol. Rev.* 202, 175-190.

Wong, S.H., Walker, J.A., Jolin, H.E., Drynan, L.F., Hams, E., Camelo, A., Barlow, J.L., Neill, D.R., Panova, V., Koch, U., *et al.* (2012). Transcription factor ROR α is critical for nuocyte development. *Nature immunology*

Yang, L., Anderson, D.E., Baecher-Allan, C., Hastings, W.D., Bettelli, E., Oukka, M., Kuchroo, V.K., and Hafler, D.A. (2008). IL-21 and TGF-beta are required for differentiation of human T(H)17 cells. *Nature* 454, 350-352.

Yang, Q., Saenz, S.A., Zlotoff, D.A., Artis, D., and Bhandoola, A. (2011). Cutting edge: Natural helper cells derive from lymphoid progenitors. *J. Immunol.* 187, 5505-5509.

Yang, X.O., Pappu, B.P., Nurieva, R., Akimzhanov, A., Kang, H.S., Chung, Y., Ma, L., Shah, B., Panopoulos, A.D., Schluns, K.S., *et al.* (2008). T helper 17 lineage differentiation is programmed by orphan nuclear receptors ROR alpha and ROR gamma. *Immunity* 28, 29-39.

Zhao, Y., Lin, Y., Zhan, Y., Yang, G., Louie, J., Harrison, D.E., and Anderson, W.F. (2000). Murine hematopoietic stem cell characterization and its regulation in BM transplantation. *Blood* 96, 3016-3022.

Ziegelbauer, K., Speich, B., Mausezahl, D., Bos, R., Keiser, J., and Utzinger, J. (2012). Effect of sanitation on soil-transmitted helminth infection: systematic review and meta-analysis. *PLoS Med.* 9, e1001162.

Ziegler, S.F., and Artis, D. (2010). Sensing the outside world: TSLP regulates barrier immunity. *Nat. Immunol.* 11, 289-293.

Appendices

Appendix 1 Backgating analysis of lung NH cells.

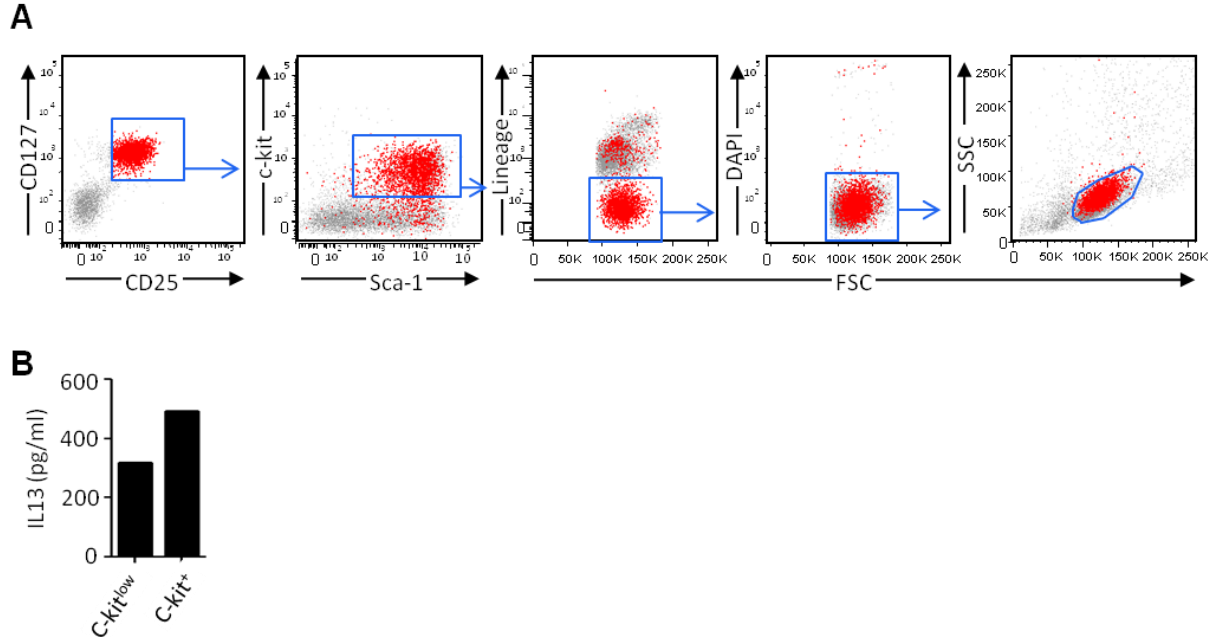


Figure 22 Backgating analysis of lung NH cells.

(A) Backgating analysis of the main Lin⁻Sca-1⁺c-kit⁺CD25⁺CD127⁺ population was conducted in FlowJo. A small number of Lin⁻Sca-1⁺c-kit^{low}CD25⁺CD127⁺ cells are present in the lung.

(B) FACS purified Lin⁻Sca-1⁺c-kit^{low}CD25⁺CD127⁺ and Lin⁻Sca-1⁺c-kit⁺CD25⁺CD127⁺ were stimulated with PMA plus ionomycin (1.0×10^3 cells per well) and culture supernatant was analyzed for IL-13 production after 3 days.

Mean of two independent experiments shown.

Appendix 2 The frequency, phenotype and cytokine production capacity of lung NH cells in *Rag1*^{-/-} mice, and myeloid and lymphoid potential of lung NH cells.

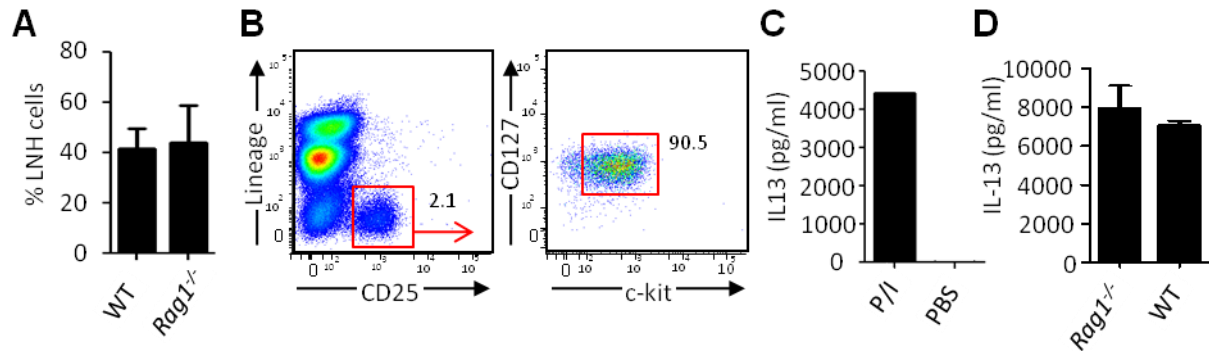


Figure 23 The frequency, phenotype and cytokine production capacity of lung NH cells in *Rag1*^{-/-} mice, and myeloid and lymphoid potential of lung NH cells.

(A) The percentage of lung NH cells amongst Lin⁻Sca-1⁺c-kit^{+/low} cells in WT and *Rag1*^{-/-} mice was compared. Data are representative of 3 independent experiments (mean and SEM).

(B) CD25 is expressed exclusively on lung NH cells in *Rag1*^{-/-} mice. *Rag1*^{-/-} lung cells were analyzed by flow cytometry, plot shown was electronically gated for lymphocytes by FSC/SCC and live cells by DAPI-positive cell exclusion. Result shown is representative of at least 3 independent experiments.

(C) *Rag1*^{-/-} lung NH cells are functionally competent. FACS purified *Rag1*^{-/-} lung Lin⁻Sca-1⁺c-kit^{+/low}CD25⁺CD127⁺ cells (3.5×10^3 cells per well) were stimulated with PMA plus ionomycin for 3 days, followed by ELISA of cell supernatant.

(D) FACS purified WT and *Rag1*^{-/-} lung Lin⁻Sca-1⁺c-kit^{+/low}CD25⁺CD127⁺ cells (1.0×10^3 cells per well) were stimulated with IL-33 (10 ng/ml) and TSLP (10 ng/ml) for 3 days, followed by ELISA of cell supernatant.

Data are representative of 3 independent experiments (mean and SEM).

Appendix 3 Lung NH cells do not have myeloid or lymphoid potential.

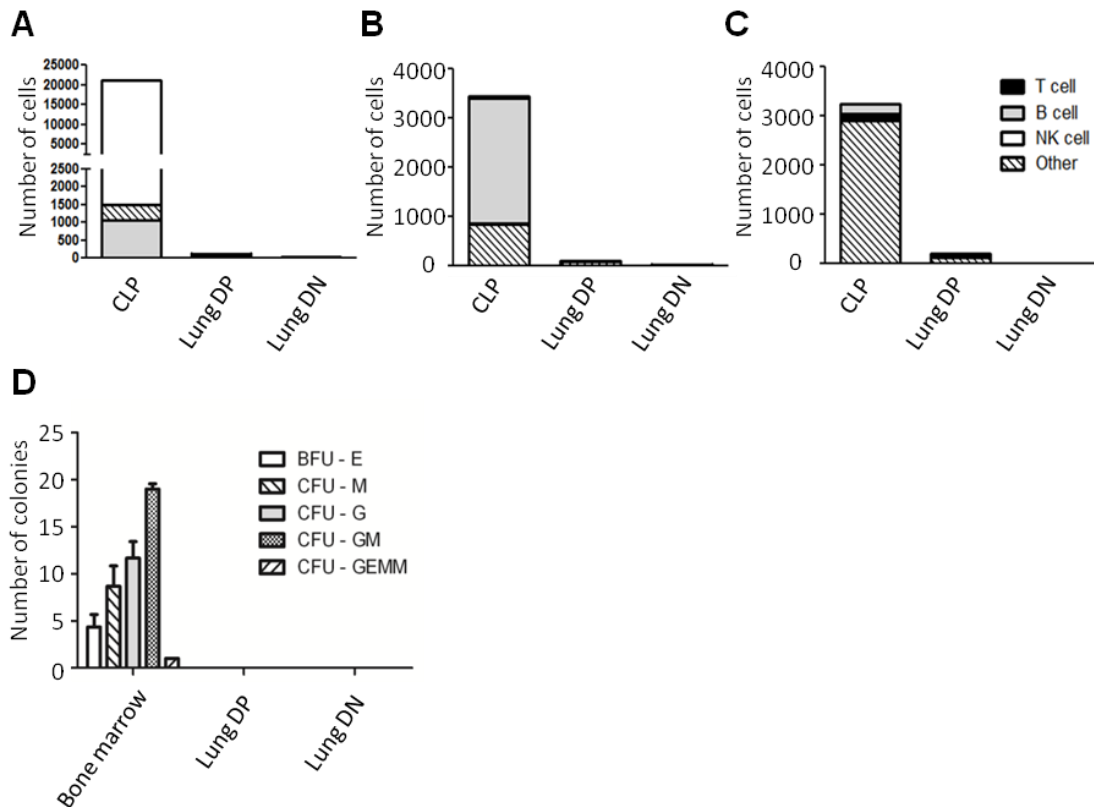


Figure 24 Lung NH cells do not have myeloid or lymphoid potential.

Lymphoid potential of FACS purified lung $\text{Lin}^- \text{Sca-1}^+ \text{c-kit}^+ \text{CD25}^+ \text{CD127}^+$ (Lung DP), $\text{Lin}^- \text{Sca-1}^+ \text{c-kit}^+ \text{CD25}^- \text{CD127}^-$ (Lung DN), or bone marrow common lymphoid progenitors (CLP) was assayed using *in vitro* differentiation cultures (1000 cells/culture) for T cell (A), B cell (B) or NK cells (C). Cells were harvested after 2 weeks, counted, and analyzed for percent CD3 ϵ (T-cell), CD19 (B-cell) or NK1.1 (NK cell) expression by flow cytometry. Data in bar charts is the mean of 2 independent experiments.

(D) Myeloid potential of FACS purified lung DP, lung DN (1000 cells/culture) or whole bone marrow control (20,000 cells/culture) was examined by methylcellulose colony forming assay. Colonies were counted and categorized based on morphology as erythroid (BFU-E), macrophage (CFU-M), granulocyte (CFU-G), granulocyte/macrophage (CFU-GM), granulocyte/erythroid/monocyte/megakaryocyte (CFU-GEMM).

Data are representative of 3 independent experiments (mean and SEM).

Appendix 4 Stimulation by PMA plus ionomycin (P/I) induced IL-5 and IL-13 production from WT and *Rag1*^{-/-} lung explants, but not from *Rag2*^{-/-}*Il2rg*^{-/-} lung explants.

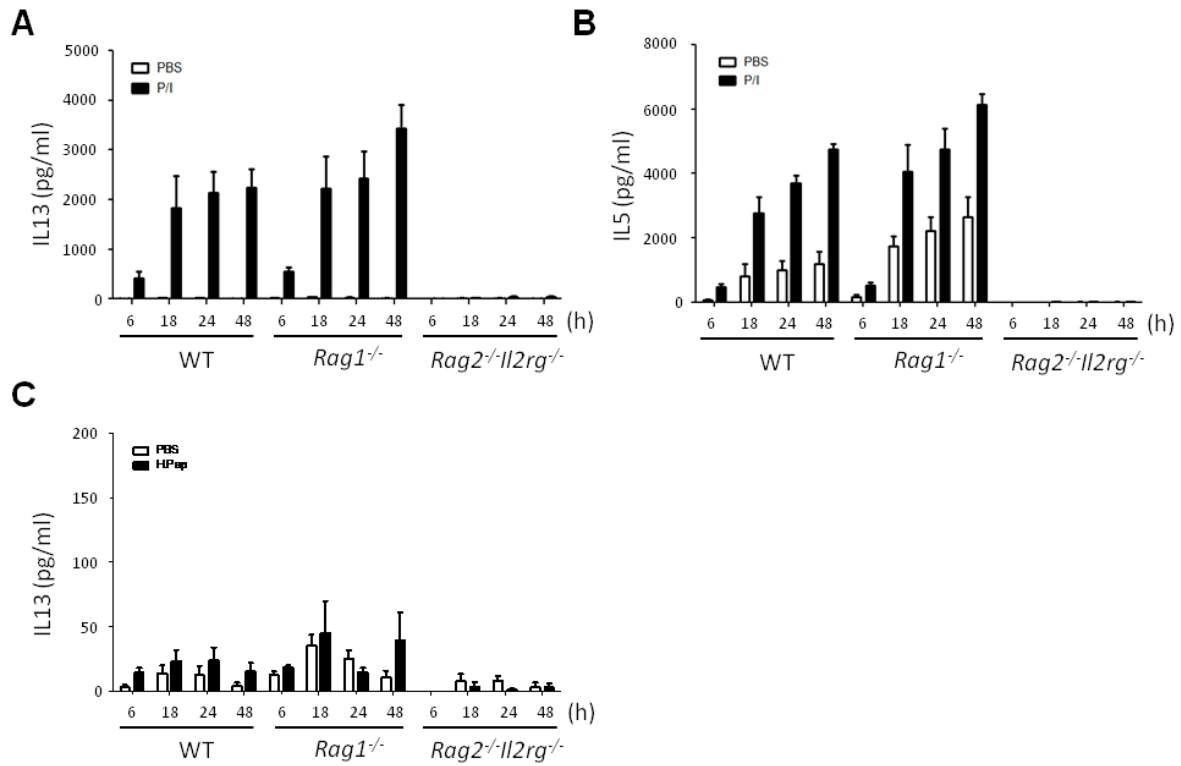


Figure 25 Stimulation by PMA plus ionomycin (P/I) induced IL-5 and IL-13 production from WT and *Rag1*^{-/-} lung explants, but not from *Rag2*^{-/-}*Il2rg*^{-/-} lung explants.

(1/6 lung in 2 ml media per well) Culture supernatant IL-13 (A) or IL-5 (B) levels were assayed by ELISA at the times indicated on the x-axis.

(C) Heat-inactivated papain and PBS were used to stimulate explant cultures (1/6 lung in 2 ml media per well) of the indicated strains, and culture supernatant was collected for IL-13 analysis by ELISA.

Data are representative of 3 independent experiments (mean and SEM).

Appendix 5 Papain stimulation induces a lung NH cell dependent Th2 response.

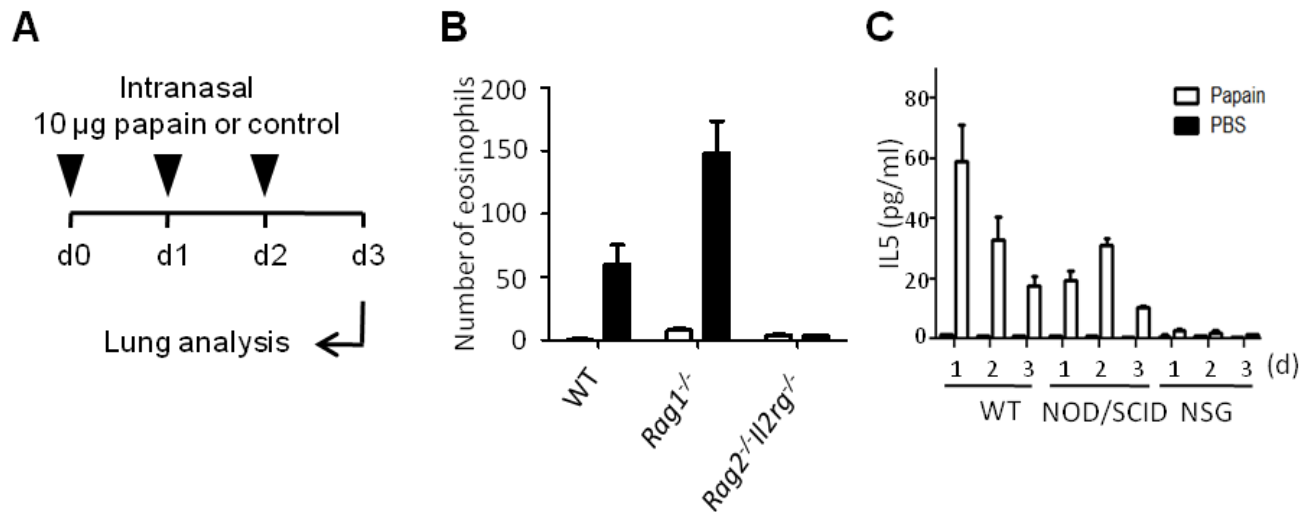


Figure 26 Papain stimulation induces a lung NH cell dependent Th2 response.

(A) Mice were injected intranasally with papain or control (PBS or heat-inactivated papain) once a day for three days. Mice were sacrificed 24 hours after the last injection and BAL was collected and lungs were dissected for analysis.

(B) Lung sections prepared from heat-inactivated (white) or papain (black) treated mice were stained with H&E stain. The number of eosinophils in ten 20× fields was counted.

(C) WT and NOD/SCID but not NOD/SCID/*Il2rg*^{-/-} (NSG) mice respond to intranasal papain treatment by IL-5 production, but not to PBS control. Blood samples were taken on day 1 to 3 after first injection and analyzed for serum IL-5 by ELISA.

Data are representative of 3 independent experiments (mean and SEM in B and C).

Appendix 6 lung NH cell depletion in *Rag1*^{-/-} mice followed by intranasal stimulation with protease allergen or house dust mite.

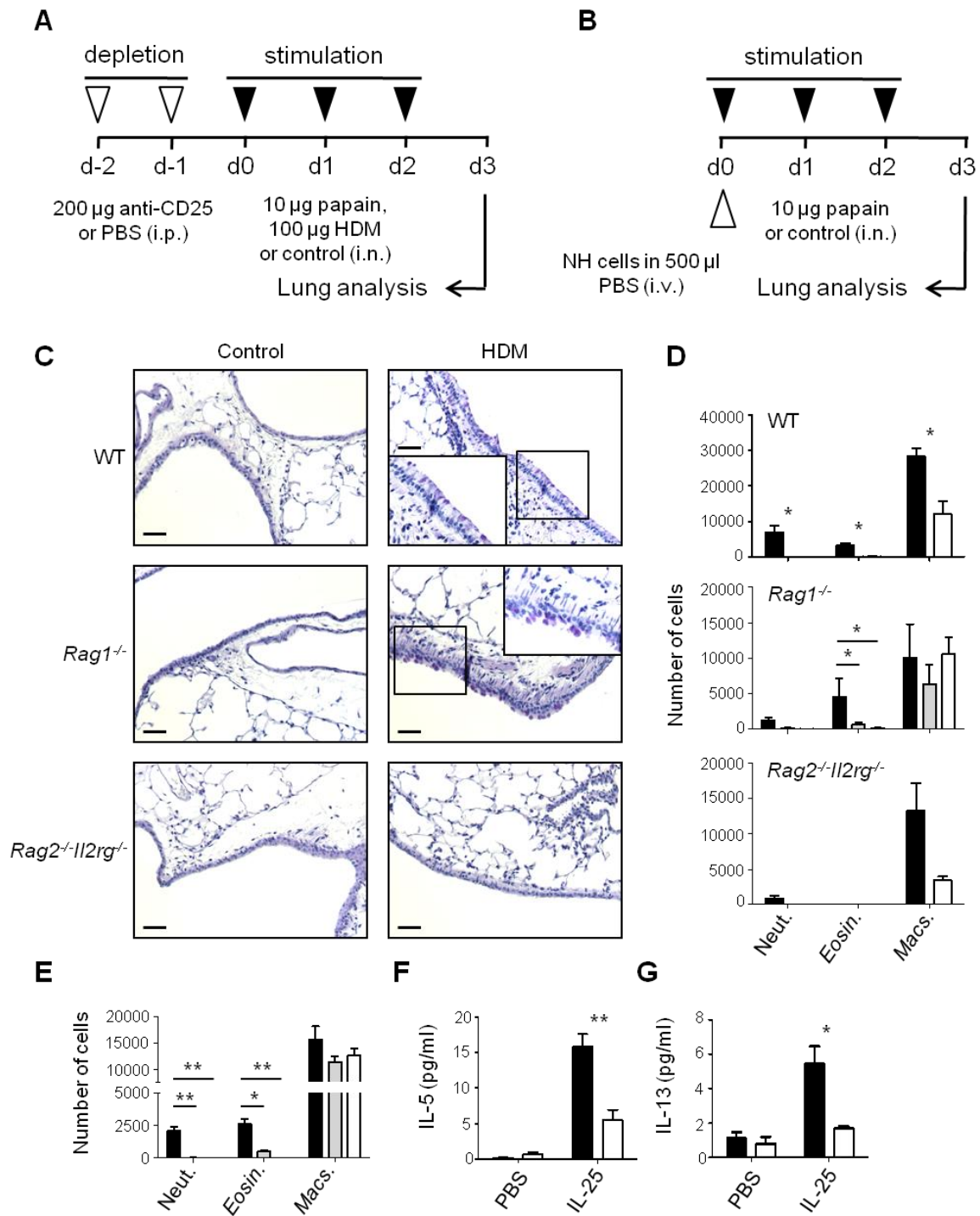


Figure 27 lung NH cell depletion in *Rag1*^{-/-} mice followed by intranasal stimulation with protease allergen or house dust mite.

(A) lung NH cells in *Rag1*^{-/-} mice were depleted by two intra-peritoneal injections of 200 µg anti-CD25 antibody (clone PC61 5.3) or PBS control. lung NH cell-depleted and control *Rag1*^{-/-} mice were injected intra-nasally with papain, heat-inactivated papain (control) or HDM once a day for three days. Mice were sacrificed 24 h after the last injection and the lungs and Bronchioalveolar lavage (BAL) were analyzed.

(B) *Rag2*^{-/-}*Il2rg*^{-/-} mice were injected i.v. with 50,000 lung NH cells or PBS, followed by intranasal stimulation with papain or heat-inactivated papain once a day for three days. Mice were sacrificed 24 h after the last injection and the lungs and BAL were analyzed.

(C) HDM stimulation causes mucus production in WT and *Rag1*^{-/-} mice, but not *Rag2*^{-/-}*Il2rg*^{-/-} mice or PBS (Control) treated mice. Scale bar represents 50 µm, magnified image taken at 63× with immersion oil.

(D) BAL cells from indicated mice strains treated with PBS (white) or HDM (black) were identified by flow cytometry and quantified. *Rag1*^{-/-} mice were not depleted and treated with HDM (black), lung NH-depleted and treated with HDM (grey), or lung NH-depleted and treated with PBS (white).

(E) BAL cells from *Rag1*^{-/-} mice treated with IL-25 (black), lung NH-depleted *Rag1*^{-/-} mice treated with IL-25 (grey) or lung NH-depleted *Rag1*^{-/-} mice treated with PBS (white) were identified by flow cytometry and quantified.

BAL fluid from *Rag1*^{-/-} mice (black) or lung NH-depleted *Rag1*^{-/-} mice (white) treated with IL-25 or PBS was analyzed for IL-5 (F) or IL-13 (G) concentration by ELISA.

*p < 0.05 **p < 0.001 (two-tailed Student's t-test). Data are representative of 3 independent experiments (mean and SEM in D, E, F and G).

Appendix 7 TSLP and/or IL-33 neutralization in explant cultures significantly decreases papain or IL-25 induced Th2 cytokine production.

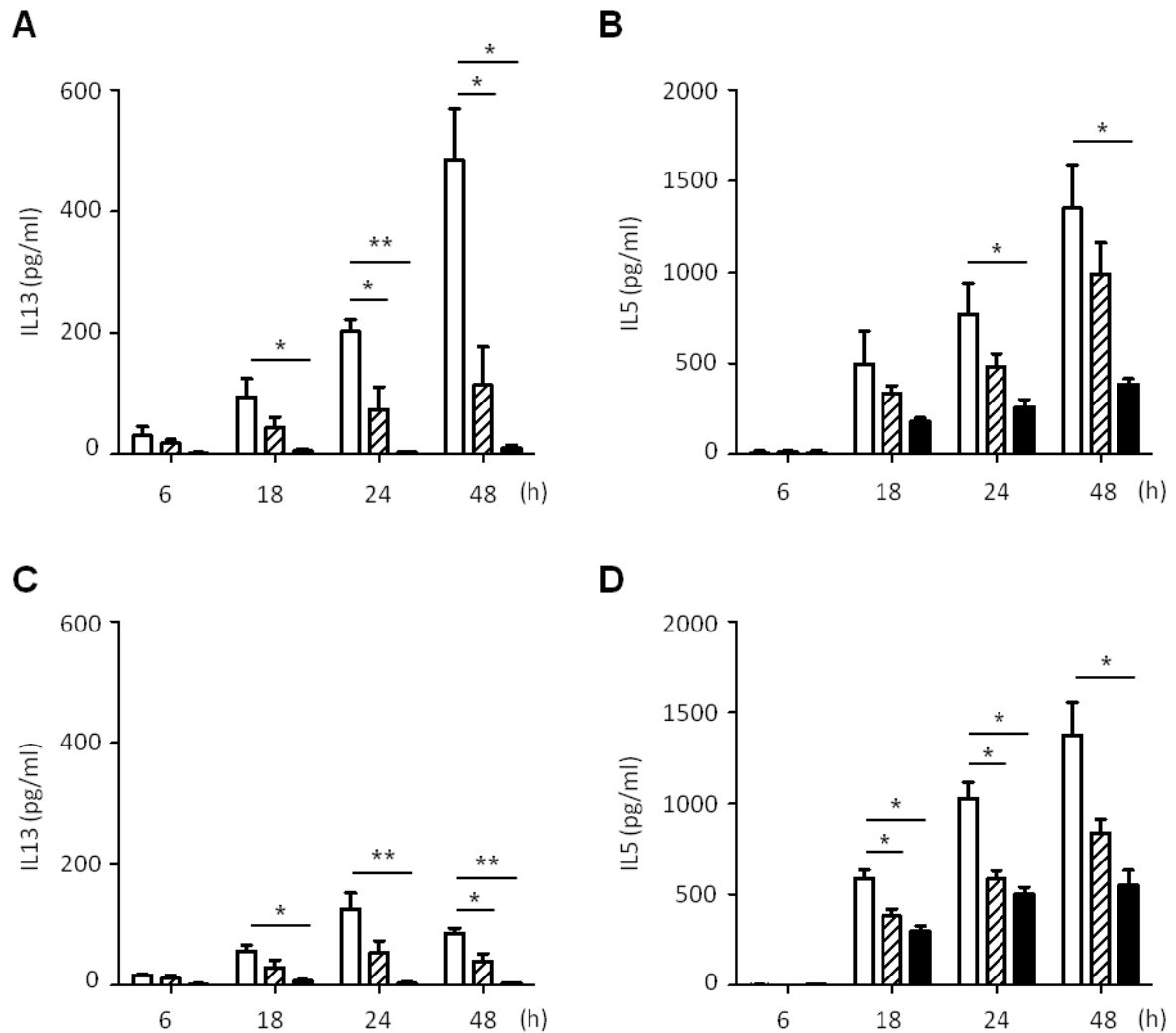


Figure 28 TSLP and/or IL-33 neutralization in explant cultures significantly decreases papain or IL-25 induced Th2 cytokine production.

Explant cultures were prepared from WT mice with anti-IL-33 (striped) or anti-IL-33 plus anti-TSLP neutralizing antibody (black), or IgG control (white). Cultures were stimulated with IL-25 (A and B) or papain (C and D). Culture supernatant samples were taken at the indicated time points and analyzed for IL-5 or IL-13 concentration. * $p < 0.05$ ** $p < 0.001$ (two-tailed Student's t-test). Data are representative of 3 independent experiments (mean and SEM).

Appendix 8 Analysis of WT NH cell gene expression and cytokine production.

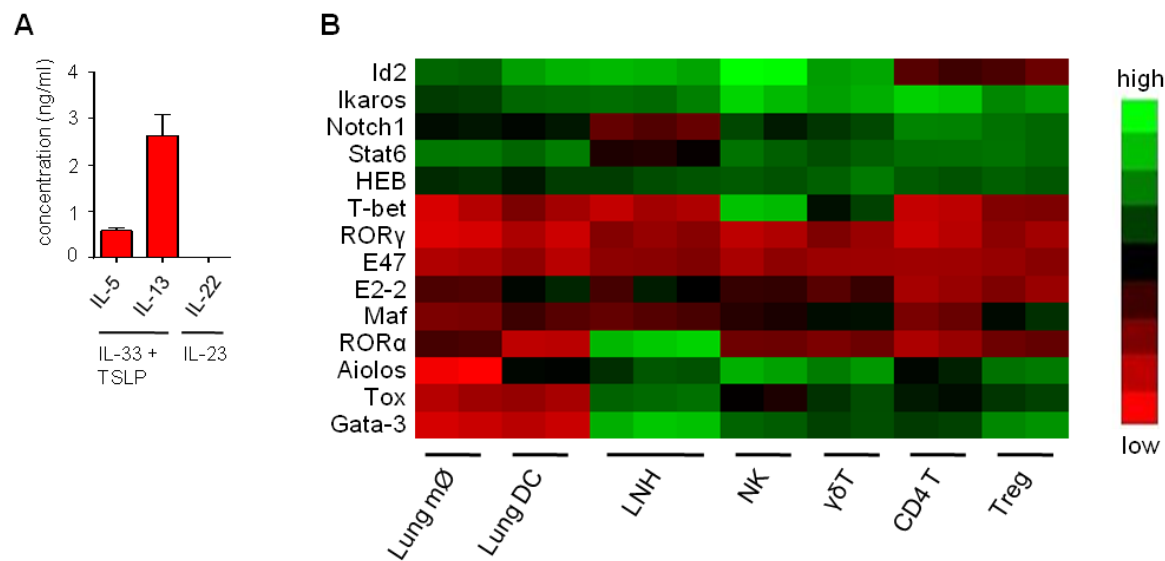


Figure 29 Analysis of WT NH cell gene expression and cytokine production.

(A) FACS purified NH cells from the lung were stimulated *in vitro* with IL-33 plus TSLP followed by analysis for IL-5 and IL-13 production after 3 days. The same populations were also stimulated with IL-23 plus IL-7 followed by analysis for IL-22 production.

(B) FACS purified naïve lung NH cells were analyzed for gene expression by Affymetrix microarray. The expression of the indicated genes in lung NH cells (triplicate experiment) were compared to available microarray results (duplicates) of other known leukocyte lineages.

Data are representative of three independent experiments (mean and SEM in A)

Appendix 9 Analysis of *staggerer* mice for NH cells and NH cell function.

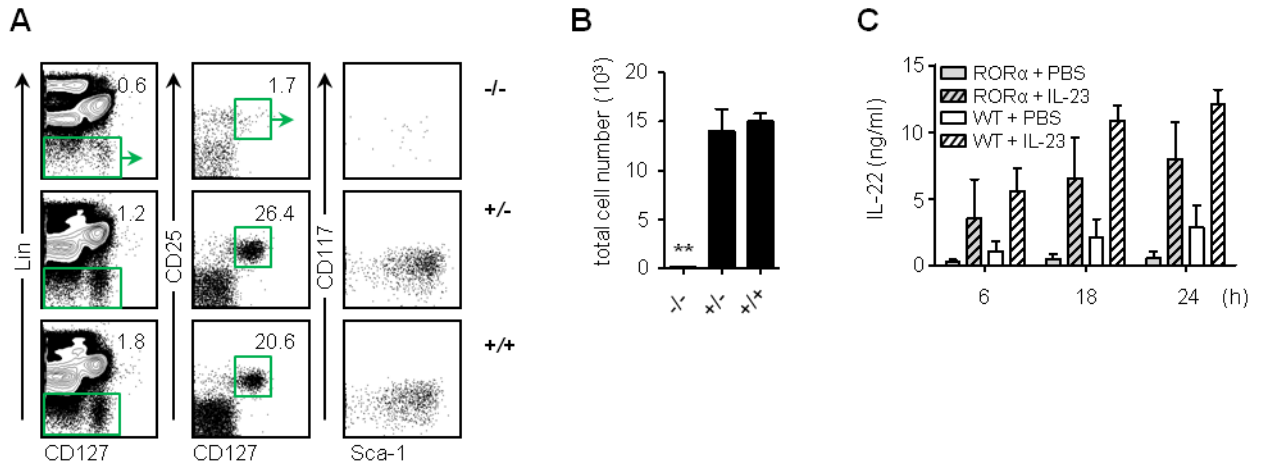


Figure 30 Analysis of *staggerer* mice for NH cells and NH cell function.

(A) The lungs of RORα-deficient homozygous *staggerer* mice (*Rora*^{sg/sg}) were compared to heterozygous and WT littermates for Lin⁻CD127⁺CD25⁺Sca-1⁺c-Kit^{-/low} NH cells by FACS. Cells were first gated for live (DAPI) leukocytes (CD45⁺).

(B) The absolute numbers of lung NH cells were quantified in homozygous knockout, heterozygous and WT littermates. A significant reduction of lung NH cells was observed in *Rora*^{sg/sg} mice, while heterozygous mice had similar numbers as WT mice.

(C) Small intestine explants cultures from indicated mouse strains were stimulated with PBS or IL-23 and analyzed for IL-22 production at the indicated time points. IL-23 stimulation induced similar levels of IL-22 production from both WT and *Rora*^{sg/sg} mice.

**p < 0.001 (two-tailed Student's t-test). Data are representative of three independent experiments (mean and SEM in B and C)

Appendix 10 *Rora*^{sg/sg} BM gives rise to normal numbers of lymphocytes and myeloid cells in the spleen and BM of congenic Pep3b hosts.

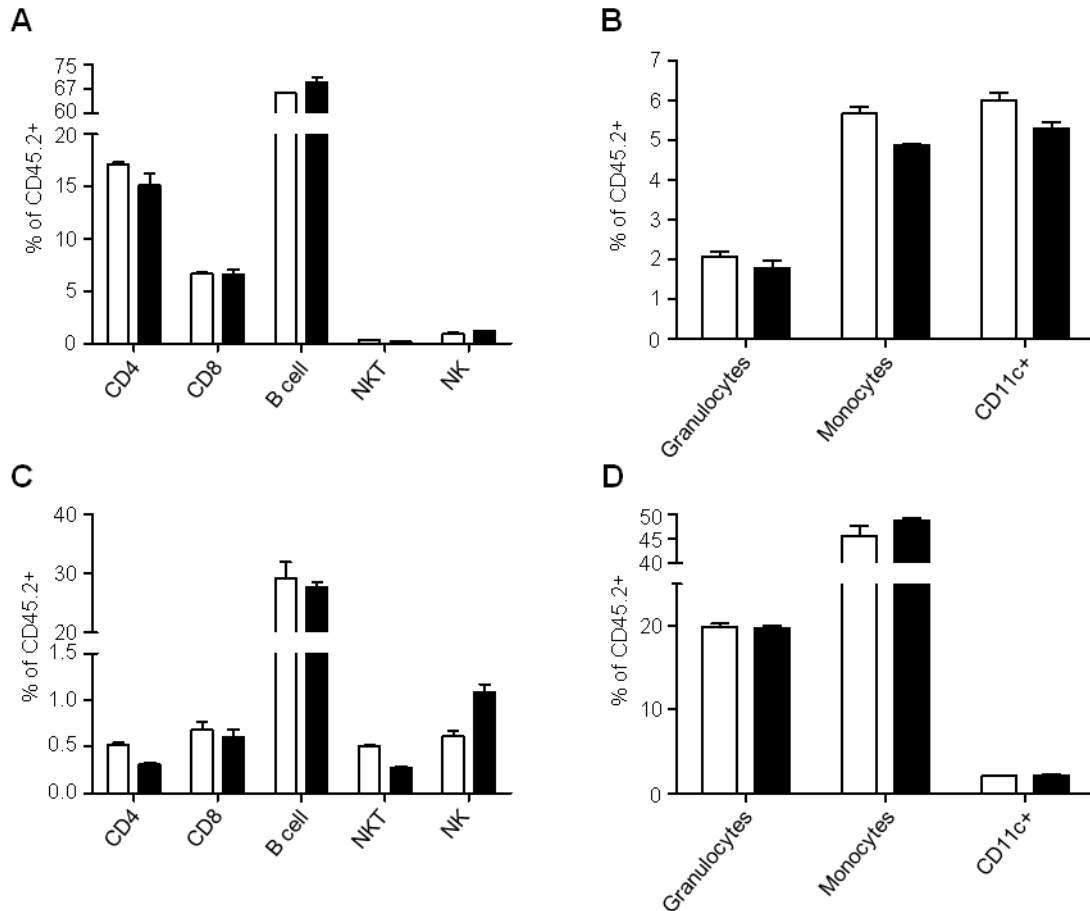


Figure 31 *Rora*^{sg/sg} BM gives rise to normal numbers of lymphocytes and myeloid cells in the spleen and BM of congenic Pep3b hosts.

Pep3b mice transplanted with *Rora*^{sg/sg} BM were analyzed after 16 weeks for donor derived (CD45.1⁻CD45.2⁺) lymphocytes and myeloid cells in the spleen (**A, B**) or BM (**C, D**). Granulocytes were identified by Mac-1 and Gr-1 expression, Monocytes were Mac-1⁺Gr-1⁻ while DC were identified by CD11c expression.

Data are representative of three independent experiments (mean and SEM in A-D)

Appendix 11 BM derived iNH cells and mature lung NH cells respond differently to *in vitro* culture conditions.

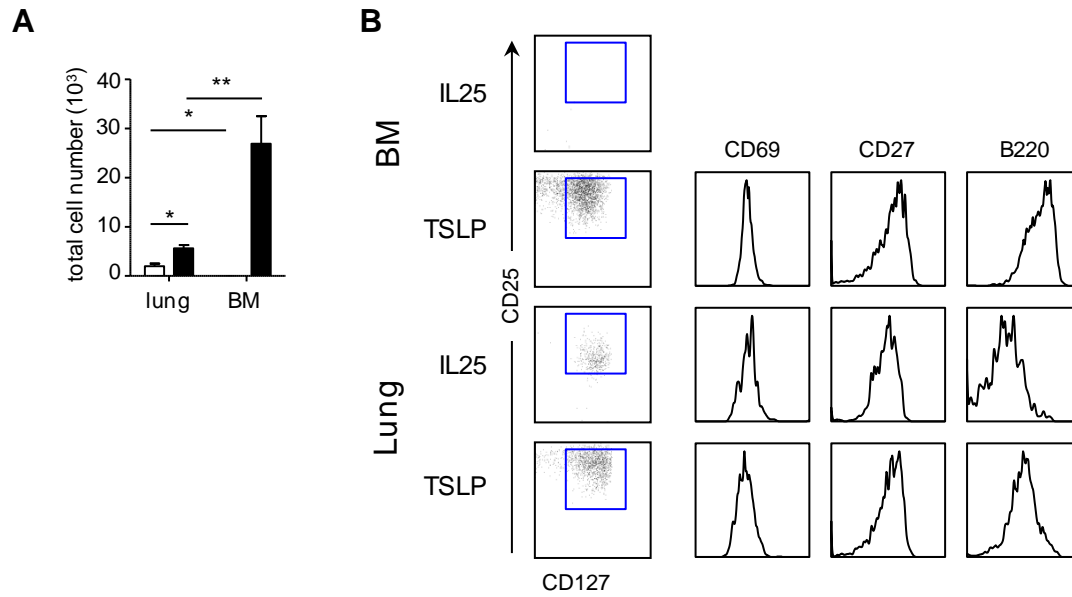


Figure 32 BM derived iNH cells and mature lung NH cells respond differently to *in vitro* culture conditions.

Purified BM iNH cells and lung NH cells (1000 cells) were cultured with IL-33 + IL-25 (white bar) or IL-33 + TSLP (black bar) for 7 days, followed by (A) cell count (B) and phenotypic analysis. Cells were first gated for live (PI) CD45⁺Lin⁻ cells.

*p < 0.05 **p < 0.001 (two-tailed Student's t-test). Data are representative of at least 3 independent experiments (mean and SEM in A).

Appendix 12 BM derived iNH cells have more efficient NH cell repopulation capacity, and are more restricted to NH cell lineage, than LMPP or CLP.

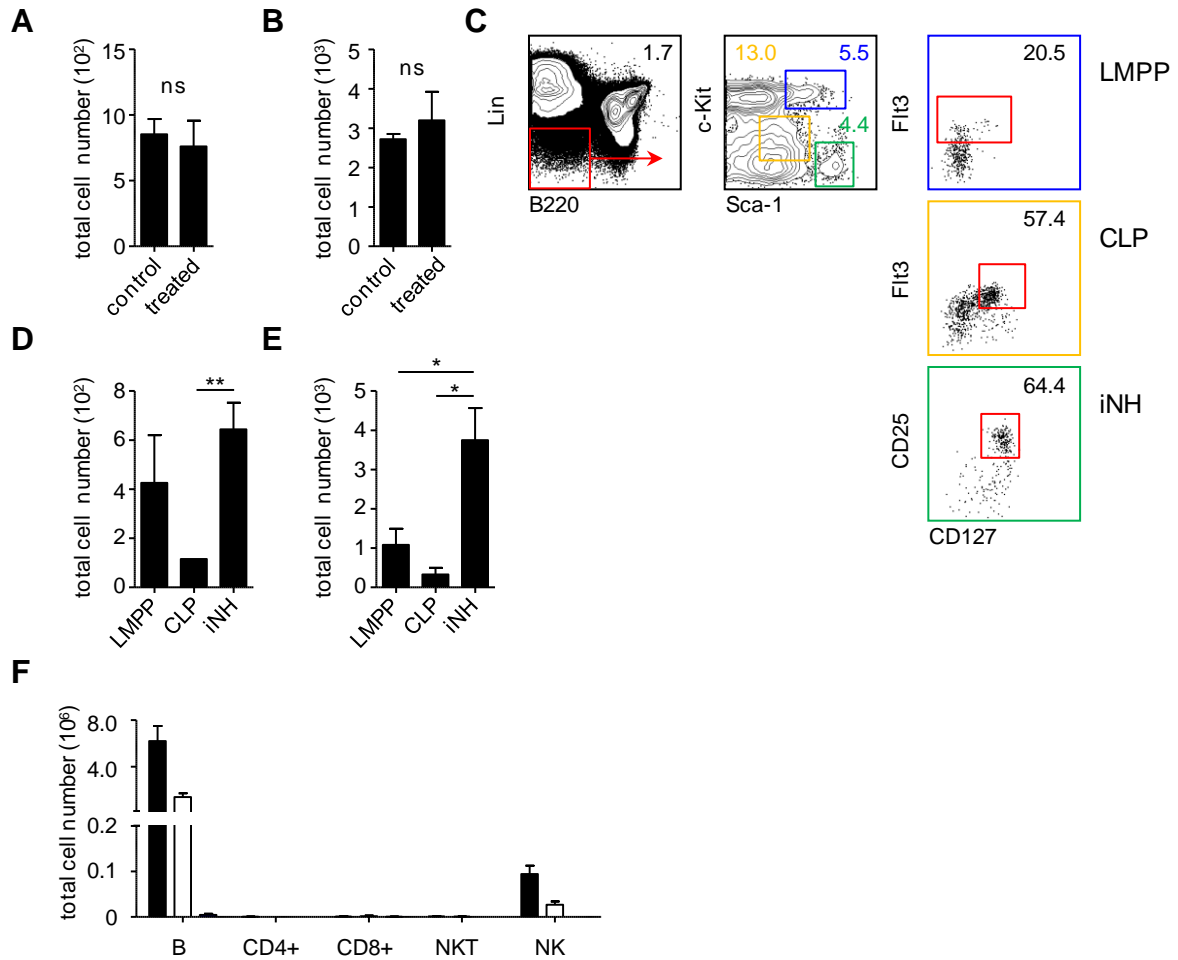


Figure 33 BM derived iNH cells have more efficient NH cell repopulation capacity, and are more restricted to NH cell lineage, than LMPP or CLP.

To determine if lung digestion conditions adversely affect progenitor function, BM was treated identical to lung (treated) or processed normally (control) and iNH cells were purified by flow cytometer followed by adoptive transplant into NSG mice. Transplanted NSG mice were analyzed after 3 weeks for the absolute number of donor derived live (PI⁻) CD45.2⁺CD45.1⁻Lin⁻CD127⁺CD25⁺ST2⁺Sca-1⁺c-Kit^{low} mature NH cells in the (A) lung or (B) small intestine.

(C) BM derived Lin⁻Sca-1⁺c-Kit^{hi}Flt3⁺ LMPP (blue box), Lin⁻Sca-1^{low}c-Kit^{low}Flt3⁺CD127⁺ CLP (yellow box) or Lin⁻Sca-1^{hi}c-Kit⁺CD127⁺CD25⁺ iNH cells (green box) were identified by flow cytometry as shown in dot plots, sorted and injected (2,500 cells per mouse) into non-irradiated NSG mice. LMPP and CLP were negative for CD25, while iNH cells were negative for Flt3 (data not shown).

LMPP, CLP or iNH cell transplanted NSG mice were analyzed after 3 weeks for the absolute number of donor derived live (PI⁻) CD45.2⁺CD45.1⁻Lin⁻CD127⁺CD25⁺ST2⁺Sca-1⁺c-Kit^{-low} mature NH cells in the **(D)** Lung or **(E)** Small Intestine.

(F) The spleens of LMPP (black), CLP (white) or iNH cell (blue) transplanted NSG mice were analyzed for the absolute number of donor derived lymphocytes.

*p < 0.05 **p < 0.001 (two-tailed Student's t-test). Data are representative of at least three independent experiments (mean and SEM in A, B, D, E and F)

Appendix 13 Gating strategies for myeloid cell populations.

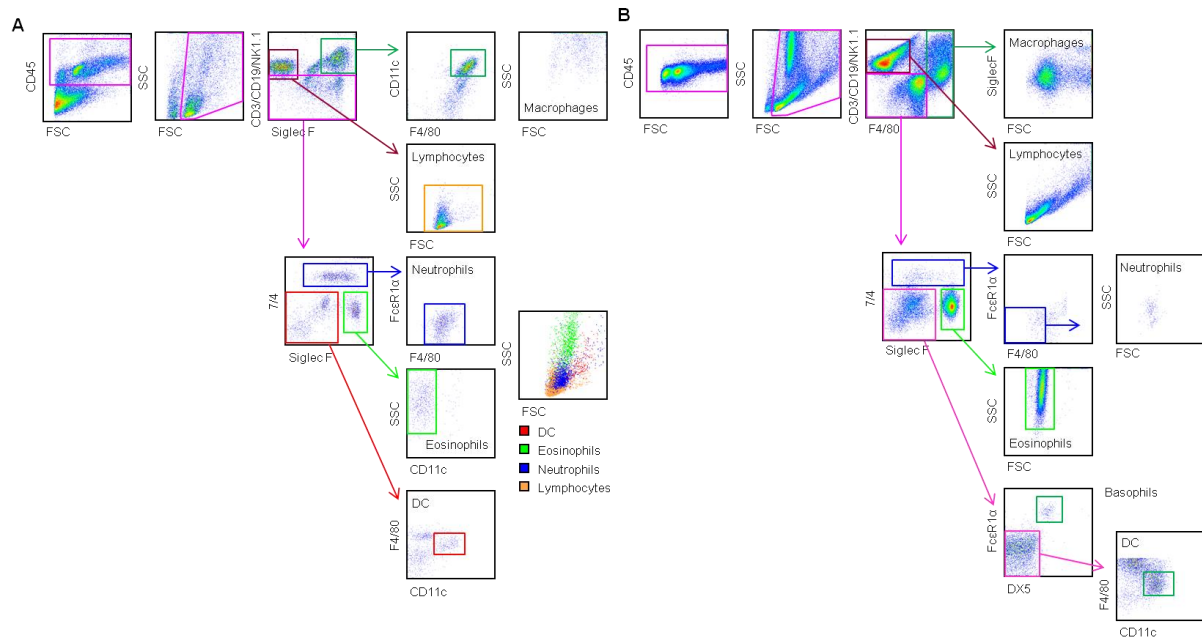


Figure 34 Gating strategies for myeloid cell populations.

Gating strategy for lung (**A**) and gut (**B**) myeloid cell populations. DX5⁺FcεR1α⁺ basophils were not detected in naïve or stimulated lungs. DX5⁻FcεR1α⁺ mast cells were not detected in lung or peritoneal lavage.

Appendix 14 Analysis of IL-25 stimulated gut NH cells.

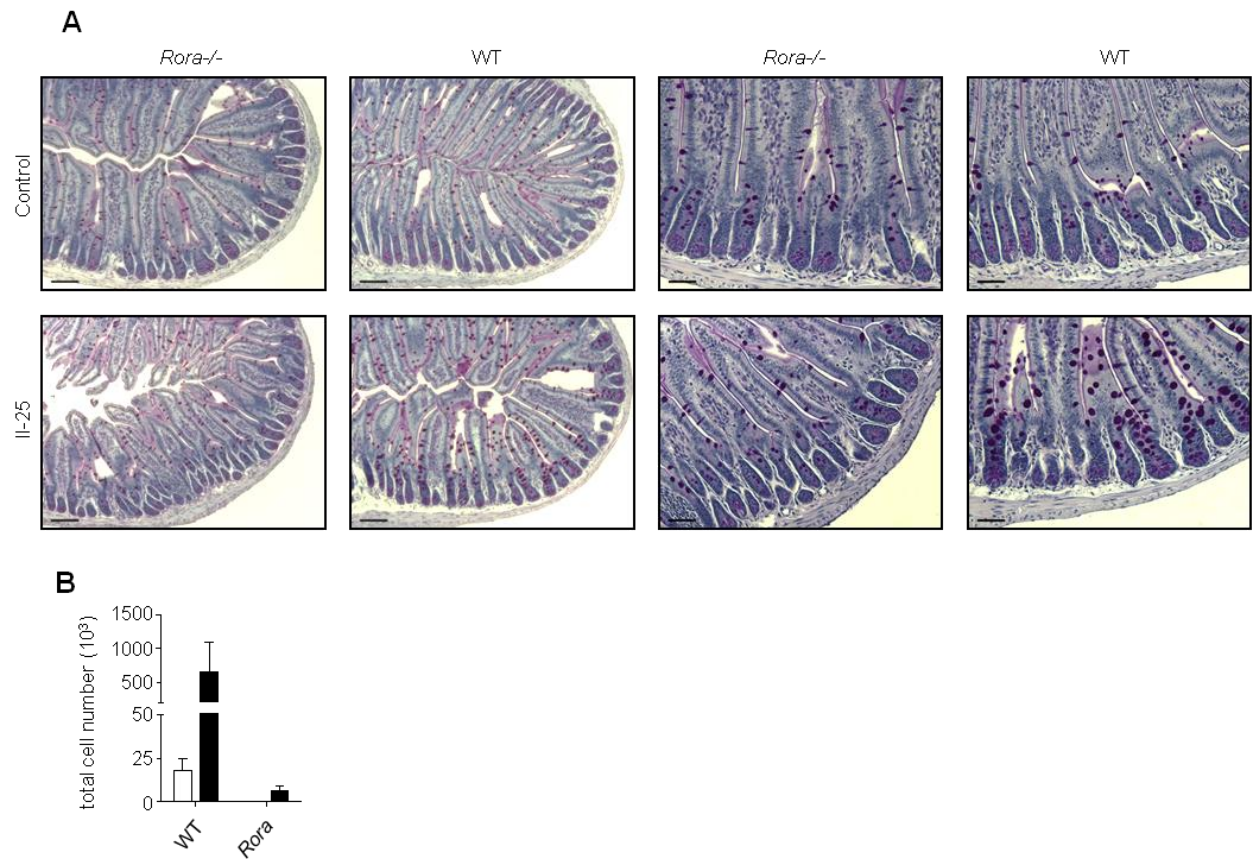


Figure 35 Analysis of IL-25 stimulated gut NH cells.

RGC mice reconstituted with *Rora*^{sg/sg} or WT bone marrow were challenged with by intra-peritoneal administration of IL-25 or PBS control once a day for 3 days.

(A) Transverse sections of the jejunum were stained by PAS (10× magnification 100 μm bar, left 20× magnification 50 μm bar, right). Goblet cell hyperplasia is observed in IL-25 treated WT intestine but not *Rora*^{sg/sg} BMT mice.

(B) Eosinophils were identified in the PL by FACS and quantified. Eosinophilic infiltration is observed in IL-25 treated WT but not *Rora*^{sg/sg} BMT mice.

Data are representative of three independent experiments (mean and SEM in B)

Appendix 15 Supplementary materials and methods

***In vitro* differentiation assay**

For lymphoid cell differentiation, FACS sorted lung NH cells or BM CLP were seeded onto pre-formed OP9 or OP9-DL1 stroma in 500 µl alpha-MEM with 10% FBS, P/S, 150 µM monothioglycerol, 30 ng/ml stem cell factor (SCF), 100 ng/ml recombinant human Flt-3 ligand (Flt3L), 1 ng/ml IL-7, and 25 ng/ml IL-15 for NK cell differentiation. Half of the media was replaced on day 7. Cultures were harvested after 14 days and analyzed by flow cytometer. For myeloid cell differentiation, FACS sorted lung NH cells or whole BM was cultured in the Methocult® myeloid differentiation assay (STEMCELL) according to the manufacturer's protocol. Colonies were scored with the aid of an unbiased expert.

Transplantation assays

Lung NH cells were sorted from B6 mice and injected by tail vein in 500 µl PBS into NOD/SCID/*Il2rg*^{-/-} mice. BM, spleens, and lungs were examined by flow cytometry after 4 weeks. PBS was used as negative control in the transplantation assays.

***In vivo* House Dust Mite stimulation**

Lipolized crude *D.pteronyssinus* (GREER Laboratories, Lenoir NC) was injected i.n. into anaesthetized mice (100 µg in 40 µl of PBS) once a day for 3 days. Lungs and BAL were analyzed as previously described.

Intranasal IL-25 stimulation

Lung NH-cell depleted *Rag1*^{-/-} or non-depleted *Rag1*^{-/-} mice were injected with 5 µg of carrier-free IL-25 (eBiosciences) in 50 µl of PBS once a day for 2 days. Mice were sacrificed 24 h after the last injection and BAL was analyzed.

Cytokine neutralization

Lung explants from B6 mice were prepared and cultured as described before. 12 cultures were prepared from a single animal and cultured in 1.5 ml of media with anti-TSLP (2.5 µg/ml) (R&D Systems) and/or anti-IL-33 (2.5 µg/ml) (R&D Systems). Explants were stimulated with IL-25 (10 ng/ml) (eBiosciences) or papain (10 µg/ml). Supernatant was analyzed for cytokines as previously described.

Eosinophil quantification

Eosinophils were quantified in 20× fields of view of H&E stained lung sections (Axioplan 2 Imaging, Carl Zeiss), captured by camera (Retiga EX, QImaging). Using the digital image to define field boundaries, eosinophils were then positively identified at 63× using immersion oil. Total eosinophil number in ten 20× fields of view was calculated per mouse lung (5 fields of view per section, 2 sections taken at different depths, separated by 500 µm).

***In vitro* expansion of BM iNH and lung NH cells**

BM iNH and lung NH cells were purified by flow cytometer and cultured (1000 cells) in 200 µl RPMI-1640, 2% FCS, 2-ME, P/S, IL-33 (10 ng/ml) plus IL-25 (10 ng/ml) or TSLP

(10 ng/ml) for 7 days. Half the media was refreshed on day 4. After culture, cells were harvested, counted and analyzed by flow cytometry.

In vivo IL-25 stimulation

Mice were injected i.p. with rIL-25 (500 ng) in 500 µl of PBS on d 0-2. Mice were sacrificed on d 3 and intestines and peritoneal lavage (PL: 8 ml PBS, 2% FCS, 10 mM EDTA) were collected. Intestines and PL cells were counted and analyzed by FACS. Intestines were fixed in formalin. Fixed tissues were embedded in paraffin and processed for H&E or PAS (+/- diastase) staining by the Centre for Translational and Applied Genomics (Vancouver, Canada).

Appendix 16 Table of primers

Primer name	Primer sequence
RORa-F	gagctccagcagataacgtg
RORa-R	gcaaactccaccacatactgg
B-actin-F	aaggccaaccgtgaaaagat
B-actin-R	gtggtacgaccagaggcatac
RORa mut-F	GATTGAAAGCTGACTCGTTCC
RORa mut-R	CGTTTGGCAAACCTCCACC
RORa wt-F	TCTCCCTTCTCAGTCCTGACA
RORa wt-R	TATATTCCACCACACGGCAA
V γ 2-F	TGGACATGGGAAGTTGGAG
V γ 1-R	CAGAGGGAATTACTATGAGC
NKG2A-F	CCTTCTCAGGAGCATCCCTGGAT
NKG2A-R	GACAAAACAGATGAGGCCAGGG

Table 2: List of primers

Table of primers used for experiments in this thesis.

Appendix 17 Table of antibodies

	target	alternative name	Detects	clone	clone (other)
cell surface	CD3ε		T, NKT	145-2C11	
	CD4		T	GK1.5	
	CD8		T	53-6.7	
	CD11b	Mac-1	Gran	M1/70	
	CD11c		DC, Gran	HL3	N418
	CD16a	FcγRIIIa	multiple	2.4G2	
	CD16b	FcγRIIIb	multiple	2.4G2	
	CD19		B	MB19-1	ID3
	CD25	IL-2Rα	lymph, progenitor	3C7	PC61.5
	CD27		T, NK, NH, progenitor	LG 3a10	
	CD32	FcγRII	multiple		
	CD34		stem cell, mast cell	RAM34	
	CD44		multiple	IM7	
	CD45		pan leukocyte	30-F11	
	CD45.1		pan leukocyte	A20	
	CD45.2		pan leukocyte	104	
	CD45RB	B220	B, progenitor	RA3-6B2	
	CD49b	DX5	NK, baso	DX5	
	CD69		T, NH	H1 2F3	
	CD90.1	Thy1.1	T, NK, NKT, NH	HIS51	
	CD90.2	Thy1.2	T, NK, NKT, NH	53-2.1	
	CD117	c-Kit	stem cell, progenitor	2B8	
	CD122	IL-2Rβ	progenitor, T, NK, NKT, NH	TM-β1	
	CD127	IL-7Rα	progenitor, lymph	A7R34	
	CD135	Flt3	progenitor	A2F10	
	CD161	NK1.1	NK, NKT	PK136	
	CD194	SiglecF	eosin	E50-2440	
	CD278	ICOS	T, NKT, NH	7E 17G9	
	CD335	NKp46, NCR1	NK, ILC	29A1.4	
	CXCR4		T, DC, NH	2B11	
	CCR6		ILC22	29-2L17	
	F4/80		macro	BM8	
	FcεRI		mast, baso, eosin	Mar-01	
	Ly-6A/E	Sca-1	multiple	D7	
	Ly-6G	Gr-1	Gran	RB6-8C5	
	Ly-76	Ter119	progenitor, RBC	TER-119	
	T1/ST2	IL-33R, IL-1RL1	myel, T, NH	DJ8	
	TCRβ		T, NKT	H57-597	
	TCRγδ		T, NKT	GL3	
intracellular	IFNγ		cyto	n/a	
	IL-5		cyto	TRFK5	
	IL-13		cyto	eBio13A	
	IL-17A		cyto	n/a	
	RORγt		TF	AFKJS-9	B2D

Table 3: List of antibodies

Table of antibodies used for experiments in this thesis. T (T cell), NKT (NK T cell), Gran (Granulocyte), DC (Dendritic Cell), B (B cell), Lymph (Lymphocyte), NK (Natural Killer cell), NH (Natural Helper cell), Baso (Basophil), RBC (Red Blood cell), Eosin (Eosinophil), cyto (Cytokine), TF (Transcription Factor), ILC22 (IL22 producing Innate Lymphocyte), Mast (Mast cell), ILC (Innate Lymphocyte).

Appendix 18 Table of cytokines

Name	receptor	produced by	function
IL-2	(IL-2R α) CD25, (IL-2R β) CD122, (IL-2R γ) CD132	T cells	lymphocyte growth and maturation
IL-3	(IL-3R α) CD123	basophils, T cells	growth factor, differentiation
IL-4	IL-4R	basophils, T cells	Th2 cytokine, Th2-skewing of CD4 T cells
IL-5	IL-5R α , IL-5R β	NH, T cells	Th2 cytokine, parrasite infection, eosinophil growth, maturation and survival
IL-6	IL-6R α (CD126), CD130	T cells, Macrophages, FALC NH	pro-inflammatory
IL-7	(IL-7R α) CD127, (IL-2R γ) CD132	stromal cells, DC, epithelial cells	Lymphocyte growth and maturation, T cell development, lymphocyte homeostasis
IL-9	IL-9R (CD129), (IL-2R γ) CD132	T cells	lung inflammation
IL-10	IL-10R α	monocytes, lymphocytes	anti-inflammatory
IL-12	IL-12R β 1, IL-12R β 2	DC, Macrophages, B	Th1 signalling, activation on T and NK cells
IL-13	IL-13R α 1, IL-4R α or IL-13R α 2	T cells, NH	Th2 cytokine, parrasite infection, induces goblet cell hyperplasia and mucus production
IL-15	(IL-2R β) CD122, (IL-2R γ) CD132	DC, Macrophages, B	T, NK, NKT cell growth and maturation
IL-17a	IL-17R	T cells, Neutrophils	pro-inflammatory, bacterial infetion
IL-17f	IL-17R	T cells, Neutrophils	pro-inflammatory, bacterial infetion
IL-18	IL-18R1, IL-18RAP	Macrophages	pro-inflammatory, T and NK cell stimulation
IL-22	IL-22R α / β , IL10R α / β	ILC22, DC, T cells	induces production of antibacterial peptide, mucosal homeastasis
IL-23	IL-12R β 1, IL-23R	DC, Macrophages	induces IL-22 or IL-17 production
IL-25 (IL-17E)	IL-17RB	Stromal cells, T cells, Mast cells	allarmin, induces Th2 response
IL-33	IL-1RAP, IL1R1 (T1/ST2)	Epithelial cells, Macrophages	allarmin, induces Th2 response
Flt3L	Flt3 (CD135)	Stromal cells	haematopoiesis
SCF	(c-Kit) CD117	Stromal cells	haematopoiesis, stem cell maintainance
TSLP	TSLPR, (IL-7R α) CD127	Stromal cells	allarmin, induces Th2 response
IFN γ	IFNGR1, IFNGR2	NK, NKT, T cells	Th1-type cytokine, viral/bacterial infection

Table 4: List of cytokines

Table of cytokines used or mentioned in this thesis.